INFORMATION TO USERS

This manuscript has been reproduced from the microfilm master. UMI films the text directly from the original or copy submitted. Thus, some thesis and dissertation copies are in typewriter face, while others may be from any type of computer printer.

The quality of this reproduction is dependent upon the quality of the copy submitted. Broken or indistinct print, colored or poor quality illustrations and photographs, print bleedthrough, substandard margins, and improper alignment can adversely affect reproduction.

In the unlikely event that the author did not send UMI a complete manuscript and there are missing pages, these will be noted. Also, if unauthorized copyright material had to be removed, a note will indicate the deletion.

Oversize materials (e.g., maps, drawings, charts) are reproduced by sectioning the original, beginning at the upper left-hand corner and continuing from left to right in equal sections with small overlaps.

Photographs included in the original manuscript have been reproduced xerographically in this copy. Higher quality 6" x 9" black and white photographic prints are available for any photographs or illustrations appearing in this copy for an additional charge. Contact UMI directly to order.

ProQuest Information and Learning
300 North Zeeb Road, Ann Arbor, MI 48106-1346 USA
800-521-0600

UMI®

GLASS CERAMICS FROM PULP AND PAPER WASTE ASH

by

Mathumathi Sivasundaram

A Thesis submitted to the
Faculty of Graduate Studies and Research
in partial fulfillment of the requirements for the degree of
Master of Engineering

Department of Mining and Metallurgical Engineering
McGill University
Montreal, Quebec
Canada

March 2000

National Library
of Canada

Acquisitions and
Bibliographic Services

395 Wellington Street
Ottawa ON K1A 0N4
Canada

Bibliothèque nationale
du Canada

Acquisitions et
services bibliographiques

395, rue Wellington
Ottawa ON K1A 0N4
Canada

Your file Votre référence

Our file Notre référence

0-612-64248-8

Canada

To my parents,
to whom I owe everything

ABSTRACT

Pulp and paper industries face tremendous problems in eliminating waste, which is in the form of sludge, wood, and reject material. Although incineration is seen as the most effective solution, this unfortunately leaves large quantities of residues such as fly ash and bottom ash. The ashes are alumino-silicate materials, which are excellent candidates for producing both glasses and glass ceramic materials.

In the present work, samples of pulp and paper incinerator residues were collected and the initial characteristics (moisture content, loss on ignition, particle size and size distribution, chemical composition) were analyzed. The major oxides were found to fall within the SiO_2-Al_2O_3-CaO (CAS) system. Moreover, nucleating agents such as TiO_2, Fe_2O_3, Cr_2O_3 and P_2O_5 were also present in the glass. Through thermal analysis (TGA and DTA) optimum heating schedules were selected for producing glass ceramic materials. It was found that the optimum devitrification temperature for fly ash was 1200° C and the final product contained anorthite with/without albite. Hardness values exceeded that of the parent glass and thus the material should be useful in glass ceramic applications.

RÉSUMÉ

Les industries de la pâte et du papier ont à faire face à de graves problèmes pour éliminer les déchets sous la forme de boues, de bois et de rebuts. Bien que l'incinération soit considérée comme la solution la plus efficace, elle laisse malheureusement de grandes quantités de résidus tels que les cendres des fumées et des foyers. Ces cendres sont des alumino-silicates, qui sont d'excellents candidats pour la production de verres et de céramiques vitreuses.

Dans le présent travail, nous avons collecté des échantillons de résidus de pâte et de papier, dont les caractéristiques initiales (humidité, perte au feu, taille de particules et distribution en taille, composition chimique) ont été analysées. Il a été trouvé que la majeure partie des oxydes se situe dans le système SiO_2-Al_2O_3-CaO (CAS). De plus, des agents de germination tels que TiO_2, Fe_2O_3, Cr_2O_3 et P_2O_5 sont également présents dans le verre. L'optimisation des protocoles de chauffage pour la production de céramiques vitreuses a été déterminée à l'aide d'analyses thermiques (ATG et ATD). Il a été trouvé que la température optimale de dévitrification pour les cendres des fumées était de 1200°C, et que le produit final contenait de l'anorthite avec ou sans albite. Les valeurs de dureté sont supérieures à celle du verre d'origine et ainsi le matériau peut être utilisable pour la réalisation de céramiques vitreuses.

ACKNOWLEDGEMENTS

I would like to express my sincere gratitude to my thesis supervisors, Professors Robin A. L. Drew of McGill University and William F. Caley of DalTech., DalHousie University, for their guidance, and encouragement throughout the whole course of study. Their enthusiasm for scientific inquiry in the field of ceramics, together with their personal attitude, patience and kindness have been inspiring during my M. Eng. Studies.

I am grateful to Professors J. A. Kozinski and Z.Altounian for providing access to the TGA and DTA equipment.

My thanks and appreciation to:

- Helen Campbell, GlennPoirier, Monique Riendeau, Mary Dikeakos, A. Ramesh, Florence Parray, Sandra Lalli, E. Siliauskas, Edwin Fernandez and Ray Langlois - for their advice and assistance in the lab.
- Michel Pernot - for translating my abstract into French.
- Carol Rousseau, Purnima Mujumdar, Genny Snider and Barbara Hanley - for their continuous help in various forms.
- My friends and fellow graduate students who created a pleasant and friendly working environment during the course
- Cynthia Macdonald who provided support and encouragement throughout my stay in Montreal.

Last but not least, I would like to deeply express my sincere gratitude to my parents, sisters and brothers for their unceasing love, encouragement and support throughout the years. Their sacrifices were remarkable.

TABLE OF CONTENTS

LIST OF FIGURES

LIST OF TABLES

CHAPTER I

INTRODUCTION

The rapid increase in municipal and industrial growth and the generations of build up of solid waste has necessitated finding new methods of disposing solid wastes. Historically, refuse disposal has been carried out according to one of three basic methods; composting, sanitary landfill or incineration [1]. Composting, the aerobic degradation of waste, is not practiced to any significant degree because of the availability and abundance of inexpensive and more effective fertilizers. Sanitary land filling, which is the permanent placement of refuse under maximum density in the earth with daily cover, is the predominant method whenever sufficient land is available at low cost near the sources of waste generation [2]. When land is not available at economical prices within reasonable distance from the centers of refuse generation, incineration presents distinct advantages and in most industrialized countries, where the population density is high and the availability of space for land filling is limited, it is seen as the most effective solution. Incineration reduces the solid waste volume by 65-70% and allows for recovery of energy as heat to make electricity or steam [3]. However the incineration process still leaves large quantities of residues such as ashes, slags and filter dusts. These by-products can sometimes contain heavy metals and lead to serious environmental hazards. This imposes the need for new alternatives for their adequate disposal or recycling in terms of environmental safeguards. Generally these hazardous ashes are stored in specially designed land sites (class 1 landfills) to provide a high level protection from the harmful effects of this waste [4].

The increasing costs associated with increasingly severe environmental regulations on storing ashes in these land fills and difficulties encountered in opening new class 1 sites are creating innovative solutions for converting ashes into an inert waste from which value can be added.

Attempts to utilize ash are not new. Several more efficient uses have been proposed in the last 40 years, including brick and ceramic tile manufacture, light weight aggregate, road pavements, fillers in plastics and paints, mineral wool and for metal recovery [5]. However these technologies face problems with cost and quality, so development of comparable technologies with added value is favored. The production of vitreous materials can be an effective route for recycling of wastes because the high temperature involved in the process leads to the complete destruction of the organic pollutants. Furthermore, heavy metals can be either incorporated in the glassy product or separated from the residue by evaporation or differential precipitation [6]. The inert vitreous product can also be used as a secondary raw material, especially in building and road construction. Unfortunately vitrification is an energy intensive process, which involves high cost [7]. Therefore more effective and economic options of improving their properties for high quality are a must.

Since the major constituents of ashes are various oxides of silicon and aluminum, these can be good candidates for glass and glass ceramic production [8]. Therefore by proper heat treatment and controlled crystallization, it should be possible to produce a new marketable material (eco-product), - glass ceramics, which can be used in many industrial applications [9].

Glass ceramics are commercially important ceramics with unique thermal shock resistance and mechanical properties. For example, properties such as strength, hardness and corrosion resistance are superior to the parent glass making them attractive materials for the construction, mechanical and chemical industries.

Of particular importance in many applications is the high uniformity of the microstructures of glass ceramics, and the absence of porosity and minor changes in volume during the conversion of glass into glass ceramic. Because the glass ceramic process begins with a glass, all the well-established glass forming techniques can be employed to manufacture components with a variety of complex shapes [10].

Glass-ceramics have now become technologically important materials since their discovery in the 1950s, and are used in microwave radomes, microelectronic substrates and packaging, domestic cooker tops and cooking utensils, astronomical telescopes, high integrity vacuum envelopes and biomedical applications [11].

Recent papers have reported on the use of vitrification and crystallization processes to recycle different wastes such as red mud from zinc hydrometallurgy, coal fly ash, iron blast furnace slag and filter dusts from waste incinerators [12]. No attempt has been made to determine the nucleation and crystallization parameters of glasses produced from pulp and paper waste incinerator residues. This thesis reports the results of a study of characterize the fly ash and bottom ash from pulp and paper incinerator waste and assesses the feasibility of producing glass ceramics from these ashes.

CHAPTER II

LITERATURE REVIEW

2.1. Solid Waste

The continuing concentration of our population in urban areas, economic and population growth, improvements in standard of living, continuing technological improvements in manufacturing, packaging and marketing have all contributed to a rising tide of scrap discarded and wastes. These solid wastes may be categorized into agricultural wastes, hospital and municipal solid waste, and industrial waste [1].

The principal constituents in agricultural wastes include crop residue, animal and poultry manure and the most common disposal practice is composting. The material components of municipal solid wastes are paper, glass, metal, plastic, rubber, textile, wood and food wastes. Although the origin of these contaminants is industrial, they are rejected by urban customers as municipal refuse [1].

Medical waste refers to any waste generated from the health care industry such as hospitals and medical laboratories. Medical wastes, in addition to general wastes, often include anatomical waste, pathological waste, and infectious waste. Thus, the mixture

contains more organic matter and plastics than municipal wastes. These wastes are usually collected and treated along with other municipal solid waste [2].
Industrial solid wastes arise from a variety of sources and can be divided into three categories [1]:

a) Waste arising from the raw materials used in industry,
b) Waste resulting from industrial processes, and
c) Waste created by worn-out products.

The wastes vary in quantity, physical and chemical compositions and properties, and in methods used for their disposal. Furthermore they are continuously changing as new technologies produce different wastes [1].

The major portion of industrial refuse consists of solid waste coming from factories, processing plants, and other manufacturing enterprises. This includes metal planting solid wastes, waste from meat packing industries, agricultural industries and food industries, plastic and paint wastes, cement, and power plant wastes, and sludge from textile and pulp and paper mills [1].

Although pulp and paper wastes are classified as general commercial waste, it is a tremendous environmental problem for the pulp and paper industry as environmental regulations become increasingly stringent while at the same time landfill space grows more scarce.

2.1.1. Pulp and Paper Waste

Large earthen impoundment, ash ponds, and landfills are common at most pulp and paper mills. As production levels and regularity requirements have changed, many mills have encountered difficulties with these process areas. Even though paper mill sludge is a relatively homogeneous material removed from the wastewater stream during the pulp and paper making process, recovery projects were virtually unheard of until the late 1980s[13]. There are three main waste streams generated in pulp and papermaking and they differ greatly in their physical and chemical properties [14]. These include the following:

Wood: Of the wood-type residues, it is the bark that is of significance in the pulp and paper industry. Bark has a high calorific value and is therefore an ideal energy source. When burning sludge, which may have too low a calorific content to ensure auto thermal combustion, bark can be cofired to enhance the heat balance. Bark does not contain any pollutants to speak of and has a low minerals content. The only factor to be considered is size, because of the risk of coarse inorganic matter being introduced into the process.

Rejects: Rejects comprise residues from various sources in the pulp production process.

Sludge: The third waste stream comprises the sludge.

There are two types of sludge produced in pulp and paper making namely,

a) **Chemical and biological sludge from the wastewater treatment system:** The characteristics of the sludge depend on the wastewater technology used in the mill, which can involve different physical, chemical, thermal and biological treatments. The paper sludge generated from the wastewater treatment units of the paper mills, with daily volume of 3000 tons (moisture content 75%) in Taiwan, is one of the major wastes in the paper industry [15].

b) **Deinking sludge:** When recycling, paper inks must be removed from the used paper before it can be efficiently reused; this process is called a deinking operation. Deinking operations involve the mechanical repulping of waste paper and the use of detergents/surfactants to remove inks and pigments. Effluents from de-inking operations include non-recoverable paper fibers, clay fillers and coating and other solids. The sludge is normally de-watered to produce a material with dry matter of approximately 30%. De-inked paper mill sludge varies in composition between mills but is normally high in cellulose and low in potentially toxic compounds [16]. It has been estimated that by the end of the decade, the world's production of deinking sludge will be more than 8 million tons per year [17].

Generally sludge is produced in two steps in the process of treating effluent. Primary clarification is usually carried out by sedimentation, but also can be performed by dissolved air flotation. In sedimentation, the wastewater to be treated is pumped into large settling tanks, with the solids being removed from the tank bottom. These solids can range from 1.5 % to 6.5% consistency, depending on the characteristics of the material [18]. Secondary treatment is usually a biological process in which microorganisms convert the waste to carbon dioxide and water while consuming oxygen. The resulting sludge is then mixed with the primary sludge prior to dewatering. The Canadian pulp and paper industries produce an estimated 1.6 million t/yr of combined primary and secondary sludge [19].

As production levels and regularity requirements have changed many mills have encountered difficulties in disposing their waste. Common problems include [20]:

Inability to accomplish design plans: Existing waste or treatment systems are not meeting original capacity and design specifications. Often, the reason is that mill-waste materials, especially sludge, change properties over time, resulting in conditions that did not exist when the facility was changed.

Expansion: Ponds and landfills are becoming filled and mills need more capacity. However, mills often have no available space for new units and are looking to expand existing sites. Again the properties of the waste make expansion difficult.

Changing operations: Mills are changing the way they handle their waste material, resulting in changing conditions at disposal facilities.

Closure: Both corporate initiatives and, in some cases, regulatory requirements have mandated that the land-based systems be abandoned and/or closed. Closure by traditional landfill capping techniques can be problematic due to unstable materials.

2.2 Solid Waste Disposal

Different strategies are used to dispose of solid waste. Growing environmental pressures and increased legislation have resulted in additional constraints on waste disposal. Typical disposal routes have included agricultural application, land disposal, incineration, and disposal at sea. For example table 2.1 shows the paper mill sludge management trends for the past 20 years [13].

Table 2.1. Paper mill sludge management trends for the past 20 years [13].

Method	1979 (%)	1988 (%)	1995(%)
Landfill/lagoon	86	74	50
Incineration	11	18	25
Land application	2	6	12
Beneficial Use	<1	1	7
Recycle/reuse	<1	1	6

However, as increasing volumes of the residues are being produced, disposal routes are diminishing. Sea disposal is no longer considered environmentally acceptable and has been banned. Growing concerns about potential long-term effects of heavy metals associated with agricultural usage of bio-solids may place additional restrictions on this route. Heavy metal contamination is also a concern in land disposal instances, and costs may prohibit their method of disposal. Incineration is currently perceived as a viable disposal option. In some instances, incineration may provide the most cost effective and environmentally acceptable option due to increasingly stringent constraints places on alternative routes of disposal. In addition, as space for dewatered sludge becomes restricted, the low residual volume from incineration increases in importance [21].

Although a portion of pulp and paper wastes are sometimes converted into organic fertilizers or recycled into construction materials, some paper factories have developed a waste incineration system to reduce the amount of waste in order to help and solve the problem of insufficient landfill sites. Further, the paper waste consists of organic fiber material and inorganic clay minerals; the thermal energy of the former can be recovered by incineration. However, the waste contains 30% non-flammable materials including clay, which are collected in the form of ashes after incineration [15].

2.2.1. Incineration

Waste incineration involves combustion under controlled conditions to convert waste into harmless end products. This is one of the intermediate processes in the eventual production of a value added product and is carried out for the following reasons [22].

a. The total amount that needs to be processed at the final stage can be reduced; and
b. This process can be carried out in a sanitary manner.

Although priority is given to reducing waste at source or recycling, incineration with energy recovery is undoubtedly an inevitable short-term solution. It is now becoming an increasingly used alternative technology for treating solid wastes with the advantage of decreasing solid waste volume by approximately 65-70% and providing heat to make electricity or steam [23]. However, the incineration process is not a final waste treatment stage. It leaves 20 – 30% of the original weight of the waste as bottom and boiler ash, and filter fly ash, all of which require further management [8]. The amount of each residue produced at an incinerator depends on several factors such as feed waste composition, incinerator technology and operation.

Bottom ash residue is the material that resides on the grate of the incinerator after combustion process is completed. This is the main waste stream from the incineration process and appears after quenching/cooling with water as a coarse, extremely inhomogeneous granulate usually containing larger fused lumps of slag, and pieces of scrap metal or wood depending on the type of waste. The slag represents 25% by volume of initial waste before incineration [4].

Fly ash is a collective term for the finer material captured downstream from the furnace, in the heat recovery and air pollution control system, and represents 3 –5 % of the initial waste volume. Fly ash consists of almost every naturally occurring element. The elemental composition of fly ash is qualitatively similar to the composition of natural earthy materials such as soils and shale [24]. The fly ash can be neutralized by adding reagents such as lime, lime wash, sodium bicarbonate or other sodium salts and may be categorized into two groups [4]:

a) Fly ash resulting from a dry exhaust gas treatment process or from a semi dry process
b) Fly ash resulting from a wet exhaust gas treatment process with or without rejection of liquid effluents and condensation process.

The bottom ash and fly ash streams are classified and managed differently due to the significant differences in their physical, chemical and leaching characteristics.

The subsequent transformation and vaporization of the volatile metals depends on the incineration environment. As heavy metals can be introduced into an incinerator without separation, some metals may be adsorbed by incombustible materials and left in bottom ash. Other metals may escape with flue gas, when passing through its dewpoint to form nuclei, or they may condense around existing particles, which can be removed by an air pollution control device as fly ash. As a result, both bottom ash and fly ash could be toxic.

The concentration of the various trace elements varies between the different types of residues whereas the major elements are nearly the same for all residues. For example several of the more volatile trace elements such as Cd, Pb, Hg, are enriched in fly ash [25].

The major elements of fly ash and bottom ash are Si, Al, Fe, Ca, Na, K and Mg and these elements are present as oxides [24]. In addition to the major elements, certain fly ashes constitute toxic heavy metals such as As, Pb, Sb, Sn, Sr and trace amounts of organic pollutants polychlordibenzo- dixines and furans [8]. The quantities may be considerable and occur mostly as water-soluble chlorides, fluorides and sulfur compounds [26].

A comparison of heavy metal concentrations of different paper-mill sludge with municipal sewage sludge is given in table 2.2.

Table 2.2. Concentration of heavy metals in different sludges in mg/kg [12].

Sludge Type	Pb	Cd	Cr	Cu	Ni	Hg	Zn
Sewage Sludge A (Germany)	137	1.7	165	460	60	1.2	1510
Sewage Sludge B (NL)	400	8	60	440	30	1	2200
Paper Sludge A (Germany)	18	1.2	27.7	30.8	24.5	0.4	137
Paper Sludge B (Germany	9.7	0.0	4.7	22	0.1	0.0	-
6 different Swedish Pulp and Paper Sludges	7-22	0.2-6	9-66	16-59	5-15	<0.04 -0.3	210-522
Range for Deinking Sludges	0-900	0-8	0-300	7-900	0-90	0-2	0-1400

The residues also differ substantially from each other in terms of water solubility. Only a small fraction, often less than 1% of the total mass of the bottom ash is soluble in water, whereas 20 –25% of the total mass of the fly ash is readily soluble in water [27].

The hazardous character of a material comes from its capacity to release heavy metals into the environment. The main route via which heavy metals enter the environment is water. Therefore the water solubility of residues and the potential leaching and release of components are important properties in relation to disposal/land filling of the residues [4].

Because of increasingly stringent environmental regulations, the incinerator ash residues are regarded as hazardous in most countries and they must be deposited in special landfills equipped with careful control of effluents. This is a costly and environmentally unsatisfactory solution. Therefore, new technological options for the decontamination of incinerator ashes must be developed with the objective of rendering a product that can be reused with no environmental risk [7].

2.3. Refuse Utilization

These environmental concerns and economic realities provide an incentive to develop new solid waste management technologies. Most attractive are those that have the potential to produce a saleable product.

Several new technologies for recycling high volume waste have been proposed. With a continuously operating processing system installed at the waste source, these technologies reduce handling, eliminate downstream liabilities, and reduce disposal costs [28]. The reuse of materials or products avoids the generation of waste.

Although recycling has had a positive effect on public attitudes towards generating waste and has been successful in diverting a fraction of a waste stream from ultimate disposal, its impact has been limited [28]. Many recycling schemes have had difficulty sustaining themselves due to widely fluctuating markets for waste materials. Moreover, the push to recycle higher percentages of the waste stream has resulted in problems with maintaining the quality of the recycled waste materials and hence the sustainability of subsequent secondary product manufacturing.

The growing production of ashes as a by-product of incineration has long caused an environmental problem with technological and economic effects in the worldwide context. Also, the increase in regulatory environmental laws demands not only major security controls over industrial waste ashes (by making them inert) but also the reuse of these wastes in other products, i.e., recycling and reutilizing. This leads to usage of incinerator residues as a raw material to make new products.

The incinerator residues have been utilized in brick and ceramic tile fabrication, lightweight aggregate, road pavements, fillers in plastics and paints, mineral wool and metal recovery by pre-treating and making them inert and inoffensive materials [5].

For example, pulp and paper incinerator ash have been used as follows [29]:

- a) Production of light weight aggregate
- b) Production of granules to carry agricultural chemicals
- c) Pelletization of sludge and non recyclable paper for use as fuel
- d) Production of ethanol from sludge
- e) Use of sludge in cement kiln feed stock
- f) Use of sludge as a hydraulic barrier material in land capping systems.

However these technologies face problems with cost and quality and wide attention is now being paid for some alternative technologies [29]. There are four generic treatment technologies, which have been used or are under consideration for recycling and reutilizing incinerator residues [30]. These include:

- a) Cement Solidification
- b) Chemical treatment
- c) Stabilizing treatment by acid and other solvent
- d) Melting and vitrification

Full–scale experience also suggests that the viability of alternative management strategies primarily depend upon four factors [29]:

a) Technical feasibility
b) Cost
c) Available markets
d) Potential liability

The relative significance of these factors varies depending on mill type, location, and waste type and company business strategy.

2.4. Melting and Vitrification

Melting of ash is one of the intermediate steps for waste processing and is attracting serious attention. The reason for the melting of ash can be grouped largely into two categories as follows [31]:

a. Reduction of incineration ash can be achieved; and
b. Toxic materials can be enclosed.

Vitrification is cost-effective and can produce an extremely durable glass form, which can isolate contaminants from the environment. Waste glass has been shown to be so stable that some vitrified wastes can be made into consumer products such as ceramic tile, building materials, or insulation. Benefits of the application of glass technology to the disposal of wastes include [32]:

- Well-characterized waste form stability
- Extremely low release rates in environmental conditions
- No combustible or pyrophoric properties

- Retention of essential release properties even if disturbed or mechanically damaged during storage or disposal
- Low generation of potentially respirable particles
- Ability to accept high loading of heavy metals
- Ability to accommodate fluctuating waste types with negligible effect on release properties
- Ability to combust limited amounts of organics
- Volume reduction, reducing disposal costs
- Total destruction of asbestos
- Scale of facility adaptable to accommodate a wide range of disposal needs

While vitrification capital cost may be somewhat higher than conventional waste solidification techniques, such as cementation, the expense is more than offset by the savings from volume reduction and reduced monitoring which are inherent in the more durable waste form [32].

Figure 2.1 shows a typical vitrification plant of municipal solid waste [4]. This process is based on maximum integration of the vitrification unit within the incineration facility. The ash and additives are continuously loaded into the furnace. By controlling the length of time the waste stays in this bath of melting products, it is possible to ensure that no elements remain unmelted and to guarantee a perfectly homogeneous end product. After passing through a settling area, the liquid product flows out through an opening towards a cooling and conditioning unit that adapts the end product according to its final use.

Since the treatment of the residues will necessarily involve high costs, the optimal results must be in obtaining recycling products of high quality for industrial applications. On the basis of these premises, the principle approach is the production of glass ceramics [33].

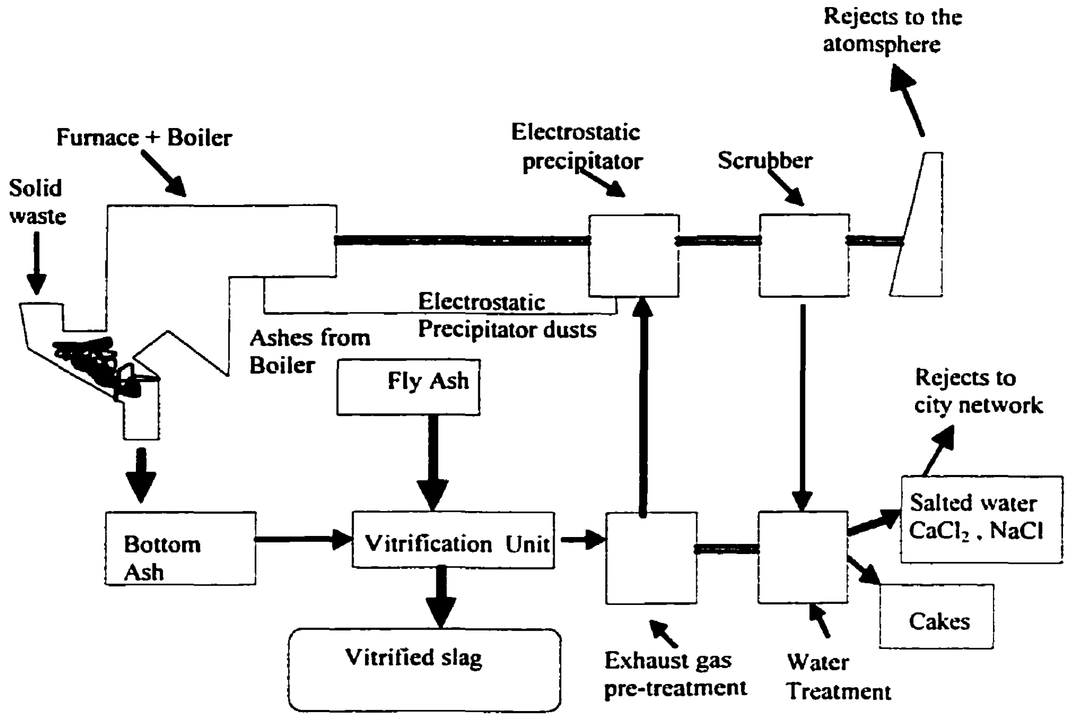

Figure 2.1. Vitrification process [4]

This inert vitreous product can be used as a raw material for making high quality products such as glass ceramics [8]. The possibility of fabricating glass ceramic materials from vitrified incinerator residues and the improvement of properties such as strength, hardness, and machinability allow them to find application in constructing diverse machine-tool pieces, and as refractory materials. Therefore vitrification can be a technically and economically acceptable process for the formation of a usable product and the reduction of the polluting properties of ashes.

2.4.1. Glass

Most mineral elements and compounds produce low viscosity liquids when sufficiently heated and crystallize quickly as the temperature falls. However, some substances produce highly viscous liquids above their melting temperatures and maintain the disordered structure of liquids as they solidify. Thus they are said to be in a vitreous or amorphous state [4]. Therefore, glass can be regarded essentially as a super-cooled liquid which, because of its very high viscosity at ambient temperatures, may be considered to be a solid. From a thermodynamic point of view these glasses would preferentially exist in crystalline form but the viscosity of the glass is too high under normal conditions of use to permit the required structural rearrangements to take place that would develop the crystalline derivative. As well, if the silica content is high enough the crystalline form is not preferential. However at high temperatures, the picture can be different and ionic movement and structural reorganization may take place [11].

Commercially available glasses, such as soda-lime-silica window and container glasses and chemically resistant borosilicate glasses, depend for their very existence on the fact that they can be brought rapidly, on cooling following shaping, through the temperature ranges at which crystallization occurs [11].

2.4.2 Glass Formation

When glass is processed by cooling from a melt, the phase transformation from liquid to solid occurs at a glass transition temperature (T_g) that lies below the melting temperature T_m at which crystallization would otherwise takes place. Referring to figure 2.2, above T_m one has a liquid; between T_m and T_g there exists a super-cooled liquid. At T_g the change in slope shows a transition to a glassy state where structural rearrangements are no longer able to takes place on a reasonable time scale [34].

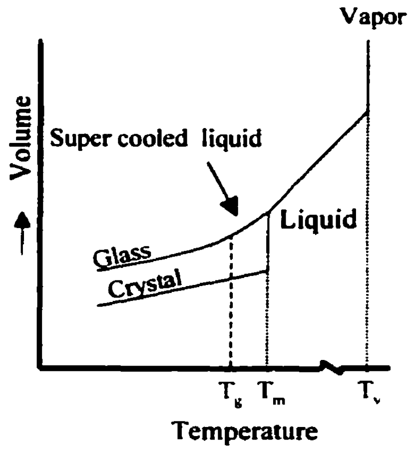

Figure 2.2.Volume – temperature relations for liquid, crystal, and glass phases [34]

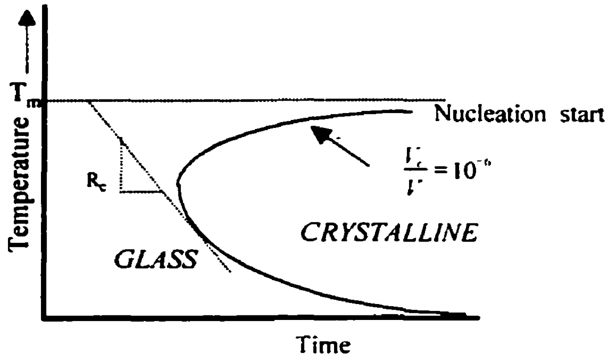

Figure 2.3.Schematic time-temperature transformation (TTT) diagram [34]

It is also clear from figure 2.3, that, when liquids cooled faster than a critical rate R_c, they avoid the crystalline transformation and form a glass. This critical rate is given by [18].

$$R_c = \frac{T_m - T_n}{t_n} \qquad (2.1)$$

Where T_m is the melting point and T_n and t_n are lower than the temperature and the time of the nose.

The formation of a glass can be obtained for a variety of different substances: elements in Group V or VI of the periodic table (Si, P), BeFe, $ZnCl_2$, some metallic alloys (Pd-Si, Cu-Zr) and pure oxides (mainly silica).

2.4.3 Oxide Glasses

Almost all the types of glass industrially produced come from oxides. Depending on their characteristics, pure oxides are more or less easily vitrified. To form an oxide glass Zachariasen enumerated the following structural rules, which are analogous to Pauling's rules for crystalline structures, for determining which compounds will form continuous random network oxide glasses [34]. Zachariasen's rules state:

1. Each oxygen atom is linked to no more than two cations
2. The number of oxygen atoms surrounding the cation must be small, four or less
3. The oxygen polyhedra share corners rather than edges or faces
4. At least three corners of each oxygen polyhedra are shared.

The oxides used in commercial glass production can be categorized into:

a) Network forming oxides

Oxides, which form glassy structure when melted and cooled, and vitrify are called network-forming oxides because of their ability to buildup continuous three-dimensional random networks. Examples are SiO_2, B_2O_3, and P_2O_5.

Glasses made solely from network formers often have limited utility. As examples shown in figure 2.4, pure B_2O_3 glass is not water resistant and pure SiO_2 glass, while valued for its chemical durability, high application temperature and thermal shock resistance, must be processed above 1750° C. Therefore to alter processing and properties, oxide modifiers and intermediates are used [19].

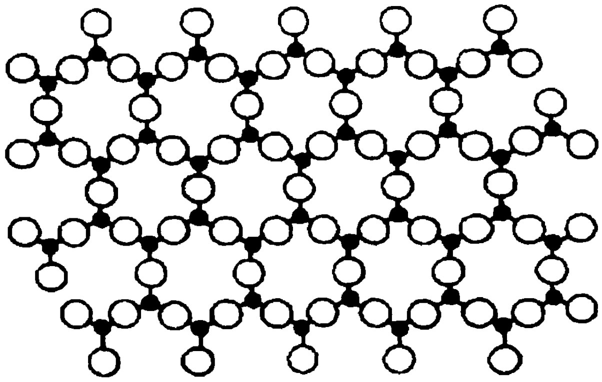

Figure 2.4. Two–dimensional schematic representation of the structure of a hypothetical crystalline compound A_2O_3 [35].

b) Modifying oxides

Modifying oxides do not form glass by themselves but, when used in certain proportions, enable the modification of the manufacturing conditions or properties of the resulting glass. This may include reducing the viscosity of the glass, increasing the thermal expansion coefficient, or lowering the melting point. Examples of modifiers are Na_2O, K_2O, and Li_2O as shown in figure 2.5 [4].

While alkaline oxides are very effective modifiers, the result is glasses that are not chemically durable. The chemical durability is greatly improved with the additional modifier CaO. Therefore oxides such as PbO, MgO, ZnO and BaO may also act as modifying oxides and prevent deterioration of the finished product.

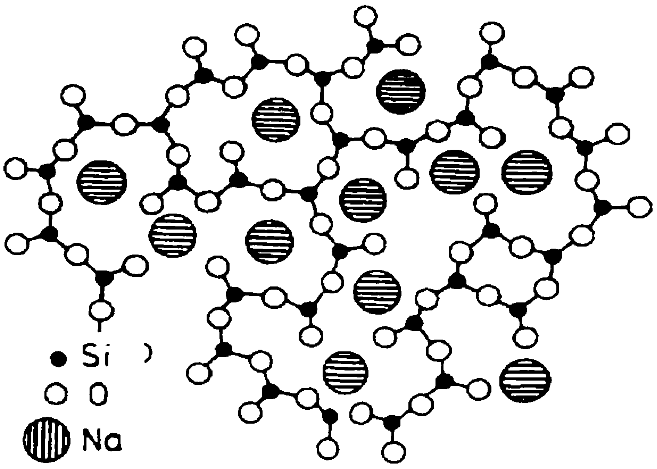

Figure 2.5. Schematic representation of the structure of a sodium silicate glass [34]

c) Intermediate oxides

Although not usually capable of forming a glass, these oxides can be incorporated into the glass network. Examples are Al_2O_3, BeO, TiO_2, and ZrO_2 shown in figure 2.6.

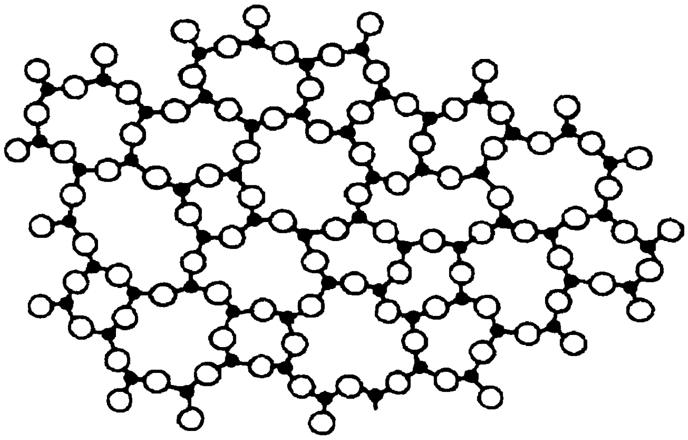

Figure 2.6. Continuous random network model of an A_2B_3 glass [34].

The following table 2.3 gives the percentages by weight of oxides in the common commercial types of glass and some special types [4]. Secondary components are always used in small proportions and are used to change the color (transition metal oxides) or manufacturing conditions (arsenic and antimony oxides) [4].

Table 2.3. The percentage by weight of oxides in common commercial types of glass and in some special types [4].

	SiO_2	B_2O_3	Al_2O_3	Na_2O	K_2O	CaO	BaO	MgO	PbO	Fe_2O_3
Sheet glass	72.5		1.5	13	0.3	9.3		3		0.1
Bottle glass	73		1	15		10				0.05
Light bulb	73		1	16	0.6	5.2		3.6		
"Pyrex"	80.6	12.6	2.2	4.2		0.1		0.05		0.05
Glass fiber	54.6	8.0	14.8	0.3	0.3	17.4		4.5		
Crystal	55.5				11.0				33	
Optical Glass	28			1.0	1				70	
Na lamp glass		36	27				27	10		
Radiation prot.glass	29						9		62	

2.4.4. Ash Glass

After magnetic removal of iron metals, the waste (municipal, building and industrial waste) is usually burned in a waste incineration plant at temperatures between 800° and 1000°C to reduce the waste and organic content. The resulting solid residuals were slag and fly ash [36].

Whatever way the ash is burned, it turns out that the ultimate waste contains two components [4]:

a) Vitrifiable compounds such as alkaline and alkaline earth oxides, silica, alumina (35-60 %)
b) Non-vitrifiable compounds such as salts (chloride, sulfate, carbonates), 25 – 50 %, heavy metals (1-5%), unburned substances and water (5 – 15 %).

Table 2.4 shows the chemical composition of paper sludge. The water content of the paper sludge is 75.4% on average. After drying, the dried portion of sludge was then burned at 700°C; the average total weight loss then amounts to 70%. In other words, the non-flammable materials in the dried sludge are only 30% and the reminder is flammable fibers.

Table 2.4. Chemical composition of paper sludge [15].

Composition (%)	Sample 1	Sample 2	Average
Moisture content	73.07	77.73	75.40
Loss of ignition	69.96	70.26	70.11
SiO_2	38.60	37.38	37.99
Al_2O_3	51.52	51.92	51.72
Fe_2O_3	2.91	3.17	3.04
CaO	4.38	5.80	5.09
MgO	3.27	2.93	3.10

Figure 2.7 shows the main composition areas of the fly ash as produced in incinerators in the ternary system CaO-Al_2O_3-SiO_2 (CAS) [9]. These ashes consist mainly of SiO_2, Al_2O_3, ($FeO + Fe_2O_3$) and CaO, MgO, SO_4^{2-}, X_2O (alkalis), TiO_2 and minor elements

such as MnO_2, SrO, BaO, V_2O_5, P_2O_5, Ga_2O_3, As_2O_3, GeO_2, MoO_3, Li_2O, NiO, PbO, and ZnO; however, it is reasonable to approximate their compositions using the CAS system.

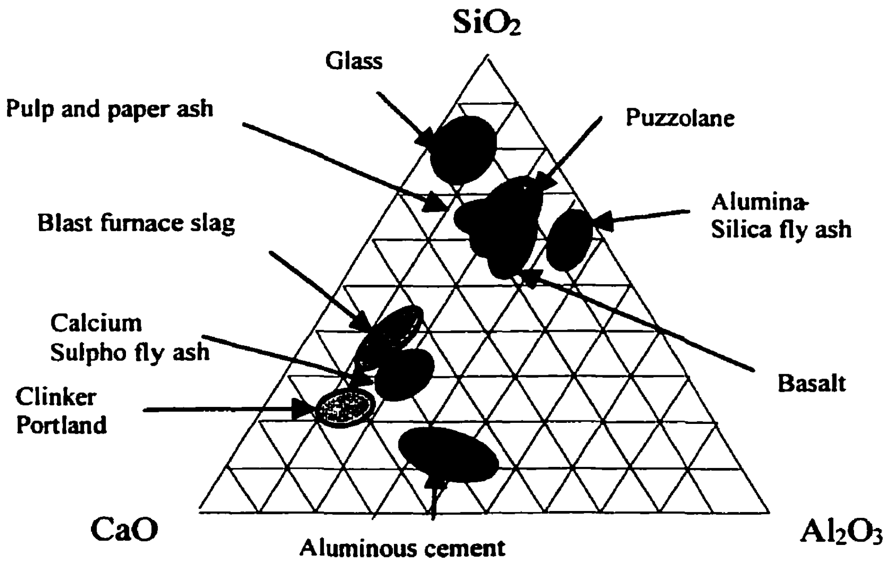

Figure 2.7. The main composition areas of incinerator fly ash as depicted in the ternary system $CaO-Al_2O_3-SiO_2$ [8].

The proportions of silica and alumina in ash represent its glass forming potential. These are the elements which will constitute the vitreous matrix of the glassy end product. A certain amount of forming oxides will be necessary to ensure the formation of glass. A minimum of oxide modifiers is also necessary; lime for durability, sodium and potassium to lower the melting point: in general ash contains enough of these. It is important that the quantities of these oxides should not exceed certain limits, in order to avoid negative effects on the life span of the glass end product [4]. For example container and window glasses have O/Si ratio of 2.3 –2.4 , but in glazes and enamels it varies from 2.25 to 2.75 [34]. After melting, most of the glass forming and modifying oxides are to be found in the vitrified end- product.

The proportions of sulfates and chlorides found in ash vary according to the type of exhaust gas treatment. The salts in ash are not miscible at high temperatures and remain outside the liquid mass. This purifies the glass and ensures its future stability. The small quantity of chemically-bound crystalline water (up to 5%) promotes the formation of silicates. The alkaline silicates that are formed are very hygroscopic and the ash humidity is bound up in hydrates, which makes the liquid more fluid [4].

Finally the quantities of heavy metals usually found in ash are so low that they neither prevent glass formation nor harm its life span.

2.5. Devitrification

Although the transparency and uniform color of many glass objects suggest a uniform material, many glasses contain a microstructure that is inhomogeneous at levels varying from a few nanometers to a few microns [34]. Commercially produced glasses contain microscopic defects due to incomplete mixing, undissolved impurities or gas bubbles. Table 2.5 shows the strength of glass compared to other materials.

Table 2.5. Strength of a glass compared to other materials [4]

Material	Strength $MN.m^{-2}$
Diamond	1800
Graphite	15
Tungsten	3000
Iron	2000
Magnesia	100
Sodium chloride	10
Silica glass	50

The fragility of glass doesn't really result from its composition but rather from its amorphous structure. An effective way of strengthening glass products is to give them a semi crystalline structure by controlled heat treatment process and/or adding nucleating agent. Such materials are called glass-ceramic materials [4].

2.5.1. Glass Ceramics

Glass ceramics are derived from the controlled crystallization of glasses to give a material consisting of one or more crystal phases and some residual glass depending on the starting composition and the heat treatment given [37]. During the crystallization process, molecular rearrangements occur to produce the appropriate crystalline phases. These phases are sometimes themselves metastable polymorphs, which under further heat treatment, can transform to the thermodynamically more stable crystal phases [38].

The established compositions and uses of glass ceramics are extensive and include the low thermal expansion, high thermal shock resistance and chemically durable Li_2O-Al_2O_3-SiO_2 compositions based on β-quartz or β-spodumene solid solution used in both transparent and opaque cookware, cooker range tops, heat-resistant windows and telescope mirror blanks. Other notable glass ceramics are the photomachineable lithium silicates, high strength alumino silicates, mechanically machineable mica based materials and a variety of compositions with hardness and wear resistance, resistance to chemical attack and oxidation, and superior optical and electrical properties [10].

2.5.2. Nucleation and Crystallization

Control of the nucleation and crystallization stages is the most critical aspect in the glass ceramic process. In addition to other structural factors, the devitrification of a glass depends on thermodynamic and kinetic behavior, which will determine the most adequate thermal cycle to obtain the final glass ceramic material.

Figure 2.8 illustrates rates of homogeneous nucleation and crystallization in a glass. For any given bulk glass, the tendency and ability to crystallize can be expressed in terms of the nucleation and crystal growth curves. Below the equilibrium melting temperature there exists a temperature interval, referred to as the metastable zone, in which nuclei do not form at a detectable rate but crystals can grow if nuclei of a sufficient size are provided by heterogeneous nucleation.

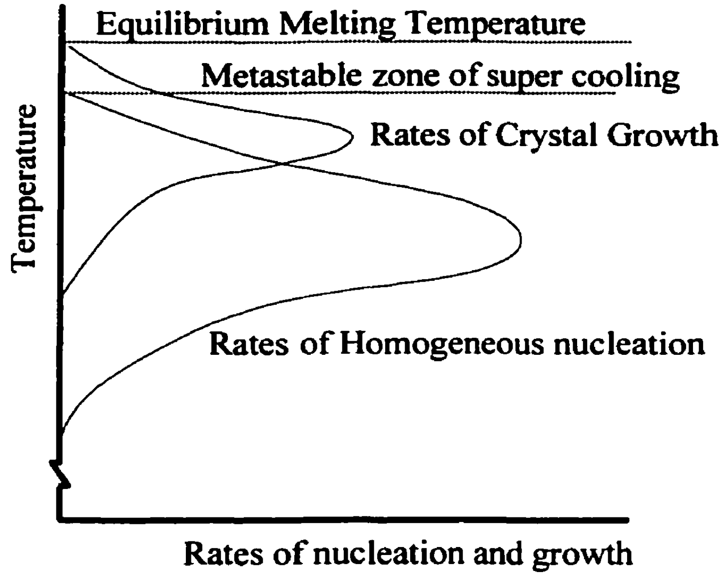

Figure. 2.8. Rates of homogeneous nucleation and crystallization in a viscous liquid [11].

At temperatures below the metastable region the crystallization process is governed by the rate of formation of nuclei and the rate of crystal growth. As the temperature falls, the nucleation and crystallization rates increase and the increasing viscosity of the glass hinders the atomic rearrangements and diffusion processes necessary for nucleation and crystal growth. Generally, the nucleation and crystallization curves overlap to some extent and this permits crystal growth to start when a large number of nuclei are present, thus enabling the desired fine crystal structure to be obtained [11].

The preparation of a satisfactory glass ceramic depends on crystallizing the glass composition under strictly controlled conditions to provide the desired closely interlocking, microcrystalline structure and smooth surface, free from cracks. In order to achieve this, it is usually necessary to include a nucleating agent in the glass that will provide the heterogeneous nuclei for subsequent crystal growth, or influence the structural reorganization in the glass in such a manner that many crystals of the desired types grow in the glass.

Table 2.6 gives some of the nucleating agents that have been used in glass ceramic processes [11]. Photosensitive metals generally required an irradiation step with ultraviolet light before functioning satisfactorily as nucleating agents [11]. Oxide nucleants are preferred to other potential nucleating agents and in some cases a combination of these oxide nucleants have been shown to give better results than individual nucleants used in the same total proportion.

Table 2.6. Examples of nucleating agents used in glass ceramics [11].

Photosensitive metals	Au, Ag, Cu
Single nucleating agents	Pt, F P_2O_5, TiO_2, ZrO_2
Variable valency oxides	MoO_3, Fe_2O_3
Complex nucleants	$P_2O_5 + TiO_2$, $P_2O_5 + ZrO_2$ $P_2O_5 + MoO_3$, $P_2O_5 + WO_3$ $TiO_2 + ZrO_2$, $P_2O_5 + TiO_2 + ZrO_2$,

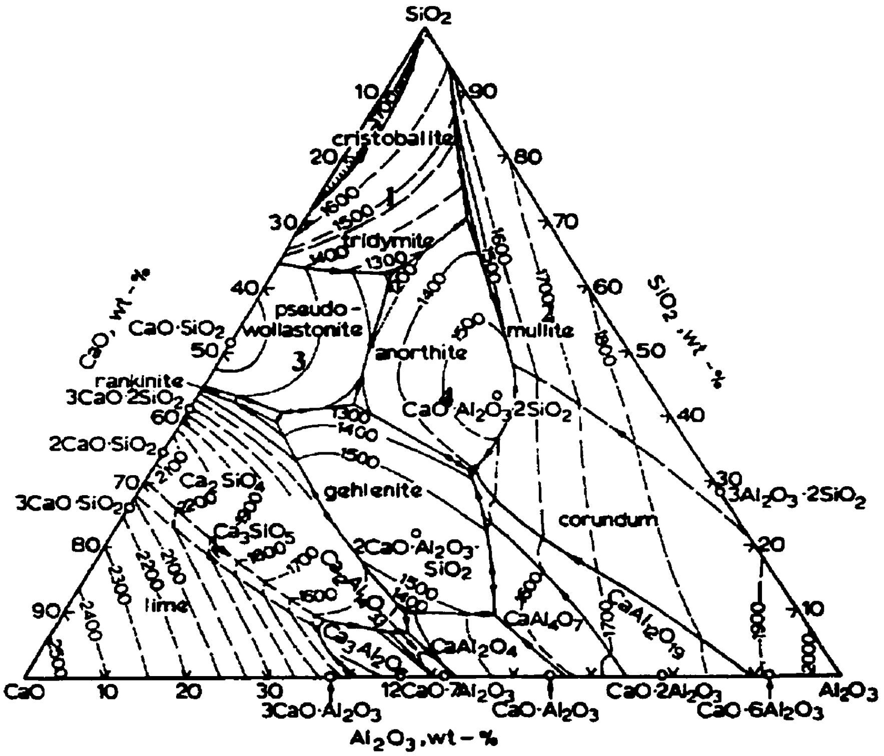

Figure 2.9. Ternary diagram of CaO-Al_2O_3-SiO_2 [39]

Figure 2.9 shows the compositions from which glass-ceramics can be made. With reference to the figure;

(a) composition 1 was obtained by using ZnS as a nucleating agent,
(b) composition 2 was with 11 % TiO_2,
(c) for composition 3, Cr_2O_3 proved a better nucleating agent than either CaF_2, Fe_2O_3 or TiO_2 and
(d) composition 4 was obtained by using MgO as a nucleating agent [39].

2.5.3. Glass Ceramic Process

The preparation of a glass ceramic involves a number of steps. First the mixture of raw materials that will form the desired composition is melted in a suitable container at a temperature generally in the range 1000 – 1700°C (depending on the composition)[11].

After refining and homogenization to provide a quality glass, the molten glass is worked by the usual methods employed in the glass industry, for example, casting, pressing, drawing or chilling to form glass frit that can be subsequently be reduced to the glass powder.

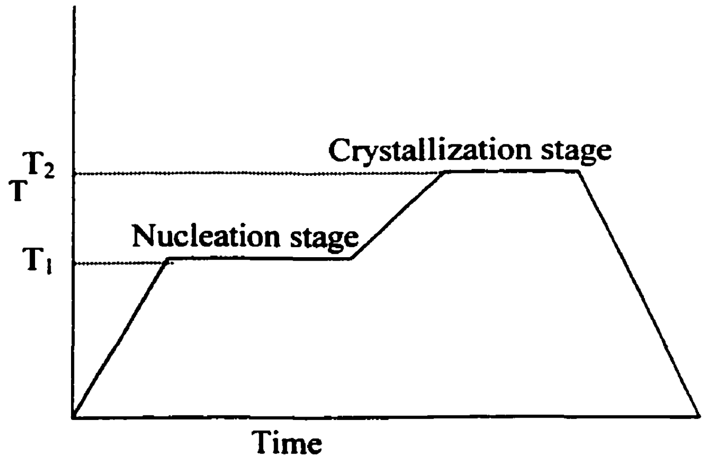

Figure 2.10. Schematic two stage heat treatment schedule for the production of glass ceramics from glasses.

Then the formed glass is subjected to a controlled heat treatment, as shown in Figure 2.10, which converts the glass to glass-ceramic. In the first stage, the object is reheated at a rate of 2 –5 ° C min^{-1} from ambient up to the nucleation temperature, T_1 and maintained for a given time. The optimum nucleation temperature, generally corresponding to a viscosity in the range $10^{11} - 10^{12}$ dPa s, is determined experimentally. At the end of the nucleation stage, the temperature is further increased at a rate less than 5 ° C min^{-1} to the optimum growth temperature T_2. This temperature is selected for the maximum development of the crystalline phase without deformation of the material by viscous flow. It is generally 25 – 50 ° C below the re-solution temperature of the crystalline phase. After holding at this temperature for the required time, the crystallized object can be rapidly cooled to ambient temperature without the need for a further annealing treatment. The periods during which the temperature is maintained for nucleation and crystallization are selected according to the chemical composition and depend on the properties required of the final product.

The heat treatment process is designed so that the microstructure of the resultant material is one in which one or more crystal phases exist together with a residual glassy phase. In any given part of a glass forming system, one crystal phase is likely to predominate on conversion to a glass ceramic. The phases that are produced are influenced not only by the major constituents in the composition of the materials, but also minor constituents in the composition of the material can also have a profound effect.

Typical examples of the principal crystal phases that develop in a number of glass ceramic forming systems are given in table 2.7. Phase composition may also be affected by the heat treatment given to the glass, particularly for glasses of high silica contents [11].

Table 2.7. Examples of crystal phases developed in glass ceramics [11]

Glass-ceramic system	Crystal phases
Li_2O-Al_2O_3-SiO_2 (low Al_2O_3)	Quartz Cristobalite Lithium disilicate Lithium metasilicate
Li_2O-Al_2O_3-SiO_2 (high Al_2O_3)	Beta spodumene Beta eucryptite
Li_2O-MgO-SiO_2	Quartz Cristobalite Lithium disilicate Lithium metasilicate Enstatitc Forsterite
MgO-Al_2O_3-SiO_2	Quartz Cristobalite Enstatitc Forsterite Cordierite
ZnO-Al_2O_3-SiO_2	Quartz Cristobalite Willemite Gahnite

2.5.4. Properties of Glass Ceramics

Glass ceramic materials can be considered as a non-porous matter consisting of fine crystals uniformly distributed throughout a residual glass phase. As glass ceramic materials contain arbitrarily oriented crystals, their properties are independent of direction. The extremely fine and uniform crystal structure, even distribution throughout the bulk of the material, and the absence of pores are important characteristics in the structure of glass ceramic materials [38].

The properties of glass ceramic materials depend primarily on the physico-chemical properties of the main crystalline phase and the size of the crystal, residual glass, the amount and morphology of glass phase present in the total bulk material and the interface formed between the crystalline and glass phase [37]. A review of some of the more important properties follows.

a) Density

Although the density of a glass ceramic material is an additive function of the densities of the crystalline and the glass phase present, it is determined by the main crystalline phase. The densities of parent glass and glass ceramic material are often different, and a volume change usually occurs during heat treatment. Oxides such as BaO, PbO, which tend to confer high densities upon glasses, also result in glass ceramics with high densities. Similarly glass ceramics having lithia as a major constituent have low densities. It is also found that the increase of the proportions of MgO, CaO, ZnO, BaO, or PbO at the expenses of Al_2O_3 or SiO_2 in glass ceramics leads to higher densities.

b) Mechanical Properties

Glass ceramics are brittle at room temperature and behave as an elastic material up to the strain that produces fracture. Mechanical properties such as strength, elasticity, hardness and abrasion resistance are influenced by particle size and volume fraction of the crystalline phase, interfacial bond strength, and differences in elastic modulus and differences in thermal expansions. Increased strength over the parent glass is a result of fine grain and uniform microstructure.

As a general rule, the strength of a glass ceramic is high compared with ordinary glass and with other types of ceramics. The Young's modulus and the bending strength of glass ceramic materials can be compared with other materials. This is shown in tables 2.8 and 2.9 [38].

Table 2.8. Young's modulus of glass ceramic materials compared with other materials [38].

Material	Young's modulus (Mpa. 10^{-4})	Material	Young's modulus (MPa. 10^{-4})
Glass-ceramic	8-14	Steatite low-loss ceramics	7.0
Fused quartz	7.4	Electroporcelain	6.7
Sodium-calcium glass	7.0	Sintered MgO	21.0
Boro-silicate glass	6.6	Marble	2.7 – 8.2
Ceramics (high Al_2O_3)	28-35	Granite	4.2 – 6.0
Sintered Al_2O_3	37.4		

Table 2.9. Bending strength of glass ceramics compared with other materials [38]

Material	Bending strength (MPa)
Glass	55 – 70
Glass ceramics	70 – 350
Glass ceramics with modified surface	Up to 1400
Electroporcelain (glazed)	86 – 140
Ceramics (high Al_3O_3)	212 – 353
Cast iron	140 – 320 [1]
Steel	300 – 1400 [1]

[1] tensile strength

The strength of glass ceramic materials varies widely depending upon the glass ceramic system and also on the heat treatment cycle employed. It is clear from Table 2.10, that glass ceramics containing MgO have greater strength, as the main crystalline phase is cordierite [38].

Table 2.10. Bending strength of various glass ceramic systems [38].

Glass-ceramic system (Nucleating agent)	Main crystalline phase	Bending strength (MPa)
$SiO_2 – Li_2O$ (Ag, Cu, Au)	$SiO_2.Li_2O$,	80 – 150
$SiO_2 – Al_2O_3$ - Li_2O (TiO_2, ZrO_2) $SiO_2 – Al_2O_3$ - Li_2O (TiO_2, ZrO_2)	β-spodumene s.s β- quartz s.s	110-180 60-110
$SiO_2 – Al_2O_3$ –MgO (TiO_2)	Cordierite	150-300
$SiO_2 – Al_2O_3$ –CaO (fluorides) $SiO_2 – Al_2O_3$ –CaO (sulphides)	Wollastonite Anorthite	70-130
$SiO_2 – Al_2O_3$ –ZnO (TiO_2) $SiO_2 – Al_2O_3$ –ZnO (ZrO_2, SnO_2)	Gahnite β-quartz s.s	70-130 60-110
SiO_2–Al_2O_3-MgO-K_2O-F (interphase between the two phases)	Fluorophlogopite	80-105

c) Thermal Properties

The dimensional changes which occur with change of temperature are of great importance from a number of points of view. For example, if a glass ceramic is required to have high thermal shock resistance, the coefficient of thermal expansion should be as low as possible to minimize strains resulting from temperature gradients with in the material. The coefficient of thermal expansion of glass ceramic materials can be very different from that of the original glass. It depends on the type of crystalline phase and the amount of crystals present in the glass ceramic substances; this can be very sensitively controlled by using a suitable heat treatment process.

Glass ceramic materials are very strong and exhibit good resistance to thermal shock. A combination of high strength and low coefficient of thermal expansion and modulus of elasticity yields a glass ceramic material with high resistance to thermal shock.

The thermal conductivity of glass ceramic materials is an important value when they are to be employed as heat conductors or as insulators. Glass ceramics have higher thermal conductivity values than glass but lower than ceramics made of pure oxides.

d) Electrical Properties

Glass ceramics have high resistivities and some can be used as insulators. The electrical conductance of glass and ceramics is dependent on the presence of mobile species, primarily alkali metal ions, and increases with increasing content of these ions [38]. Glass crystallization, incorporating alkali metal ions into the crystalline phase, decreases the electrical conductance. The electrical resistivities also decrease with increasing temperature but can be increased by having non-alkali glass ceramic materials based on SiO_2-Al_2O_3-ZnO with the additions of B_2O_3, BaO and CaO [38].

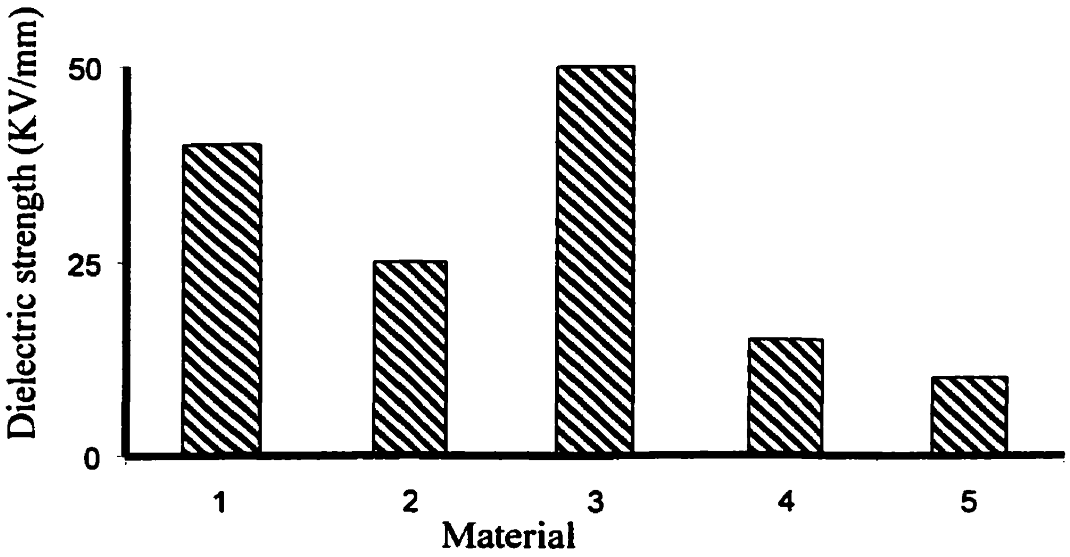

Figure 2.11. Dielectric strength of materials:

1- glass, 2- ceramics, 3- glass ceramics, 4- acrylates, 5 - nylon [38]

Glass ceramics have high dielectric breakdown strength compared with other materials as shown in figure 2.11. The dielectric breakdown strength becomes important when the glass-ceramic material is to be used at a high voltage gradient, for example high voltage insulators or condensers. Two of the factors affecting this value are the very homogeneous, free grain structure and non-porous nature of these substances [37].

In contrast to sintered ceramics, separation of micro-crystals of titanates, niobates or zirconates in the glass phase yields a pore-free material that has a controlled grain size. The ferroelectric properties of these crystals permit electrical control of double refraction or scattering, useful in telecommunications for light switches or for spectral filters. If the glass phase contains the oxides of the transition metals or rare earths, then the system can contain crystalline phases of magnetic ferrites, garnets or magnetoplumbites and the glass ceramic material can be used in high frequency technology, provided it has a high electrical resistance [38].

e) Chemical Properties

Most glass ceramic materials exhibit sufficiently high chemical resistance. The chemical stability and the durability of glass ceramics is affected by the composition of the crystalline phase and also by the composition and amount of residual glass phase and its morphology. When a glass-ceramic is chemically attacked, the initial effect is upon the glass phase present. This occurs because the early stages of attack involve ion exchange between hydrogen and mobile cations in the glass. Subsequently the silica network structure can be attacked by a process of hydration. The greater mobility of alkaline metal ions in the glass phase as compared with that of similar ions incorporated in crystal phases will lead to greater reactivity of the glass phase and inferior resistance to chemical attack [37]. Therefore, the achievement of higher chemical durability in glass ceramics requires the volume of residual glass phase to be small and also that the chemical composition of the phase favors good stability.

The chemical composition of the residual phase is affected by the heat treatment process and also by the initial glass composition. A silica-rich glass phase containing in addition

Al_2O_3 and ZnO together with alkaline earth oxides will favor the attainment of good chemical durability.

f) Optical Properties

The most important optical property is radiation transmission. Although some glass ceramic materials are translucent or transparent or transmit infrared radiation. Most of the materials are opaque. The passage of light is affected primarily by the crystal size and if the crystals are smaller than the wavelength of visible light, then the glass ceramic material is transparent. Further, the factors affecting the passage of light are the optical anisotropy and difference in refractive index between the glass and crystalline phases [38].

Transparent glass ceramic materials with high permittivity show good electro-optical properties and when an electric field is applied, they rotate the plane of polarization of the beam of plane- polarized light transmitted through them.

2.5.5. Types of Glass Ceramics

According to the nature of the raw materials used in the manufacture of glass-ceramics, these can be classified as [40]:

1) Technical glass-ceramics

Glass ceramics for domestic or technical use are made from pure materials. They are generally white and grouped according to the major components like Li, Mg, B, Ba. In order to vary the final properties of these products, TiO_2 or P_2O_5 is used as a nucleating agent.

2) Glass-ceramics for architectural or industrial uses of the petrurgical type

Raw materials used for making this type of glass ceramics are obtained from rocks, minerals and mixture of both. They can be produced also by sinter nucleation and crystallization.

3) Glass ceramics from waste incinerator residues

A great deal of work has been carried out in various parts of the world to investigate the preparation of glass ceramics from waste products such as blast furnace slags and power station fly ash. Much of the work on this type of material has been carried out in Eastern Europe although there has been a significant amount of work in the UK on blast furnace slags.

2.5.6. Glass Ceramics from Waste Incinerator Ashes

To date, glass ceramics are produced using waste materials such as coal ash, iron and steel slags, radioactive wastes, municipal incinerator wastes, sewage sludge and goethite industrial wastes. None of the reports addressed production of glass ceramics using pulp and paper incinerator residues

Table 2.11. The ash composition for different paper-mill sludge [14]

Type of Ash	SiO_2	Al_2O_3	CaO	MgO	Fe_2O_3	P_2O_5
Paper mill sludge (UK)	41.95	24.15	24.85	6.7	0.9	0.2
Paper mill sludge(Germany)	37	23	35	2.2	-	-
Paper mill sludge and sewage (Germany)	51.9	2.5	23	0.47	0.58	1.0

Table 2.11 shows the ash composition for different paper-mill sludge [14]. The major chemical components of ashes are SiO_2, and Al_2O_3. However in this case the CaO content is higher than for the original sludge, because limestone, $CaCO_3$ is added into the co-generation energy recovery system to absorb SO_x contained in the exhaust gas.

It is clear that sludge compositions are suitable to make glass and glass ceramics. Furthermore for common compositions of glass-ceramic systems, the SiO_2 and Al_2O_3

contents along with their ratio are especially important as this determines the melting temperature. In addition, the presence of Fe_2O_3 can reduce the melting temperature of the system and the alkaline earth oxides such as CaO and MgO influence glass forming behavior and the nucleation and crystal growth mechanisms of the derived glass. Finally, the type of glass ceramics manufactured from slags, red muds, and ashes from a combination of solid residues may have applications in the construction industry.

CHAPTER III

OBJECTIVES

The purpose of this work was to investigate the feasibility of making glass ceramics from pulp and paper incinerator residues. Two types of ash were investigated;

a). Fly ash
b). Bottom Ash

The ashes were characterized for the suitability for vitrification and devitrification. The vitrified and devitrified products were characterized for their physical properties.

CHAPTER IV

EXPERIMENTAL METHODOLOGY

4.1. Characterization Techniques

4.1.1. Starting Material

All the experiments were performed using fly ash and bottom ash supplied by a Canadian pulp and paper company. Table 4.1 shows the elemental analysis of these ashes as reported by the supplier.

The appearance of fly ash was found to be much darker in color and finer than bottom ash, which contained very coarse particles and wood particles.

From the supplier's specification it is clear that the major chemical components are SiO_2, Al_2O_3, CaO. The chemical composition of ash is typical of the most common glassy ternary system. Significant amounts of oxides of Mg, Mn, Mg, Na, K, P are also present, which can be to used as nucleating agents for nucleation and crystallization.

General Information

Table 4.1. Solid analysis of fly ash and bottom ash of a Canadian pulp and paper company collected on August 26, 1998.

	Fly Ash	Grate Ash
% Solids	68.98	64.23
Elements (mg/kg)		
Si	240,000	150,000
Al	10,000	52,000
Ca	43,000	66,000
Fe	16,000	12,000
Mg	10,000	6800
Mn	1400	2000
K	3700	7800
P	7400	3100
B	72	70
Na	12000	2900
S	2100	4300
Heavy Metals (mg/kg)		
As	<	13
Cd	0.3	8.9
Cr	28	31
Cu	33	330
Pb	14	99
Mo	6	7.0
Hg	0.35	<
Ni	30	22
Se	<	<
Zn	940	1500

"<" – Less than Method Detection Limit (MDL)

These ashes were characterized by means of moisture content, loss on ignition (LOI), thermogravimatric analysis, particle size analysis (sieve), chemical analysis (XRF), microstructural features by SEM and optical microscope, mineralogical analysis by XRD, EDS & EPMA in order to study the vitrification and devirtification effect.

4.1.2. Moisture content

The moisture contents of fly ash and bottom ash were determined according to ASTM C 311-94 a. A 20 g as-received sample was dried to a constant weight in an oven at 105 – 110 ° C. The percentage of moisture content was calculated to the nearest 0.1 % by following equation.

$$\text{Moisture content, \%} = (A/B) \times 100 \text{-----------------------} \quad (4.1)$$

Where A=weight loss during drying

B= Weight as-received

4.1.3. Loss On Ignition

Loss on ignition of these ashes were determined in accordance with the procedures outlined in test methods ASTM C 114, except that the material remaining from the determination of moisture content shall be ignited to constant weight in an uncovered porcelain crucible at 1000 ° C. The percentage of loss on ignition was calculated to the nearest 0.1 as follows.

$$\text{Loss On Ignition, \%} = (A/B) \times 100 \text{--------------------------} \quad (4.2)$$

Where A= weight loss between 110 °C –1000 °C

B= Weight of moisture free sample used.

4.1.4. Thermogravimetric Analysis (TGA)

In order to study the behavior of fly ash and bottom ash when heated, a Thermogravimetric Analyzer (TGA) was used (figure 4.1). This instrument allows for precise control of heating rate, maximum temperature and sample atmosphere as well as giving the possibility to monitor the weight of a sample throughout a run.

The TGA consists of a furnace and an electronic recording balance. It is linked to a computer, which acts as an interface between the instrument and the user. Prior to a run, the user programs the heat profile, the furnace atmosphere and other operating parameters. The Data Acquisition System (DAS) allows the user to control operating parameters during a run and to collect the data.

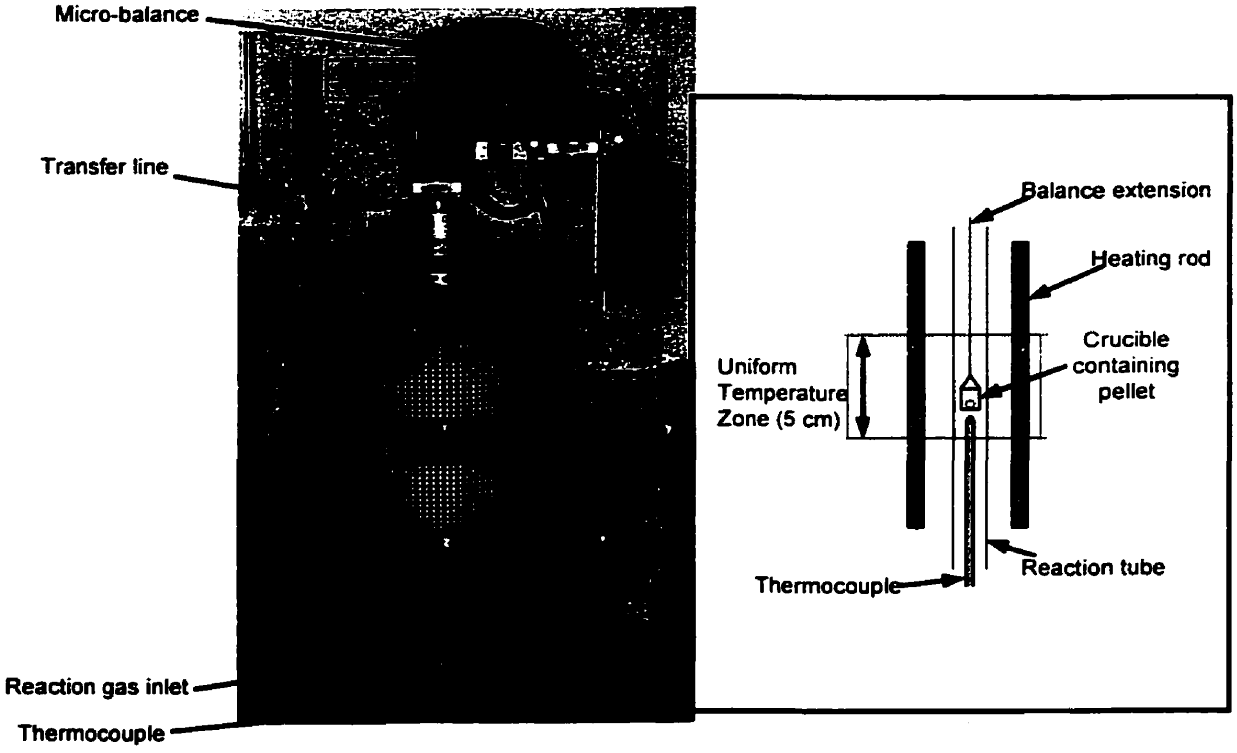

Figure 4.1: Thermogravimetric furnace

The model utilized in this study was a Cahn TG-171, which has a maximum operating temperature of 1700°C. The balance has a sensitivity of 1 μg, a 100 g weight maximum and a 10 g dynamic weight range.

The furnace consists of a cylindrical ceramic reactor tube surrounded by silicon carbide heating elements. Due to the inflow of reaction gases by the bottom and of purge gases from the balance by the top, the temperature within the furnace was not uniform. However, at a suitable distance from the ends of the reactor tube, there was a certain part of the furnace, which was at uniform temperature. This zone, approximately 50 mm in height, was called the Uniform Temperature Zone (UTZ). It was important to ensure that the sample and the thermocouple are both placed within the UTZ.

1 g and 0.5 g of bottom ash and fly ash were placed in an alumina crucible respectively. A platinum wire was attached to the crucible to form a bucket. The bucket was then hooked to a sapphire rod, which was connected to an electronic balance. A thermocouple, placed approximately 1 cm below the crucible, enables the software to monitor the temperature. A B-type thermocouple, which can be used up to 1700°C, was used in this study. The atmosphere of the furnace was controlled by reaction gases, which enter by the bottom of the reactor and flow upwards and around the sample.

The time evolved, weight and temperature profiles, collected by the DAS, provide information on the temperature ranges at which reactions take place and on their extent and speed.

Here the heating rate was 10 ° C/min and the maximum temperature attained was 1400 ° C.

4.1.5. Particle Size Analysis

Since these samples contained agglomerates, the particles were separated by the sedimentation method. First, distilled water with 1% sodium silicate was added to the ashes and stirred gently for 2 minutes and allowed to settled. Then the uncleared water was drained off. The same procedure repeated until clarified water was obtained. Finally two drops of 0.1 % $MgCl_2$ was added to the solution in order to settle all the suspending particles. After 24 h the clear water was drained off and the settled particles were dried in an oven to remove the moisture. These dried particles were then subjected to a sieve analysis.

Sieving is the most widely used technique for sizes down to 44 μm. A set of sieves often followed a √2 progression of sizes. Agglomeration becomes a problem below about 44 μm and can introduce error in the analysis.

Sieving is the classification of particles in terms of their ability or inability to pass through an aperture of controlled size. Particles are introduced onto a stack of sieves with successively finer apertures below, and the particles agitated until blocked by an aperture smaller than the particle size. For an equal weight of sample, the number of particles increases as $(\text{size})^{-3}$, and apertures of the finer sieves become blocked ("blined") if the sample size is too large and the sieving mechanism is inefficient.

In the present work a weighed amount of these ashes were placed in a set of screens with the screen size of 850, 600, 425, 300, 212,150, 106, 75,53,45, 38μm and sieving was done for 15 minutes. Then the ash in each screen was carefully removed and the weight was determined to the second decimal place.

4.1.6. Chemical analysis

Chemical compositions of these ashes were determined by X-ray florescence spectroscopy. Fluorescence spectroscopy has been used widely as an analytical tool in variety of chemical and biomedical investigations as it presents many advantages, being rapid, sensitive, specific and non destructive.

The instrument used was a Philips PW2400 3kW automated XRF spectrometer system with a Rhodium 60 kV end window X-ray tube, five X-ray detectors, five primary beam filters, eight analyzing crystals, two fixed channels for simultaneous measurements of Na and F, and a 102 sample autochanger.

The major elements Si, Ti, Al, Fe, Mn, Mg, Ca, Na, K, P and the trace elements Ba, Ce, Co, Cr, Cu, Ni, Sc, V, Zn were analysed using 32 mm diameter fused beads prepared from a 1:5 sample: lithium tetraborate mixture. The accuracy of silica is within 0.5%. For the other major elements it is within 1%. For trace elements the accuracy is within 5%. The limiting factor for accuracy is the degree of scatter of analyses from which the values are determined.

Loss On Ignition can also be determined by XRF. Here the samples were heated to 1000° C and the loss on ignition was calculated. A minimum weight of 10 g of samples was needed to perform the analysis.

4.1.7. Microstructural Characterization

Scanning Electron Microscopy

The scanning electron microscope (SEM) is a versatile instrument capable of producing an image with high resolution. Images displayed on the CRT can result from secondary electrons or backscattered electrons captured by the detector. In this work a JEOL-JSM 840A Scanning Electron Microscope (SEM) was used. In order to prevent a negative charge build up on the specimen surface, all the SEM samples were Au-Pd coated prior to examination. Semi quantitative microchemical analyses were done using an Energy Dispersive Spectroscopy (EDS) analyzer (model Tracor 5500) attached to the SEM.

The particles present in the as-received ashes were identified according to their morphology and analyzed chemically using EDS after being separated into different fractions by hand picking. This is done by placing the sample under an optical microscope and by using a needle; the different particles were classified and separated. The different particles appeared in different color and shapes under optical microscope, which made easy the separation procedure.

Electron Probe Microanalysis

The compositional analysis was performed using electron probe microanalysis (EPMA) of as-received particles after hand picking. Vitrified and devitrified products were also examined in a CAMEBEX EPMA with a wavelength dispersive system (WDS) using an accelerating voltage of 10 kV. All the samples were mounted in epoxy resin and surfaces were ground by using 200, 400, 600,800, and 1200 μm grit silicon carbide paper. Once the surface was smooth, it was polished using alumina media to 5, 1 and 0.1 μm grit. The samples were carbon-coated using an EDWARDS E306A coating system for EPMA analysis.

The microstructural features of vitrified and devitrified specimens were studied to determine any aspects of structural changes, which might have occurred as a result of crystallization.

4.1.8. X-Ray Diffractometry

In order to make a quantitative phase analysis, X-ray diffraction was carried out on as received ashes after beneficiation, vitrified product and devitrified product to determine the crystalline phases present in each fraction of the ashes. The specimens were exposed to filtered Cu Kα radiation on a RIGAKU ROTAFLEX RU-200 B diffractormeter. The angular range between 10 to 100° was investigated with an angular velocity of 0.6 ° /min, accelerating voltage of 40 kV (± 0.1%) and a beam current of 20 mA (± 0.1%). The phases present in the samples were identified by comparing the diffraction patterns obtained with the XRD reference patterns available on the base data in the computer.

To verify the amorphous nature of the as quenched glass and to investigate the crystalline phases grown during the heat treatments, the thermally processed samples were finely ground and then analyzed. The crystalline phases present in the devitrified product were identified using JCPDS-XRD spectra data as the internal references standard.

4.1.9. Differential Thermal Analysis

Differential thermal analysis is a measurement of the temperature increase or decrease involved in a chemical or physical change or in a phase transformation in a material on heating/cooling. For thermal analysis a DTA 7 Series/ UNIX was used. This equipment has advantages including high sensitivity, automation, broad temperature range, rapid cooling, and simplicity of operation.

The DTA 7 furnace employs Pt and Pt-30% Rh windings. The furnace provides a uniform temperature environment for the sample and reference materials. This equipment can be used from ambient temperature to 1600 °C.

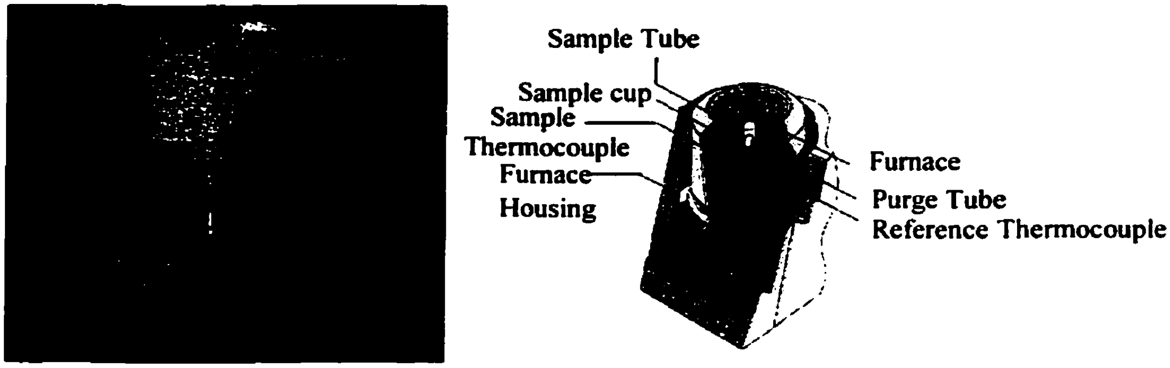

Figure 4.2. Differential Thermal Analyser

Analyses were carried out in air under one atmospheric pressure. Pt crucibles were used and α-alumina powder was used as the reference material. The samples were heated to 1400 ° C and the heating rate was 10 °/min. The glass transition temperature and melting temperatures were determined by heating as received samples after beneficiation.

In order to determine the crystallization temperature, glass powder was used and for this, ashes were heated to 1500 ° C and the melt quenched in water to obtain glass fragments. The glass fragments were well dried in an oven and hand ground using an alumina mortar and pestle. The ground powders were screened using a 200 μm sieve. The samples were stored in vacuum desiccators until used for the DTA measurements. The same procedure was repeated to measure the crystallization temperature of glasses.

4.1.10. Thermodynamic Evaluation

A thermodynamic analysis to calculate the melting point and liquid content of the ashes was carried out with the aid of a computer program named F*A*C*T (Facility for the Analysis of Chemical Thermodynamics).

F*A*C*T is a fully integrated thermochemical database program which couples proven software with self-consistent critically assessed thermodynamic data. This program is capable of performing thermodynamic calculations and supplying data and properties of various stoichiometric compounds and solutions. The analysis carried out in the present work was based on the routines EQUILIBRIUM to predict the melting temperature and the amount of liquid present at that temperature. The EQUILIB program can compute multicomponent multiphase equilibra including non-ideal alloys, slags, mattes and molten salts drawn from the F*A*C*T solution databases. Equilibrium routine determines the chemical species when specified elements or compounds react or partially react to reach a state of chemical equilibrium. The input consists of three entries:

i) The reactants,
ii) The final conditions, Temperature and Pressure, and
iii) The species selection, a list of possible product phases, such as ideal gas phase, pure solids, liquid ideal solution.

The input consists of a species, a group of species or a balanced chemical reaction. The temperature, hydrostatic pressure, phase and activity of each species may also be specified on a second line in the form of subscripts. Data is retrieved from the F*A*C*T database and a tabular display or spreadsheet is generated containing the change in the required thermodynamic properties of the system for a particular temperature or range of temperatures, which may be used directly to create a graph of a thermodynamic property (slag liquid content) as a function of temperature.

Oxide percentages determined by chemical analysis were used in this study. All ten oxides (SiO_2, Al_2O_3, TiO_2, MgO, CaO, MnO, K_2O, Na_2O, Fe_2O_3, P_2O_5) and the weight in grams were input in the database. The activity and pressure were kept as unity and the temperature versus liquid content was plotted using F*A*C*T EQULIB program for both fly ash and bottom ash.

4.2. Melting and Vitrification

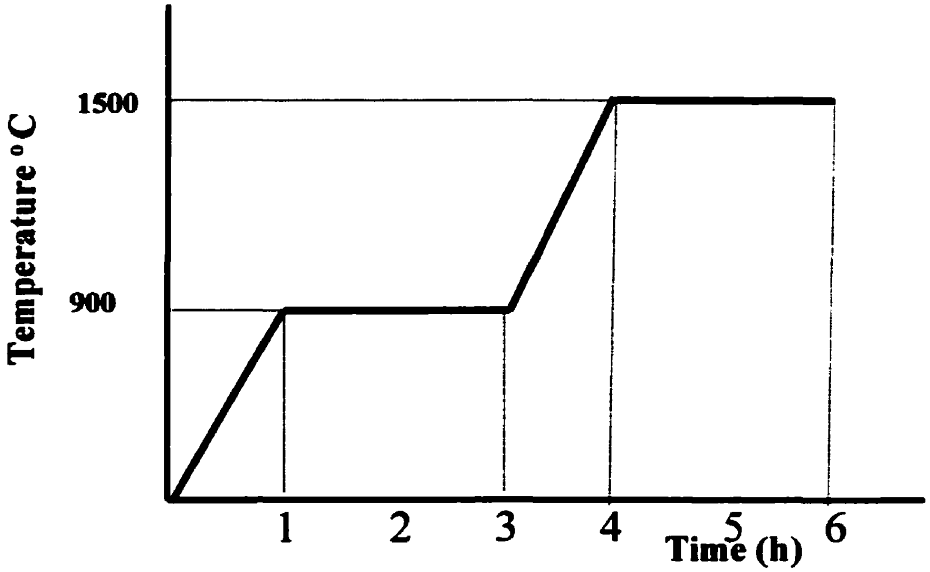

Figure 4.3. Two stage heat-treatment schedule for vitrificaation

The melting of ashes was done in two steps. As received ashes after beneficiation were placed in platinum crucibles and melted at 900 ° C using a heating rate of 10 ° C/min. For the degassing process the mixtures were held at 900 ° C for 2 h. Then the mixtures were heated to 1500 ° C. To homogenize the melt the samples were held at 1500 ° C for 2 hrs. The Pt crucible containing the glass melt was removed from the furnace and quenched in distilled water to obtain a clear glass. It was not possible to pour the glass melt from crucible due to the high viscosity and difficulty in controlling the temperature.

After quenching the glass fragments were well dried in an oven and part of the glass fragments was hand ground using an alumina mortar and pestle. The ground powders were screened using a 200 μm sieve.

The bulk glass and glass powder were subsequently used for devitrification process

4.3. Devitrification

In order to understand the crystallization effect, both bulk glass pieces and glass powder were subjected to a controlled heat treatment process. Cylindrical compressed samples were prepared with glass powder of 200 µm sieve by cold uniaxial pressing at 100 MPa.

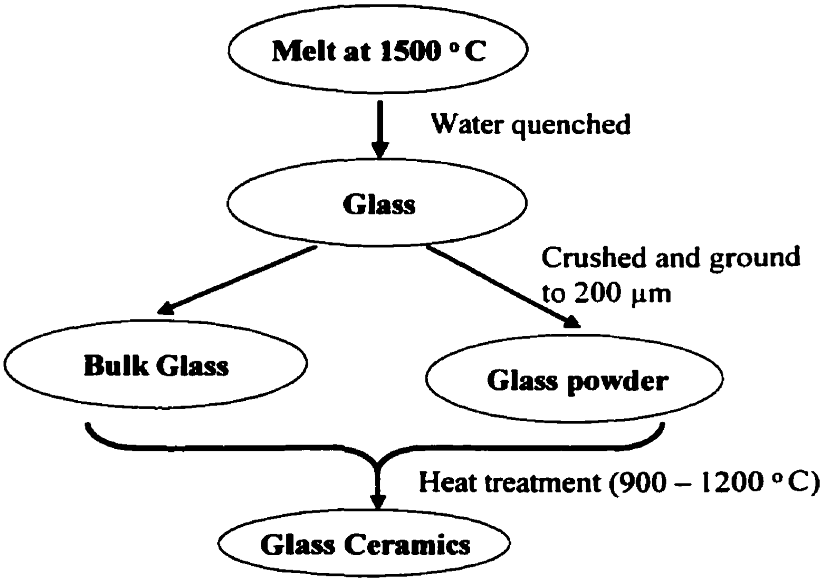

Figure 4.4. Flow chart for devitrification process

Bulk glass pieces and cylindrical samples were placed on an alumina brick and a sintering operation was performed at temperatures of 900, 1000, 1100 and 1200 ° C for 2 h at heating rate of 10 °/min using a silicon carbide Blue M furnace. The samples were subsequently cooled to room temperature. The devitrified products were characterized by X-ray diffraction, scanning electron microscopy and electron probe microanalysis.

4.4. Mechanical Testing

4.4.1. Microhardness

Hardness measurements were done on vitrified and devitrified products to assess the changes occurring in the microstructure due to heat treatment. Hardness testing procedures can be divided into two groups: macrohardness and microhardness testing. Macrohardness testing refers to testing with loads equal to or over one kilogram; microhardness testing refers to testing with loads less than or equal to 1000 g. A load of 500 g was selected and the time of indentation was fixed at 15 seconds. The microhardness tester used was a Leco, model M-400-G2. The diamond indenter used was a Vickers indenter ground in shape of a square based pyramid with an angle of 136^o between the faces. The tip of the diamond was cleaned before starting each series of test. The surface condition of the specimens was critical; thus a good metallographic finish was necessary to ensure that the tip of the indentation could be sharply focused and measured.

The surface of the specimen must be completely normal to the indenter to ensure a symmetrical indentation. For this reason, the mounted sample was placed in a universal clamp and leveling vice. At least five indentations were made per sample, and the size of the indentation was precisely measured with a microscope having a good resolving power. A microprocessor with digital read-out display automatically converted the measurements to Vickers microhardness values. For each condition an average value was calculated.

4.4.2. Fracture Toughness

Fracture toughness measurements were conducted by Vickers indentation technique [41]. Development of radial cracks around Vickers indentation in brittle materials has been long noticed. The cracks were first regarded as a nuisance to effective hardness measurements. However, it is possible to empirically correlate the fracture toughness of a material with the crack length. The advantages of such a technique are:

a) Many tests can be performed on a small sample not suitable for conventional fracture toughness tests, and
b) The ease, simplicity and short time required for testing.

The fracture mechanics analysis is based on the propagation of a half penny-like crack, which forms below the indenter. The general complexity of the elastic / plastic contact field description led to the development of semi-empirical models relating the fracture toughness, K_c, the hardness, H, the crack length, c, the indentation diagonal, a, the constraint factor, ϕ, (about 3 for Vickers indenter's), Poisson's ratio, v, the friction between the indenter and the material, u, and the plastic zone radius, R_y [41].

K_{Ic} by Vickers indentation technique

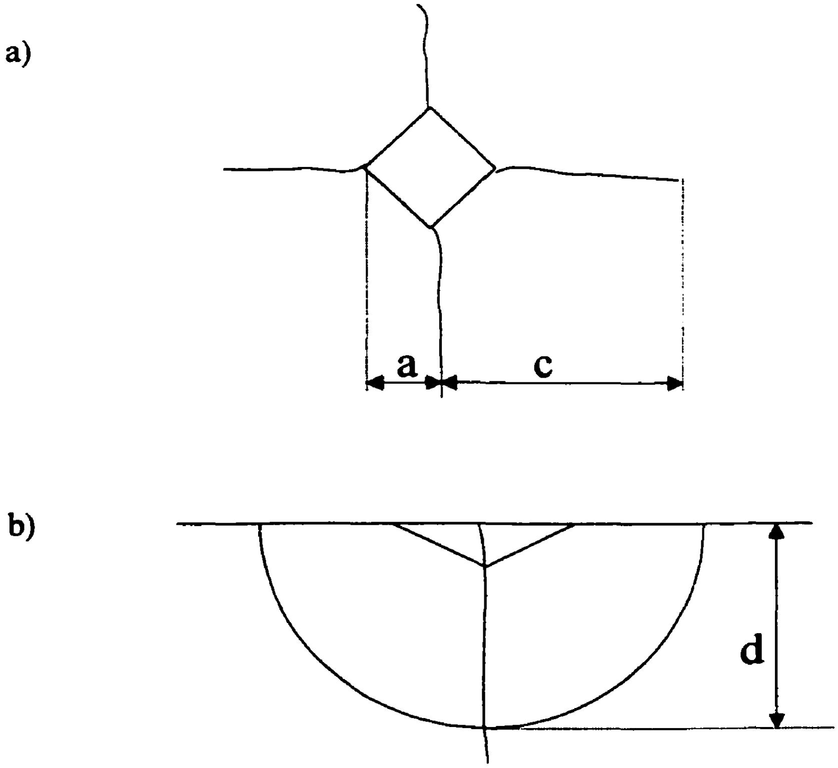

Figure 4.5. Vickers indentation technique a) crack length at the indentation corners b) half penny like crack.

Initial experimental studies indicated that the fracture toughness was strongly dependent on the ratio c/a, but was not affected by v, and u. A correction taking into account the residual stresses left by the indenter and the plastic zone had to be introduced in terms of hardness to elastic modulus ratio, H/E. The following relation was obtained [41]:

$$K_c\phi / H a^{1/2} = 0.45\,(c/a)^{-3/2}(H/\phi E)^{0.4} \text{-----------------------------} (4.3)$$

Two conditions have to be fulfilled for this technique to be valid:

a) A half penny-like crack has to be developed so that the crack length, c, is representative of the crack depth, d
b) The c/a ratio has to be greater than 2 to ensure that the crack crosses the plastic deformation zone.

Residual stresses at the surface of the specimen, i.e. due to machining or fast cooling rates, are known to seriously affect the fracture toughness measurement.

In the present study, specimens used for the fracture toughness determination were annealed glass and glass ceramics specimens obtained from heat treating bulk glass and glass powder. The samples were ground and polished to 0.05μm alumina.

CHAPTER V

RESULTS AND DISCUSSION

5.1. EXPERIMENTAL RESULTS ON CHARACTERIZATION OF RAW MATERIALS

Residues removed from the wastewater stream produced by the pulp and papermaking process is generally known as sludge. Mills produce various amounts of sludge, depending on their raw material, process and final product. Also the sludge is distinctly different in composition. The sludge differs between virgin and recycled mills; however, significant variations also exist within the same categories.

In practice, this sludge is mixed with other waste like wood, and rejects before incineration. Fly ash and bottom ash are a particular variety of waste materials from incineration that is generated by the pulp and paper industry in a very large volumes; gigascale quantities. This class of industrial by-product material, if not utilized is generally land filled as a part of daily management practices. In order to be utilized as a raw material, the physical and chemical properties of these by-products are important.

Large numbers of factors combine to increase the complexity and variability of ashes. The heterogeneity of ashes occurs as a result of

a) Variation in the ratio of wood, sludge and recycle material
b) Batch to batch changes.

Both lead to different interbedded minerals, which are differentiated largely on the basis of chemical composition and variations during formation and collection at the plant. The consequences of these variations can be examined at both micro and macro levels.

Pulp and paper mill incinerator wastes are composed of fibrous organic matter that characteristically feature:

- High moisture content, and
- High loss on ignition

5.1.1. Moisture Content and Loss On Ignition

Table 5.1. Moisture content and Loss On Ignition of fly ash and bottom ash of pulp and paper waste residue

Ash	**Fly Ash**	**Bottom Ash**
Moisture content (%)	**29.56**	**30.41**
Loss On Ignition (%)	**17.43**	**11.33**
Total volatiles	**46.99**	**41.74**

From table 5.1 the moisture contents of fly ash and bottom ash are 30% on average. After drying at 120 ° C for constant weight to remove the moisture, the dried portion of these ashes was then burned at 1000 ° C for 2 h. The average weight loss amounts to 17.4 % and 11.3% for fly ash and bottom ash respectively. Thus, the non-flammable materials in the dried ashes are only 53 % and 58 %, and the remaining portion is combustible material. Previous studies yielded different moisture contents: fly ash 39% and bottom ash 24 % [42] and loss on ignition differed from 13 -27% [43]. This is due to the heterogeneous nature of as received samples.

The ignition loss can increase the porosity and decrease the densification. Organic compounds gasify and/or oxidize to CO_2 and H_2O. In addition, inorganic compounds such as $CaCO_3$ may decompose into CO_2 at higher temperature. All these reactions involving organic and inorganic components during burning can contribute to weight loss of the material.

5.1.2. Thermogravimatric Analysis

The thermogravimatric analysis of bottom and fly ashes is given in figure 5.1. The first mass loss with TGA peak temperature of 90- 100 ° C results from evaporation of surface and crystal water, whereas the second, quite low degradation step at about 225° C results from the incineration of residual carbon. From table 5.1 we can see the loss on ignition in fly ash is higher than the loss on ignition of bottom ash. This is due to evaporation of organic materials. The result can be confirmed by this TGA graph since the slope of the curve for fly ash from 200 to 600 ° C is sharper than that for bottom ash.

The third mass loss in the region of 625- 750 ° C probably results from calcium carbonate decomposition. This is very low compared to the decomposition temperature of calcite (898 ° C), but its decomposition pressure reaches about 0.1 bar at 730 ° C. Therefore the degradation of calcite at about 750 ° C can be explained by a shift of weight during thermal treatment in an open system.

The final weight loss occurs in the range 950 -1025 ° C, a decomposition of sulphate compounds, probably calcium sulphate, can be assumed. Formation of calcium sulphate in fly ash is due to the addition of limestone, $CaCO_3$ as a neutralizing agent into the co-generation energy recovery system to absorb SO_x contained in the exhaust gas.

Weight loss due to water, carbon dioxide and sulphur dioxide could also be explained by this thermogravimatric analysis. Evaporation of heavy metals and heavy metal compounds could not be demonstrated due to the very low concentration of heavy metals in the ashes.

Evaporation of crystal and surface water and incineration of organic carbon are complete at temperatures below 600 ° C. As decomposition of calcium carbonate takes place within the temperature region of 650-950 ° C the sample was kept for 2 h at 900 ° C for degassing.

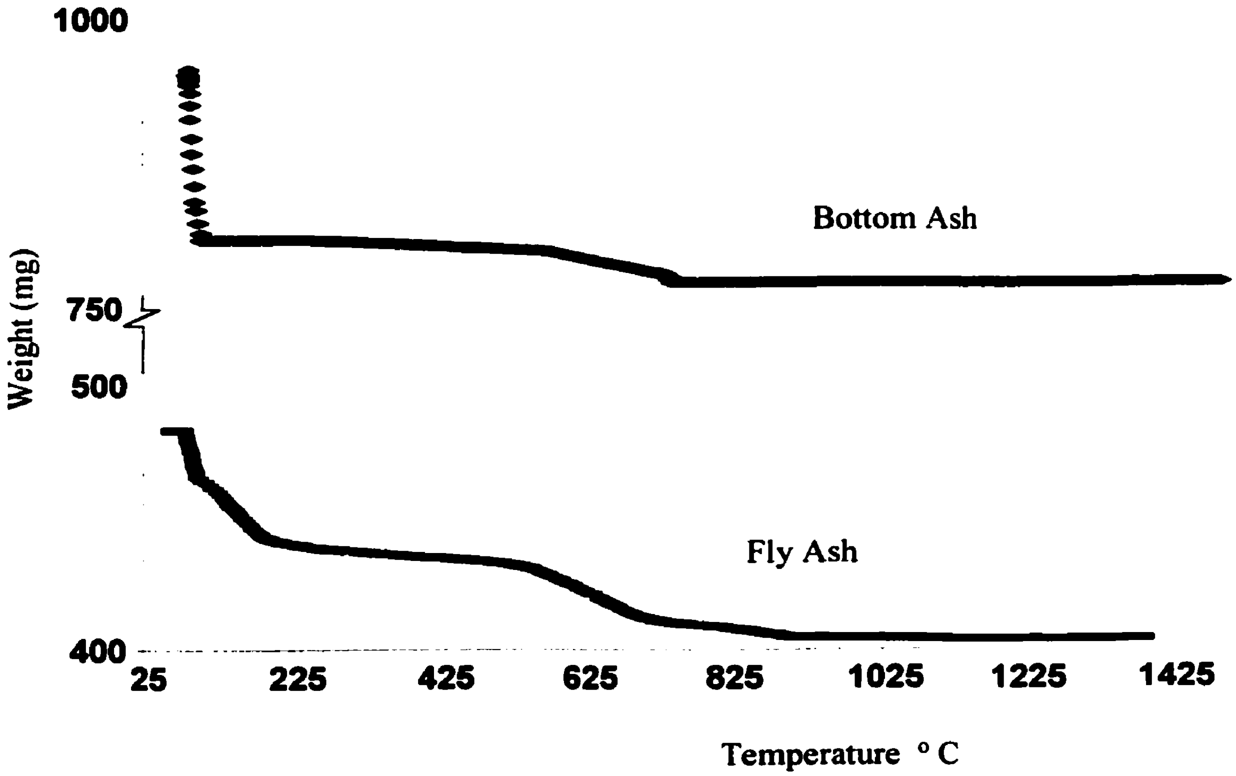

Figure 5.1. Thermogravimetric analysis of ashes

Change in color can also be observed from low temperature to high temperature. The color of the low temperature ash was grayish-black compared to a yellowish-white color of higher temperature ash. This also indicates that a temperature of at least 650 ° C may be required to achieve complete burnout of the waste residues.

5.1.3. Particle Size Analysis

Ashes from pulp and paper incineration are white yellowish to gray, containing single black mainly carbonaceous particulates. The dusts are highly hygroscopic and tend to agglomerate. Therefore the particles are first separated into single particles by the sedimentation method.

Cumulative particle mass size distributions of fly ash and bottom ash are presented in figure 5.2. The figure shows that these residues have a wide particle size range from about 1- 1200 μm. As can be seen, the bottom ash is significantly coarser than the fly ash. The mean particle size (D_{50}) of fly ash is around 180 μm, whereas the average particle size of bottom ash is around 1000 μm.

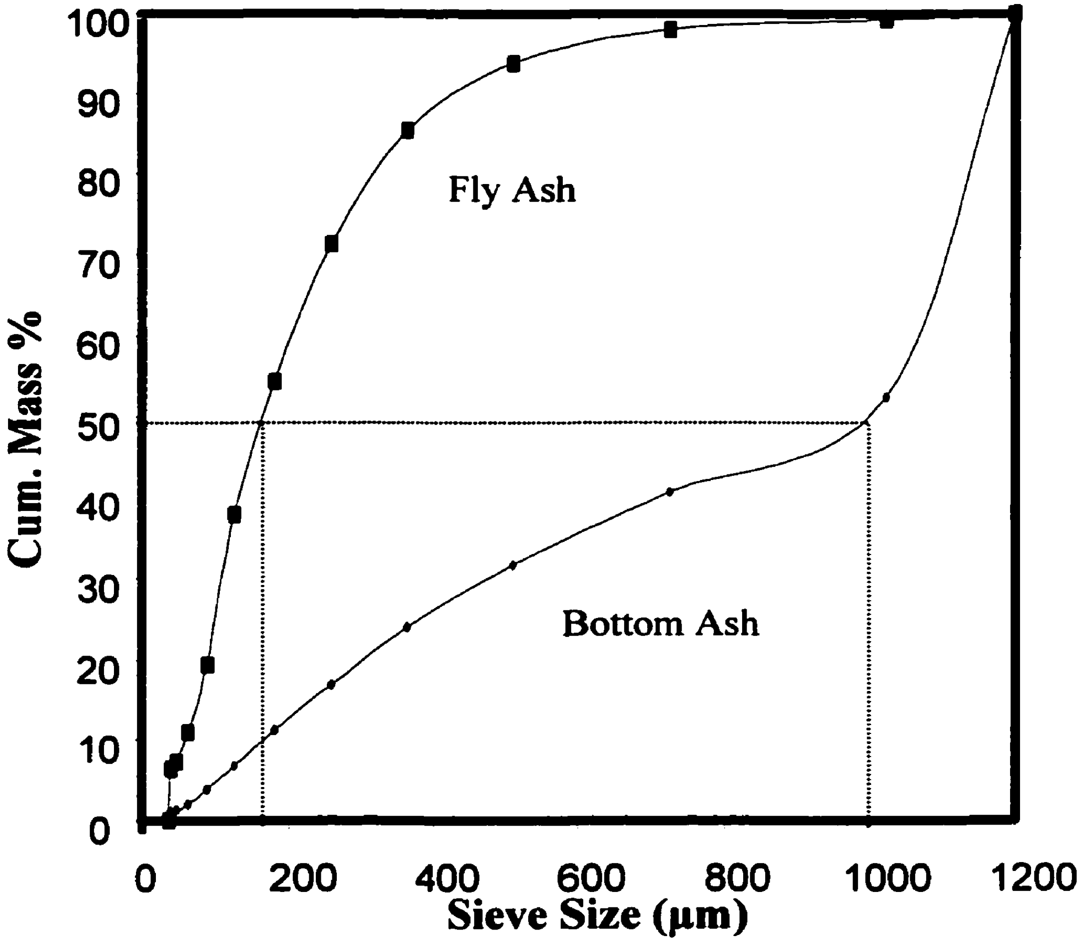

Figure 5.2 Cumulative particle size distribution of ashes.

The specific surface areas was measured by the nitrogen adsorption Micromeritics 2000 BET technique The measurements for fly ash bulk samples were 22.3 m^2g^{-1} and for bottom ash 6.6 m^2g^{-1}. From this we can conclude that fly ash is finer and has more porous particles than bottom ash.

5.1.4. Microstructural Characterization

During the combustion process, temperatures in the boiler flame may exceed 1600 ° C and are suffiently high to melt most of the inorganic material present in the waste. Although several dozen minerals are reported in ash, most occur infrequently or in trace amounts. The majority of mineralization is from aluminosilicates, carbonates and silica.

With the exception of silica, all minerals are substantially decomposed during burning; the clay minerals loses water and may melt to form glasses which dissociate on cooling into various glassy and crystalline components; the carbonates are decomposed to release CO_2 and form CaO, MgO and mixed oxide combinations. Interaction between physically associated minerals is also expected to bring about chemical reactions at elevated temperatures through which new glassy and crystalline phases are formed. Under the high temperature conditions in the boiler flame, a series of complex physio-chemical changes occurs in the particles, the most notable being their rapid conversion to a spherical form as a result of surface tension forces acting on the melt to minimize surface free energy. As the particles exit the flame in the gas stream, they rapidly move into a lower temperature regime where they are quenched into a glassy solid state. The rate of quenching will depend to a large extent on the size of the particle: large particles will quench more slowly allowing crystallization to occur in the still-molten interior. In addition, although some of the bloated particles burst as molten droplets, most are quenched in the same way as solid particles as they exit the flame and are preserved as hollow spheres with varying wall thickness. A second consequence of the presence of glasses during vitrification is their possible involvement in secondary reactions with glasses leading to either polymerization or depolymerization.

Scanning electron microscope observations, energy dispersive X-ray analysis, XRD, and EPMA have provided considerable information on the physical characteristics of ashes. The shapes of the ash particles vary depending on the mineral concerned. Most of them are irregular and angular.

The major portion of most fly ash consists of particles resulting from the cooling of molten droplets of fused materials in pulp and paper waste. Fusion of minerals such as quartz, feldspar and clay results in glassy spherical particles. Sometimes, however, large grains of quartz and feldspar do not fuse and remain intact as angular fragments.

Figures 5.3, and 5.4 show the micrographs of fly ash particles after beneficiation. Particles in this sample were extremely heterogeneous in size and shape. They are mainly formed via sintering of sludge minerals and were composed mostly of small, spherical aluminosilicate particles interspersed with larger irregular carbon particles, which appeared to be incompletely combusted.

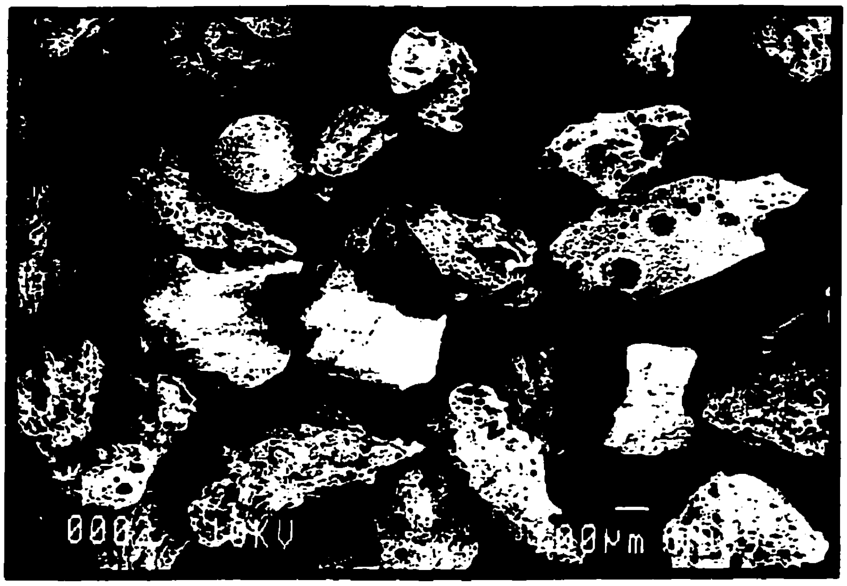

Figure 5.3 Scanning electron micrograph of fly ash after beneficiation shows spherical aluminosilicate particles.

A similar pattern has been identified in fly ashes from coal sources. The sphere formation results from the melting of mineral inclusions in coal on a non-wetting surface, namely carbon [44].

Figure 5.4 Scanning electron micrograph of fly ash after beneficiation shows larger irregular carbon particles

Their typical size of 400 -500 µm was significantly larger than that of paper additive minerals such as talc, kaolinite confirming that one agglomerate included a large number of the ash-forming particles. Some spherical particles, evidently formed via melting, were also observed. However these particles were typically below 100 µm implying that melting had occurred only in a very limited region, e.g. on the surface of burning char. Many individual spherical particles or their agglomerates were formed via vaporization and condensation. Some longer chain-type agglomerates were observed indicating that the concentration of vaporized material had locally been sufficient to allow particle coalescence and agglomerate growth to proceed further. Again the sphere formation may result from melting of mineral inclusions in ash on a non-wetting surface (carbon). The optimal temperature for ceno-sphere formation, on the basis of ash density, is reported to be 1230 °C[45]. At higher temperatures gas evaluation is too rapid and gas will escape from the molten ash; at lower temperatures, sphere formation is too slow relative to the duration of the molten state with the furnace.

The net outcome is that fly ash is typically heterogeneous as a result of the presence of a mixture of unburned carbon, and detrital minerals (such as quartz), which are flame-modified or fire-polished broken shards, and a considerable proportion of fine, spherical aluminosilicate particles.

Figure 5.5 Scanning electron micrograph of bottom ash after beneficiation

Figure 5.5 presents a scanning electron microscope of the bottom ash after beneficiation. Here two kinds of particles can observed and these are mostly mixed particles. There are silicate particles adhering to the surface, which can be melted at the temperatures of combustion inside the burning chamber. As their main constituents were glass, these were classified as glassy particles. When compared with fly ash particles, these bottom ash particles are dense and less porous. This can be confirmed from the specific surface area measurements. Both fly ash and bottom ash contain carbonaceous semi-burned particles, paper and cardboard carried practically unaltered by the gas flow.

5.1.5. Chemical Analysis

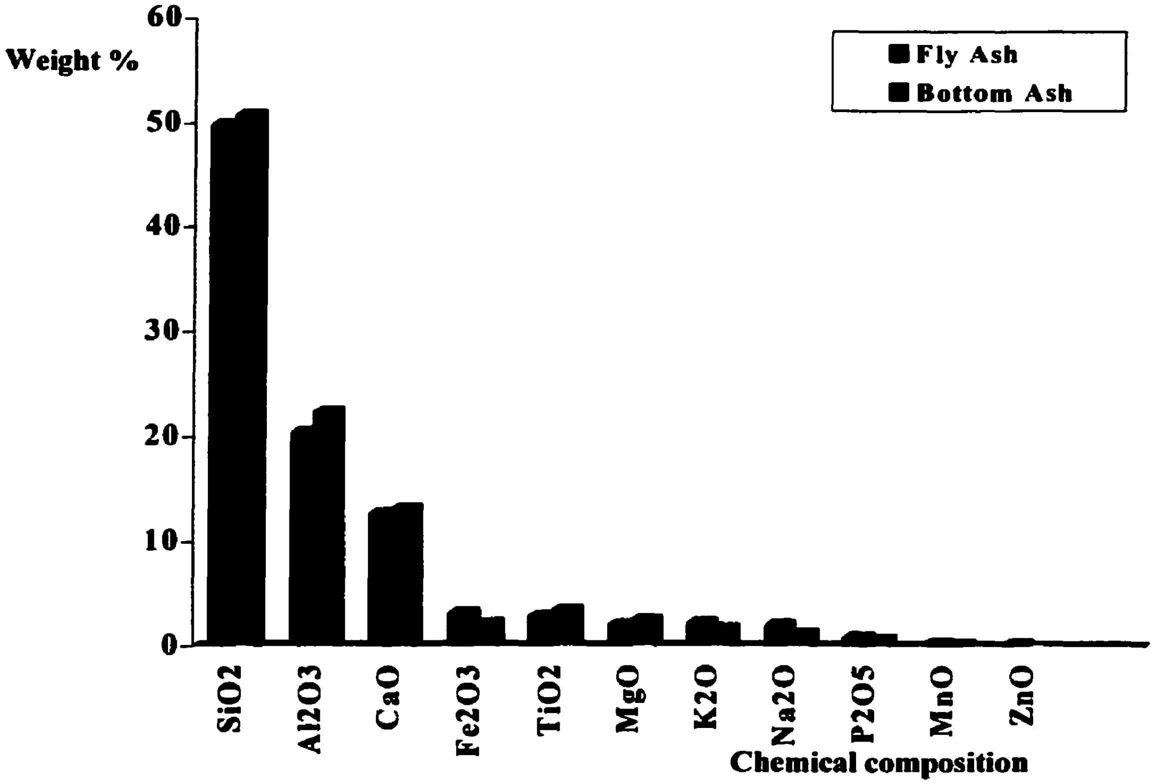

Figure 5.6 Chemical compositions of ashes

The chemical compositions of the ashes are presented in fig. 5.6. The concentrations of major elements Si, Al, Ca, Fe, Ti, Mg, Mn, K, and P in fly ash and bottom ash are similar. This similarity is not surprising because the major elements are not volatile and should partition somewhat evenly between the two ashes. In all the samples a certain amount of unburned carbon was found beside these compounds.

All the elements are calculated as oxides. Oxidized compounds of Si, Al, Ca amounts for nearly 80 % of the composition ash. Other elements such as Ti, Fe, Mg, K, N, and P are minor constituents and account for a small percentage of the bulk composition. All other elements such as Cr, Zn, Ni, Cu and Be occur in the parts per million range and collectively seldom exceed 1% of the bulk composition.

From figure 5.6 it can be seen that Al_2O_3, SiO_2, CaO are the major ash forming oxides and probably come from kaolinite and calcite minerals in the sludge. Fe_2O_3 and TiO_2 are from inks and came from de-inking sludge. Bark and waste wood ash include high concentrations of silicon and calcium and minor concentrations of aluminum, potassium and sodium. These are the major sources for K_2O, Al_2O_3 and minor sources for SiO_2 and CaO. Quartz sand was used as bed material in most incinerators. Thus, the SiO_2 content of bottom ash is higher than that of fly ash. Finally MgO and TiO_2 originate from talc, which is used as a brightening agent in paper manufacturing.

The sum of oxides plus LOI is near to 98 % in fly ash and 99 % bottom ash, the remaining could corresponds to elements such as Cl and S that cannot be determined by this method. The chemical composition of ashes is typical of the most common glassy ternary system. In is important to note that species known to be nucleating agents, such as TiO_2, P_2O_5, and Fe_2O_3, are present in reasonable amounts, which are able to act as nucleating agents for nucleation and crystallization.

5.1.6. X-Ray Diffractometry

As mentioned earlier, during the combustion process, temperatures in the incinerator may exceed 1600 ° C. This is sufficiently high to melt most of the inorganic material present in the pulp and paper waste. The majority of the minerals formed are quartz, anorthite, mullite, lime and hematite. The following figures 5.7 and 5.8 show the minerals obtained in the present work using XRD.

The X-ray pattern of as received fly ash samples after beneficiation is presented in figure 5.7. Results from XRD analysis of crystalline phases indicate that $CaCO_3$ converts to CaO and reacts with kaolinite forming calcium aluminosilicate compounds like anorthilte and albite.

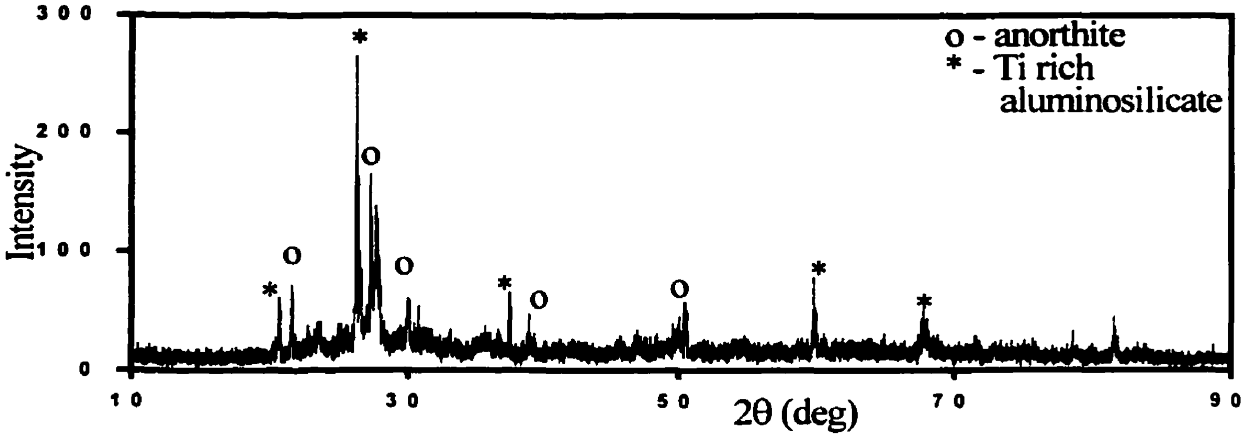

Figure 5.7. X- ray diffraction pattern of fly ash after beneficiation

Although the samples are principally composed of glassy material, several distinct peaks were observed and the following minerals were identified for fly ash: quartz, anorthite, and traces of lime.

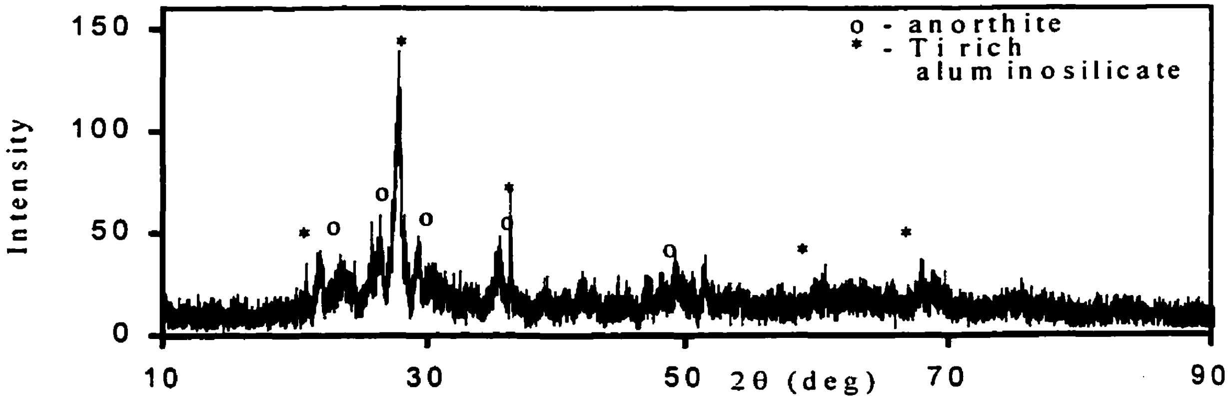

Figure 5.8. X-ray diffraction pattern of bottom ash after beneficiation.

Figure 5.8 shows the XRD pattern of bottom ash particles after benefaction. This indicates that the most abundant minerals in the crystalline phase of the beneficiated bottom ash are anorthite, quartz, titanium rich silicate, and calcite.

Microchemical characterization by EPMA was attempted to better identify the crystalline phases present in as received particles. The EPMA analysis shown in figure 5.9 suggested that the as received particles after beneficiation contain mainly two crystalline phases, anorthite and titanium rich aluminosilicate.

Figure 5.9. Micrograph of as received particle after beneficiation

Table 5.2 gives the EPMA analysis of the crystalline phases in the as received ash particle. The analyses show that the primary crystalline phase is anorthite.

Table 5.2. EPMA micro chemical analysis of as received particles

Oxides										
Na_2O	MgO	CaO	SiO_2	FeO	Al_2O_3	P_2O_5	TiO_2	K_2O	MnO	Total
0.62	0.45	19.94	43.19	0.75	33.47	0.46	0.84	0.38	0.06	100.16
0.87	0.58	19.22	44.17	0.87	32.39	0.47	0.85	0.53	0.06	100.01
0.83	0.48	19.69	43.44	0.87	33.58	0.47	0.92	0.38	0.08	100.70
0.76	0.56	19.60	43.89	0.99	32.51	0.46	0.96	0.44	0.07	100.23

It should be also noted that the individual substances are not homogeneously distributed over all particle sizes. Some heavy metals may be normally entrained from the combustion chamber as volatile chlorides and condensed on the fly ash in the colder part of the incinerator. The external surface is decisive in this context so that these substances become enriched in fine dust. On the other hand, particulate carbon is primarily entrained and gets enriched in the coarse dust [45].

A summary of minerals in bulk raw material after beneficiation as a function of particle size fraction is given in appendix.

5.1.7. Thermal Analysis

Chemical reactions or structural changes within a crystalline or glassy substance are accompanied by the evolution or absorption of energy in the form of heat. When a substance crystallizes, an exothermic effect occurs since the free energy of the regular crystal lattice is less than that of the disordered liquid state. Conversely, the melting of a crystal gives rise to an endothermic effect. Chemical reactions between two substances may also give rise to endothermic or exothermic effects. Differential thermal analysis is a technique which enables reactions or phase transformations to be studied for substances at high temperatures.

In this method the material under test, in the form of a finely divided powder, is placed in a small platinum capsule. Adjacent to the test capsule is a second capsule containing alumina which does not exhibit endothermic or exothermic effects. The two capsules are heated together at a constant rate and the differential temperature is plotted as the ordinate against the reference sample temperature. Exothermic effects are indicated as peaks on the curve obtained and endothermic effects as dips in the curve.

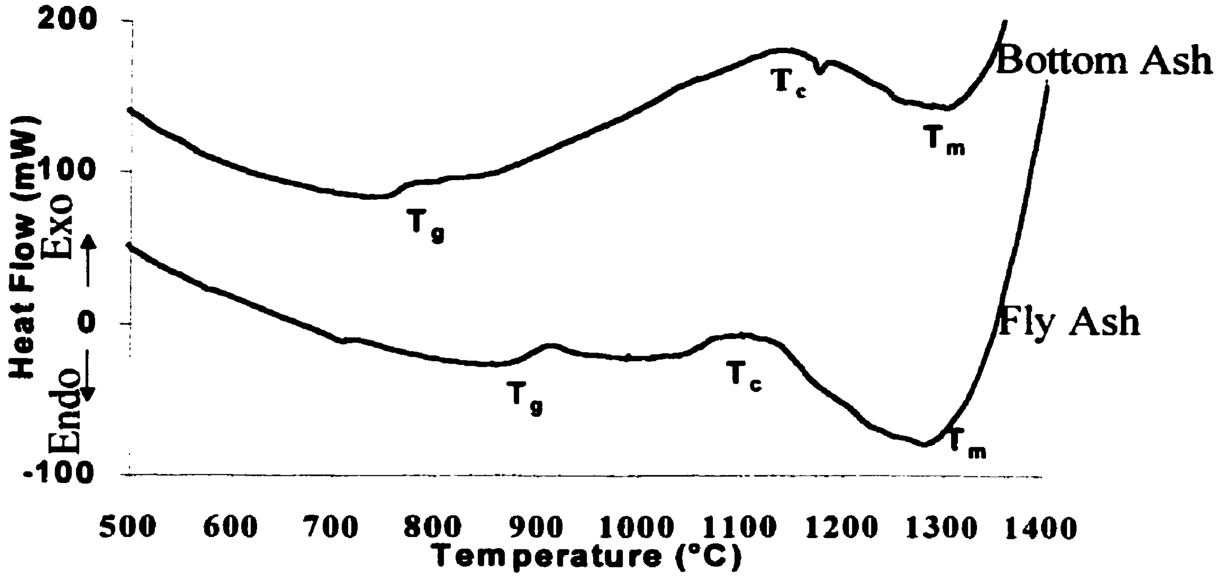

Figure 5.10. Differential thermal analysis curves for fly ash and bottom ash

The D.T.A. curve obtained for fly ash and bottom ash shows a number of features and these can be seen in figure 5.10.

The DTA curves for fly ash and bottom ash samples show a glass transition at 875 and 750 ° C. Fly ash shows two exothermic crystallization peaks whereas bottom ash shows one exothermic crystallization peak and just after that an endothermic peak, which could be due to melting of localized compounds. Finally there is an endothermic reaction indicating formation of a liquid phase for these ashes. For fly ash it is approximately 1285 ° C and for bottom ash is around 1300 ° C.

Table 5.3. Glass transition, crystallization, and melting temperatures of fly ash and bottom ash

Ash	Glass Transition Temperature (° C)	Crystallization Temperature (° C)	Melting Temperature (° C)
Fly Ash	875	1100	1285
Bottom Ash	750	1175	1300

DTA was only used to determine the melting temperatures for ashes. The temperature was determined to be 1300° C. However, when these ashes were melted at 1300° C, it was found that the ashes are actually only partially melted, and were very difficult to pour due to their high viscosity. Therefore, in order to provide a better estimate of the melting temperature and amount of liquid content for ease of pouring, the F*A*C*T program was used to estimate the melting point..

5.2. Thermodynamic Evaluation of CaO-SiO_2-Al_2O_3 System

Calculations using F*A*C*T indicate the onset of melting for fly ash is around 1325 ° C. Also, the liquid content increases with increasing temperature, and after it reaches a critical temperature the amount of liquid content becomes constant. Figure 5.11 gives the percentage of liquid slag as a function of temperature..

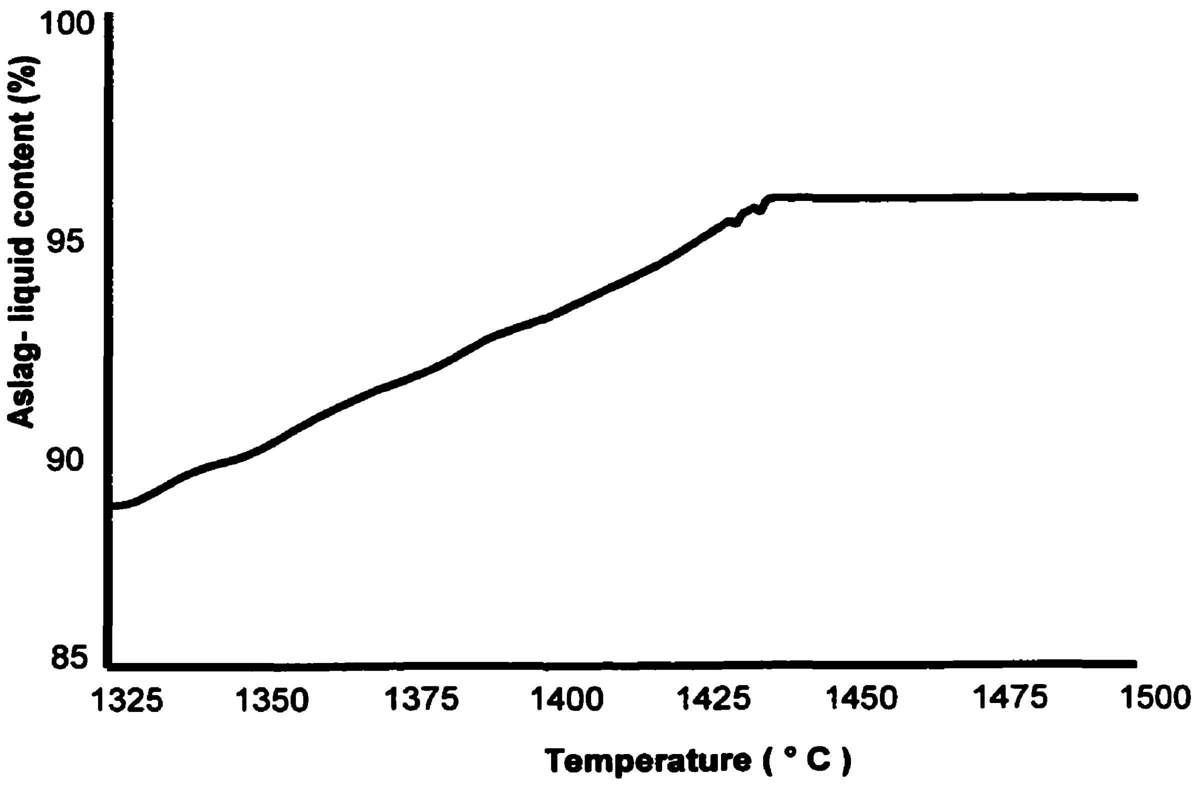

Fig. 5.11 Slag liquid content of fly ash against temperature

It was found that the maximum liquid content of 95.7 % can be obtained when fly ash heated to 1440 ° C. Unlike fly ash, the bottom ash starts to melt at 1550 ° C. The liquid content obtained at 1550 ° C is 83.27 % and it remains more or less the same up to 1700 ° C. This is because of the Al_2O_3/CaO ratio. The viscosity increases with increasing Al_2O_3/CaO ratio, reaching a maximum at the molecular ratio of Al_2O_3/CaO =1, above which the viscosity decreases. This is why the maximum liquid content was obtained at lower temperature for fly ash (1440 ° C) than compares to bottom ash (1550 ° C).

Table 5.4 Viscosity of Al_2O_3 – SiO_2 – CaO melts at temperatures of 1450 ° – 2100° C [46].

Weight %			Viscosity η 0.1 Nsm^{-2}						
CaO	Al_2O_3	SiO_2	1500° C	1600° C	1700° C	1800° C	1900° C	2000° C	2100° C
60	40	0	-	-	0.8	0.6	0.5	-	-
50	50	0	5.7	2.3	1.2	1.0	-	-	-
40	60	0	-	3.3	1.7	1.1	-	-	-
30	70	0	-	-	1.8	1.1	-	-	-
20	80	0	-	-	-	1.1	0.7	0.6	-
0	100	0	-	-	-	-	-	-	0.5
50	30	-	-	2.4	1.4	1.0	0.7	0.6	-
40	40	20	-	4.0	2.0	1.3	0.9	-	-
30	50	20	11.5	4.7	2.5	1.5	1.2	1.0	-
20	60	20	-	-	2.7	1.6	1.3	-	-
0	80	20	-	-	-	-	-	0.8	0.6
50	10	20	3.9	2.1	1.3	1.0	0.8	0.6	-
40	20	40	9.2	4.3	2.2	1.8	1.4	1.2	-
30	30	40	25.7	11.0	5.3	2.8	2.0	1.6	-
20	40	40	-	19.9	9.6	5.3	3.1	--	-
0	60	40	-	-	-	-	2.4	1.5	1.2

Table 5.4 shows a detailed study of the viscosity of Al_2O_3 – SiO_2 – CaO melts at temperatures of 1450 ° – 2100° C [46]. The isoviscosity curves (isokoms) for 1500° C are shown in figure 5.12 [46]. As the CaO-Al_2O_3 binary melts the viscosity increases slightly with increasing concentration of Al_2O_3. Over the composition range 0-60 wt.% SiO_2 for the Al_2O_3–SiO_2 melts, the viscosity increases gradually with increasing concentration of silica.

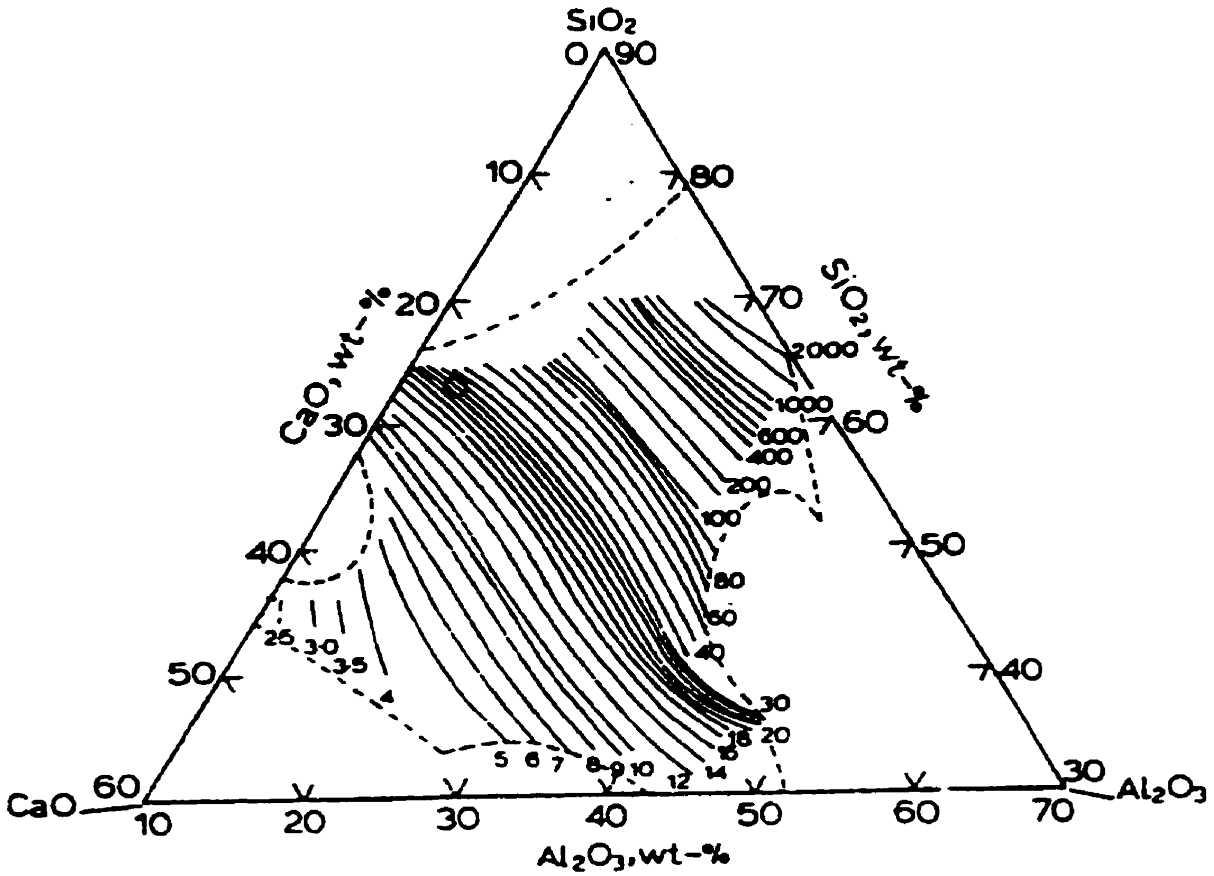

Figure 5.12. Isokoms(P) for CaO-Al_2O_3 – SiO_2 system at 1500° C[46]

Although the effect of other elements such as the alkali metals would have to be taken into account in the calculation, the system Al_2O_3 – SiO_2 – CaO does provide a useful first approximation to the behavior of these ashes. The thermodynamic calculation can be confirmed by referring to the ternary diagram shown in figure 5.13. Here the optimum melting temperature of fly ash is around 1440 ° C whereas for bottom ash it is 1550 ° C.

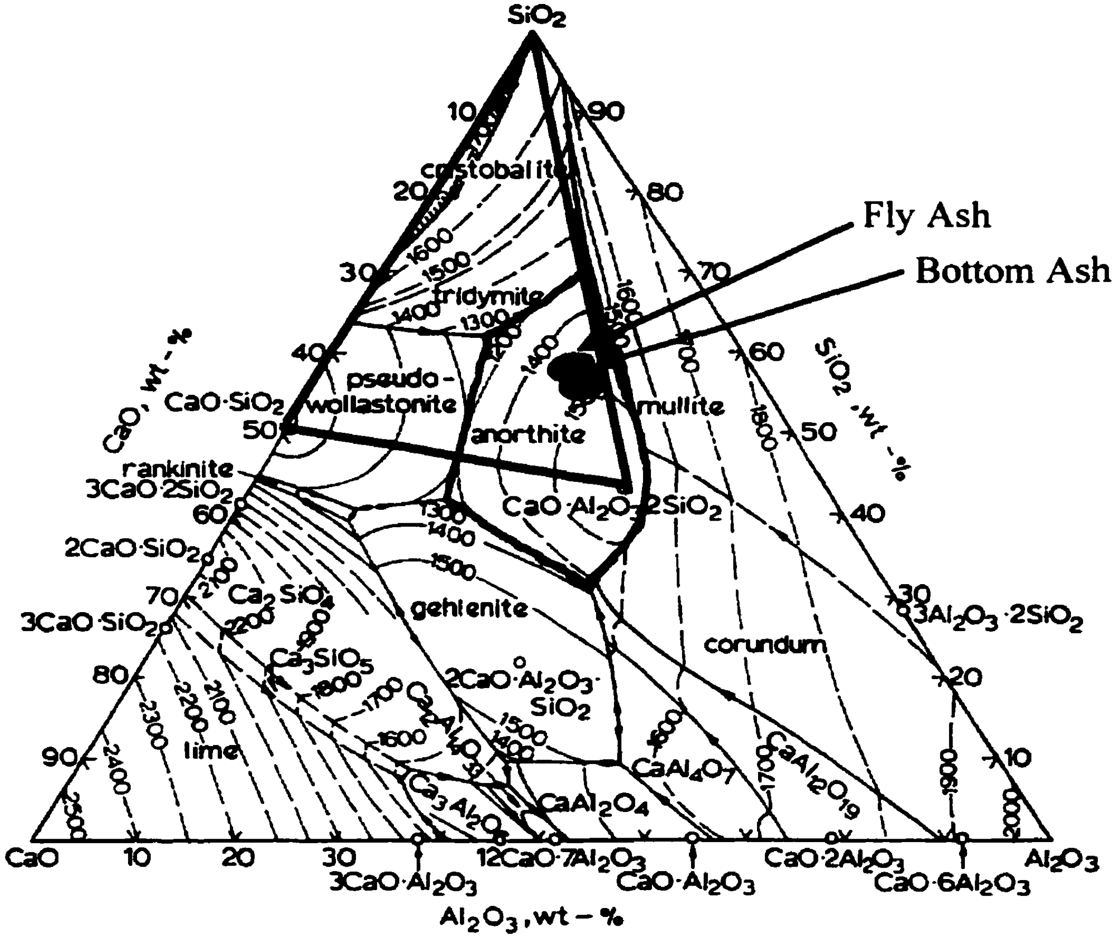

Figure 5.13 Ternary diagram of $CaO-SiO_2-Al_2O_3$ indicating that both the fly ash and bottom ash fall within the anorthite region.

5.3. Experimental Results on Vitrification

When cooled rapidly, many molten liquids form solids in which the atoms do not achieve the degree of crystalline order that would develop at a slower rate of cooling. In silicate and aluminosilicate systems structural disorder can be considered in terms of three influencing factors: [35]

a) disorder due to rapid quenching
b) disorder due to network isomorphic substitution and
c) disorder due to cation modification

Of these, the last two are different aspects of polymerization. Disorder introduced by quenching can be illustrated by consideration of two forms of silica, namely. crystalline silica and glassy silica. However, most glasses are more complex than vitreous silica and results from co-melting silica with other oxides such as network formers and modifiers.

As network formers and modifiers are added, the network may be visualized as becoming progressively depolymerized, the resulting glass being composed of increasingly smaller aluminosilicate oligomers, with a large number of terminals. negatively charged bridging and non-bridging oxygen (NBO) atoms.

It can be seen therefore that disorder in glasses is associated with both network substitution and the depolymerization of networks by modifier addition leading to a high NBO content. Due to the complex chemical nature of ashes both mechanisms of disorder will prevail in their structures.

In practice, the degree of disorder can be clearly understood from XRD patterns and electron microscopy can be used to reveal the structure –property relations in the vitreous state through macro to nano-structural levels of observation.

5.3.1. Electron Microanalysis

The microstructural studies were performed on freshly fractured specimens of vitrified samples using scanning electron microscopy. Figures 5.14 and 5.15 show the scanning electron micrograph of fly ash and bottom ash glass respectively. The glasses obtained in this work were transparent and colored. Fly ash glass appeared to be dark greenish color whereas bottom ash glass appeared as a dark brownish color glass. Coloring ions (Fe, Cu) in ashes caused the formation of colored glass. The glasses become darker with increasing carbon content. Thus fly ash glass is darker than bottom ash glass as carbon content in fly ash is higher than in bottom glass. They had featureless surfaces and were-bubble free and homogeneous.

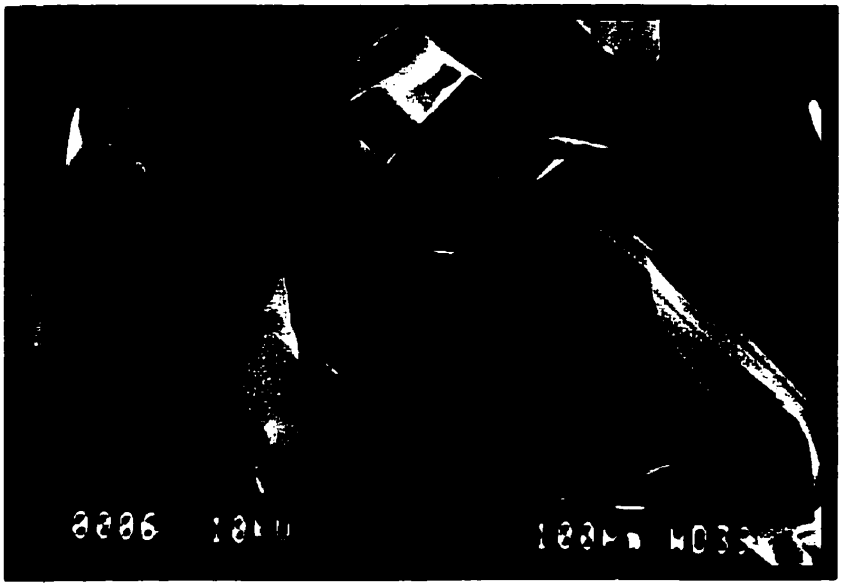

Figure 5.14. Scanning electron micrograph of fly ash glass particles

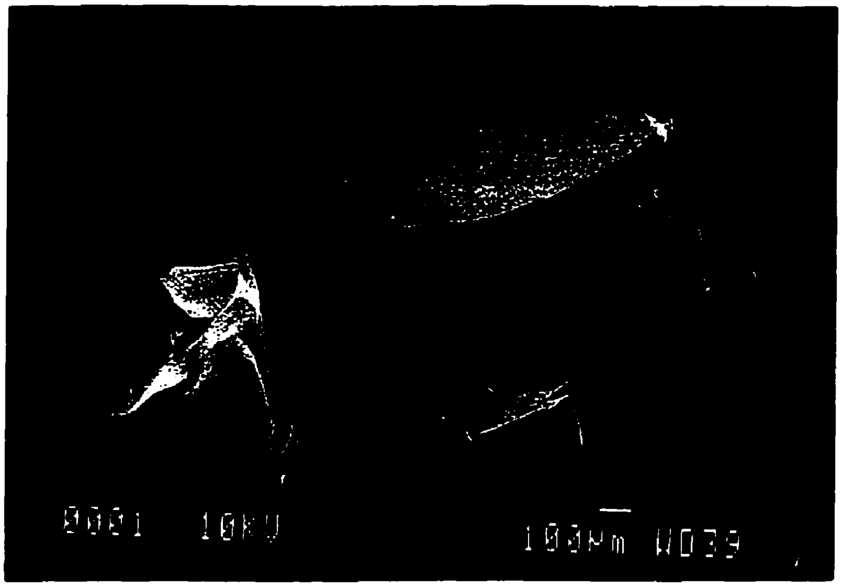

Figure 5.15 Scanning electron micrograph of bottom ash glass specimens

5.3.2. X-ray Diffractometry

X-ray diffraction patterns of bulk vitrified product of fly ash shown in figure 5.16 and 5.17 indicate the amorphous state of fly ash glass and bottom ash glass respectively. In both cases, the spectra show presence of a non-crystalline material (silica), and absence of any distinct crystalline species.

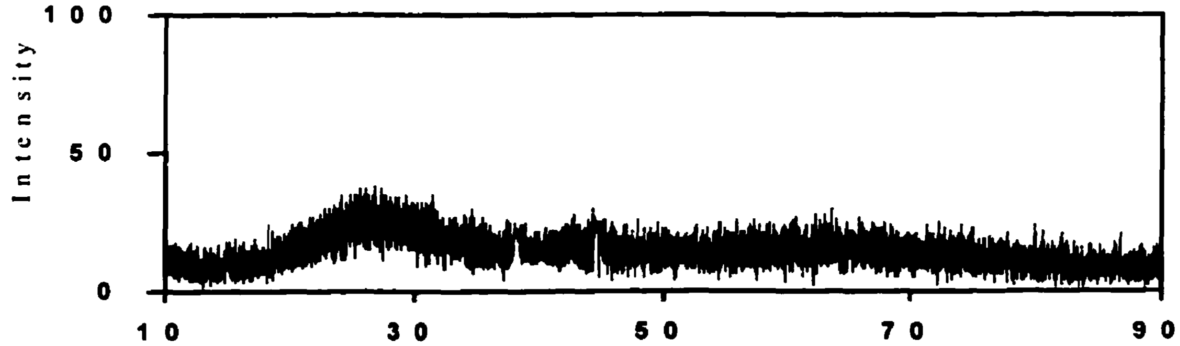

Figure 5.16 X-ray diffraction pattern of fly ash glass

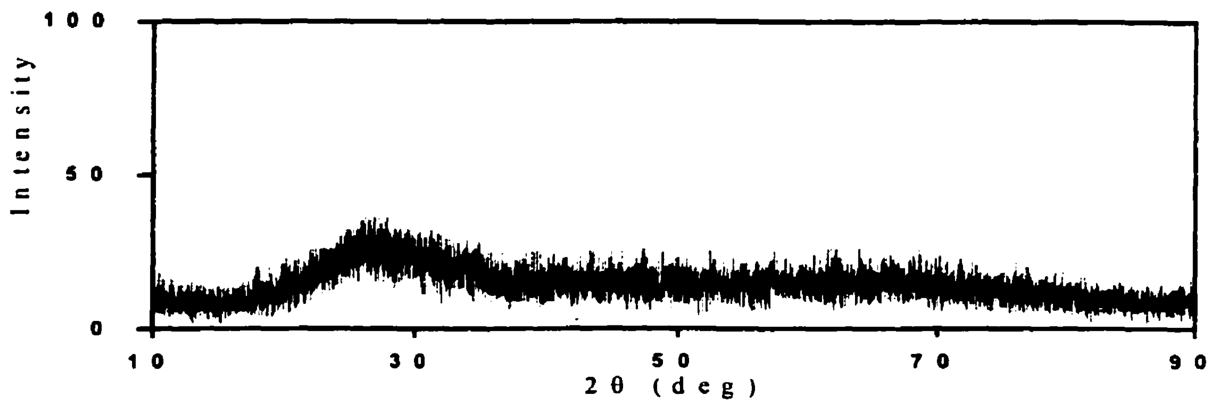

Figure 5.17 X-ray diffraction pattern of bottom ash glass

The EPMA micro chemical analysis form different areas of fly ash and bottom ash glass is given in table 5.5.

Table 5.5. EPMA micro chemical analysis of fly ash and bottom ash

Ash	Oxides										
	Na_2O	MgO	CaO	SiO_2	FeO	Al_2O_3	P_2O_5	TiO_2	K_2O	MnO	Total
Fly Ash	2.14	2.15	14.48	47.83	2.98	22.16	1.22	3.19	2.30	0.33	98.78
	2.12	2.09	14.21	48.75	2.94	21.81	1.14	3.12	2.34	0.36	98.87
	2.11	2.17	14.54	48.03	3.01	21.97	1.15	3.21	2.29	0.31	98.77
	2.27	2.10	14.06	49.45	2.82	21.32	1.09	3.13	2.46	0.31	99.00
Bottom Ash	1.29	2.26	14.42	45.77	1.54	27.30	0.86	4.14	1.52	0.19	99.30
	1.24	2.35	14.58	46.14	1.57	26.75	0.87	4.30	1.50	0.15	99.42
	1.24	2.31	14.54	45.92	1.57	26.69	0.86	4.26	1.49	0.18	99.05
	1.25	2.29	14.81	45.68	1.60	26.69	0.90	4.36	1.48	0.16	99.21

The major glass components of these glasses are CaO, SiO_2, Al_2O_3. The CaO. and SiO_2 percentages of fly ash and bottom ash are almost same. However the average Al_2O_3 content of fly ash is 22% whereas in bottom ash it is 27%. Both glasses have nucleating agents such as Fe_2O_3, TiO_2 and P_2O_5 in significant quantities, which can act as nucleating agents during the crystallization process.

5.3.3. Differential Thermal Analysis of Fly Ash Glass

Figure 5.18 reports the DTA trace of the fly ash glass samples, performed at 10 °/min heating on 200 µm powdered samples.

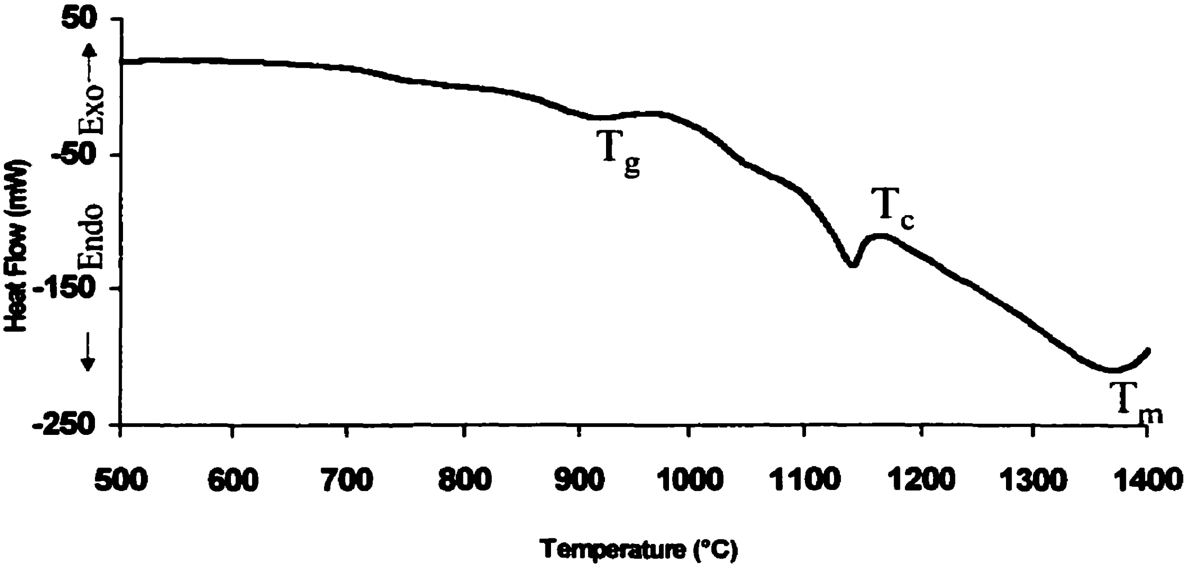

Figure 5.18. Differential Thermal Analysis of fly ash glass

As a glass is heated, its heat capacity changes within a narrow temperature range called the glass transition temperature, which corresponds to the temperature at which the glass network acquires sufficient mobility to change from a rigid to plastic solid. It is observed that the glass transition takes place at 925° C. As the crystallization takes place, the heat of crystallization is evolved and all of the material shows a wide exothermic band from 925 ° to 1025 ° C interval indicating the structural reordering of the glassy network. For temperatures between 1100° to 1200° C, there is a sharp decrease in the curve indicating partial melting of the powder. At 1150 ° C there is an exothermic peak indicating crystallization of glass. Finally there is a decrease in the DTA curve observed at about 1400° C, where melting is completed.

5.4. Experimental Results on Devitrification

CaO-Al_2O_3-SiO_2 (CAS) system glasses are one of the fundamental silicate systems that have been used widely in many fields of industry. The crystallization of CAS system glasses has been investigated by many researchers. The crystallization of CAS system glasses is very complicated and depends on the different glass compositions or glasses system. Glasses generally crystallize by their surface or internal (volume) crystallization [47]. Although both crystallization mechanisms can occur simultaneously and competitively, one mechanism usually dominates over the other. Glasses crystallize in the whole body when the content of SiO_2 in the CAS glasses is low. When the SiO_2 content is high, the glasses crystallize only on the surface but if some nucleating agents such as TiO_2, Cr_2O_3, P_2O_5 and Fe_2O_3 are added to the glasses they can crystallize in the whole body.

Particle size has a great effect on crystallization of glass particles. The total effective surface area to the volume ratio increases with decreasing particle size for a fixed amount of sample [48]. The dominance of surface crystallization should be observed with increasing particle size, because the total effective surface area to volume ratio decreases, hence the number of surface nuclei available for crystallization increase with increasing particle size. When the internal nucleation is dominant, the contribution of number of internal nuclei compared to that of the surface nuclei in the sample increases with decreasing particle size [48].

Two types of glass samples, bulk glass and glass powder of 200 μm, were chosen for nucleation and crystallization studies in order to understand both surface and volume crystallization. Glass samples were heat treated at different temperatures and the results for the development of crystalline phases as identified by XRD and EPMA are given in table 5.6.

Heat Treatment Temperature (° C)	Bulk Glass	Glass Powder
900	Glass (XRD)	Glass (XRD)
1000	Glass (XRD)	Glass (XRD) (Just nucleation start)
1100	Nucleation (XRD)	Nucleation (XRD & EPMA)
1200	Partially crystallizes (XRD & EPMA)	Fully crystallized (XRD & EPMA)

Table 5.6. Nucleation and crystallization temperatures for bulk glass and glass powder

From table 5.6 it can be seen that heat treatment has a great effect on structure and function of glass ceramics and by controlling the process of heat-treatment, desired crystalline structures and phases can be achieved. The DTA curve for fly ash glass shows the glasses characteristic temperatures corresponding to endothermic and exothermic peak. At temperature T_g, the glass transition temperature, the viscosity of glass is about 10^{12} Pa s. However, the most effective nucleation temperature of glass generally corresponds to a viscosity of 10^{12} Pa s [48]. Thus the nucleation temperature is usually selected at temperature slightly above T_g.

5.4.1. X-ray Diffraction

The XRD analysis of devitrified glass obtained from bulk glass is shown in figure 5.19. While the DTA curve indicates a transition at around 925° C, the XRD pattern demonstrates that the material is completely amorphous up to at least 900 ° C.

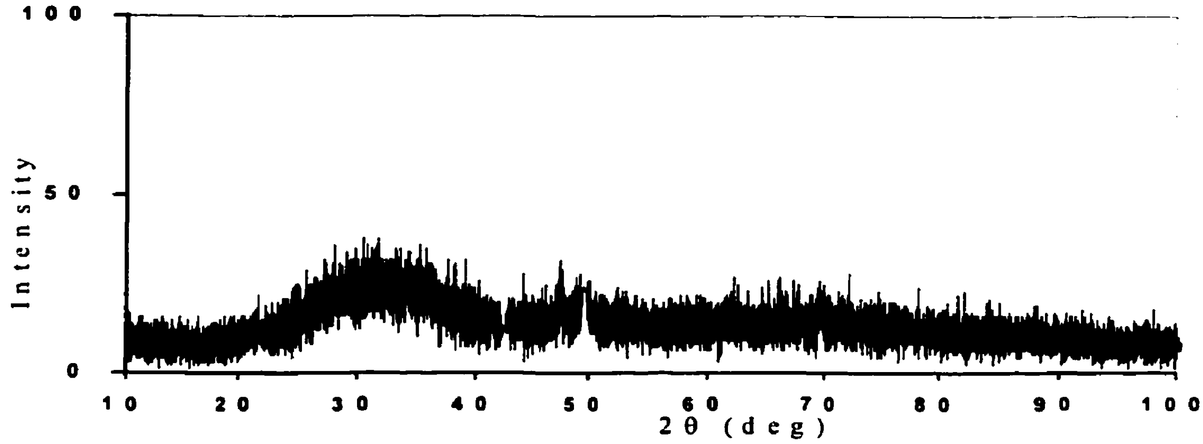

Figure 5.19. XRD pattern of fly ash bulk glass heat-treated to 900 ° C

The XRD pattern shown in figure 5.20 is typical of a non-crystalline pattern. It can be seen that there is a single peak, which indicates where the nucleation and phase separation takes place.

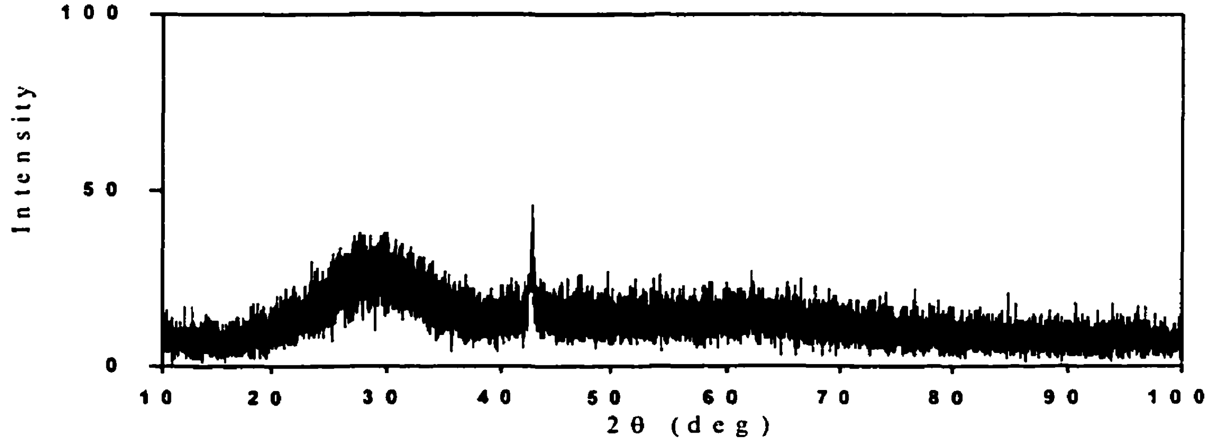

Figure 5.20. XRD pattern of fly ash glass powder heat-treated to 1000 ° C

Figure 5.21 shows that at 1100° C, although the specimen quite amorphous, it has developed the crystalline phases anorthite ($CaO.Al_2O_3.2SiO_2$) and/or albite calcian $(Na,Ca)Al(Si,Al)_3O_8$. As a matter of fact, the highest intensity peaks match with both anorthite and albite and it is difficult to determine whether both crystalline phases are simultaneously present at this temperature.

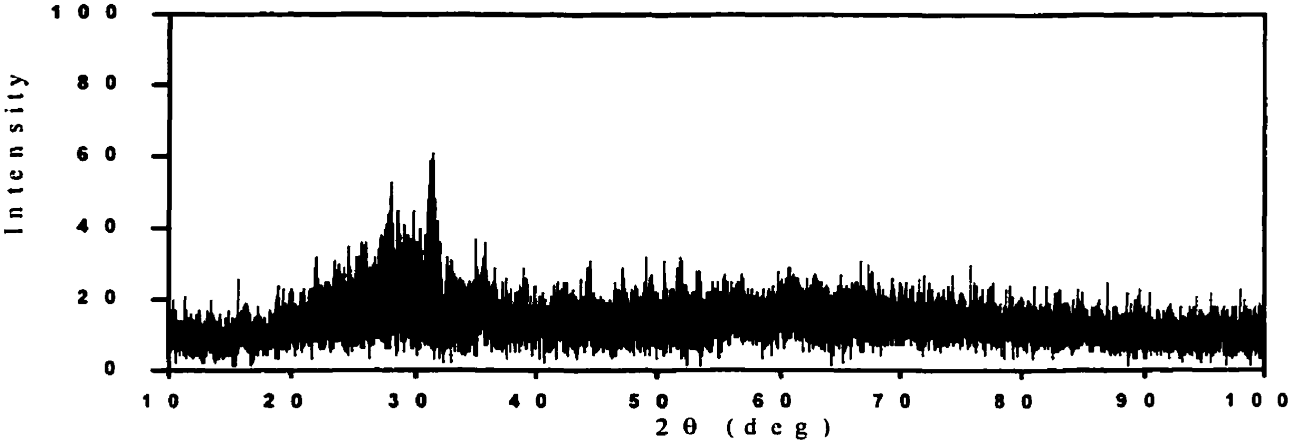

Figure 5.21. XRD pattern of fly ash bulk glass heat-treated to 1100 ° C

The DTA curve shows an abrupt change between 1100° and 1200° C due to partial melting of the sample; this result agrees with the XRD pattern at 1100 ° C which presents the characteristic broad peak of amorphous material and some unidentified crystalline phase. It can be seen in figure 5.22, at higher temperature i.e. 1200 ° C there is no doubt that both phases coexist since the XRD pattern shows that the amorphous phase has practically disappeared and both anorthite and albite combine with TiO_2 to form complex aluminosilicate crystalline phases. Further increase in temperature leads to melting.

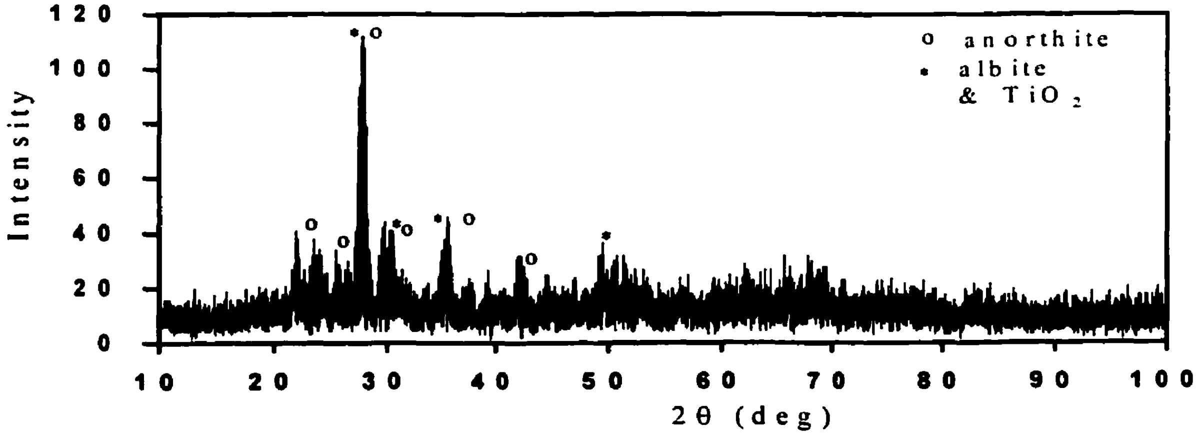

Figure 5.22 XRD pattern of fly ash glass powder heat-treated to 1200 ° C

Microchemical characterization by EPMA and SEM was attempted to resolve the crystalline precipitates in the devitrified product.

5.4.2. Microstructural Analysis

Electron microscopy permits very detailed study of the process of conversion of glass into a glass ceramic material. In addition to qualitative evaluation of microstructural changes, it also permits quantitative measurements, especially of the number of particles, their size and distribution. The properties of materials at individual stages in the transformation of a glass to a glass ceramic material are very different and thus a suitable technique for sample preparation must be selected.

The X-Ray diffraction pattern of the devitrified glass ceramics suggested that the crystallized glass probably contained two crystalline phases, anorthite and albite calcian, $(Na,Ca)Al(Si,Al)_3O_8$, a aluminosilicate, both combined with titanium oxide in the devitrified product.

The EPMA data collected from four separate locations on a devitrified fly ash bulk sample are summarized in table 5.7.

Table 5.7. EPMA analysis of devitrified fly ash bulk glass at 1100 ° C

Oxides										
Na_2O	MgO	CaO	SiO_2	FeO	Al_2O_3	P_2O_5	TiO_2	K_2O	MnO	Total
1.60	2.24	25.03	40.32	2.46	19.22	0.00	3.57	2.79	0.65	97.89
1.31	2.31	24.09	40.22	2.45	19.09	0.00	3.52	3.91	0.72	97.62
1.22	1.99	22.99	40.17	2.45	19.10	0.00	3.51	5.38	0.60	97.39
1.56	2.18	23.85	40.50	2.42	19.14	0.00	3.53	4.13	0.50	97.80

Analysis of table 5.7 indicates it is most likely representative of the anorthite and a complex titanium rich aluminosilicate with residual silica. This result corresponds to the XRD analysis of figure 5.22 and the scanning electron micrograph shown in figure 5.23 confirms the results.

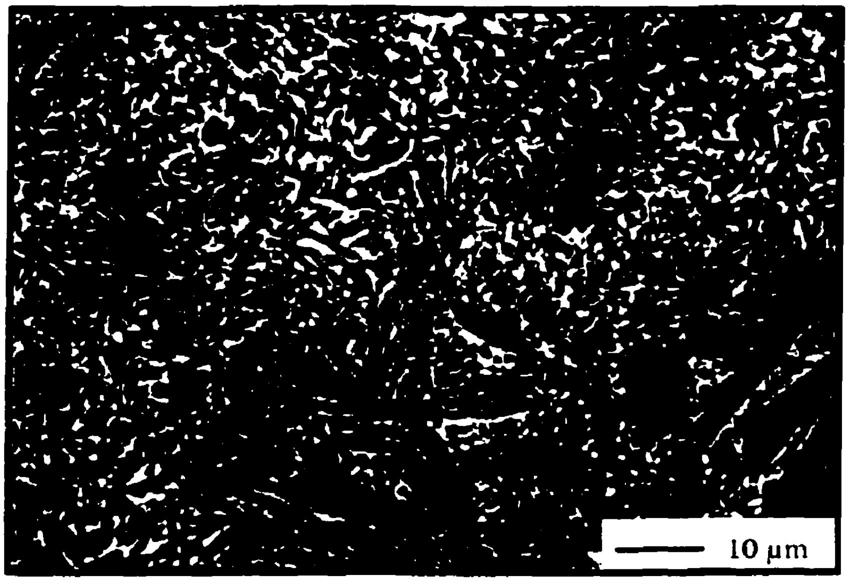

Figure 5.23. Scanning micrograph of fly ash glass heat treated to 1100° C

The SEM micrograph shows that both phase separation and nucleation take place in the interior. There is a field of phase separation for two types of liquids occurs near to high content of SiO_2 in the line between CaO and SiO_2 of the CAS system. As the composition of glass is located in the area of crystal anorthite, which is closed to the siliceous glass-forming field of sub-stability and non- uniformity, they display the phenomenon of phase separation [47]. In the structure of glass, O^{2-} is attracted to near Si^{4+} in the form of $(SiO_4)^{4-}$. At the same time the network modifiers also have a tendency to attract O^{2-} with a partial negative charge (non-bridge oxygen), so the network modifiers compete with Si^{4+} for O^{2-} [35]. When the surrounding temperature is the temperature T_g, the structure of the glass becomes relaxed and diffusion of ions is easier. For glass with more network modifiers, non-bridged oxygen are concentrated in the area that contains more network modifiers and the glass separated into two phases, which are the phase with more Si^{4+} and the phase with more network modifiers. The conditions of nucleation are that ions diffuse together from the uniform glass base, and the ions are rearranged to give the structure of the crystals.

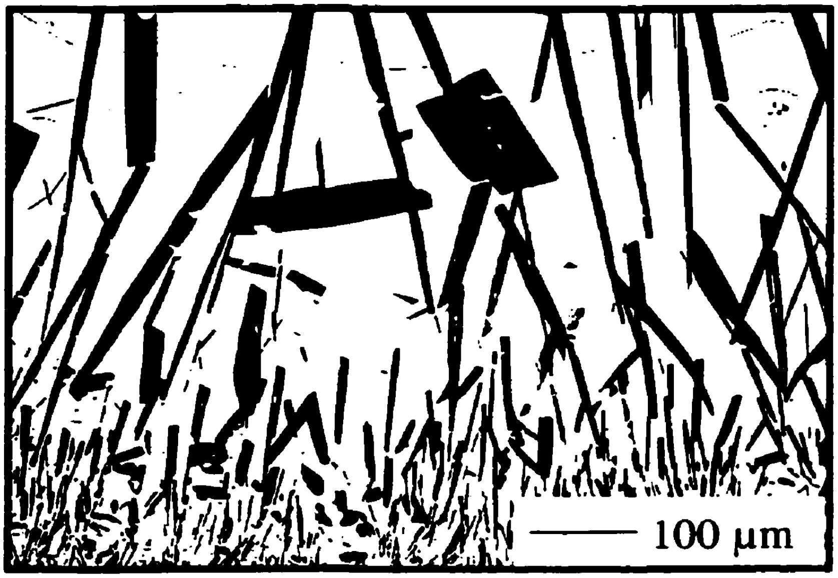

Figure 5.24. Scanning electron micrograph of bulk fly ash glass heat treated to 1200° C

Large anorthite dendrites that grow from the surface to the interior are shown in figure 5.24. This is due to the presence of micro-cracks, and impurities on the surface of the glass, which, result in heterogeneous nucleation. The crystals on the surface grow to make contact with each other and then a layer of surface crystals moves forward into the interior. This can be seen in figure 5.25. The table 5.8 shows the EPMA micro chemical analysis of fly ash bulk glass heat treated to 1200° C and confirms that the crystals are anorthite.

Table 5.8. EPMA analysis of devitrified fly ash bulk glass at 1200° C

Oxides										
Na_2O	MgO	CaO	SiO_2	FeO	Al_2O_3	P_2O_5	TiO_2	K_2O	MnO	Total
0.53	0.10	19.74	43.73	0.89	35.05	0.25	0.16	0.31	0.00	100.75
0.61	0.09	19.74	43.51	0.88	34.83	0.22	0.16	0.34	0.04	100.44
0.47	0.10	19.72	43.96	0.82	34.65	0.26	0.14	0.33	0.03	100.51

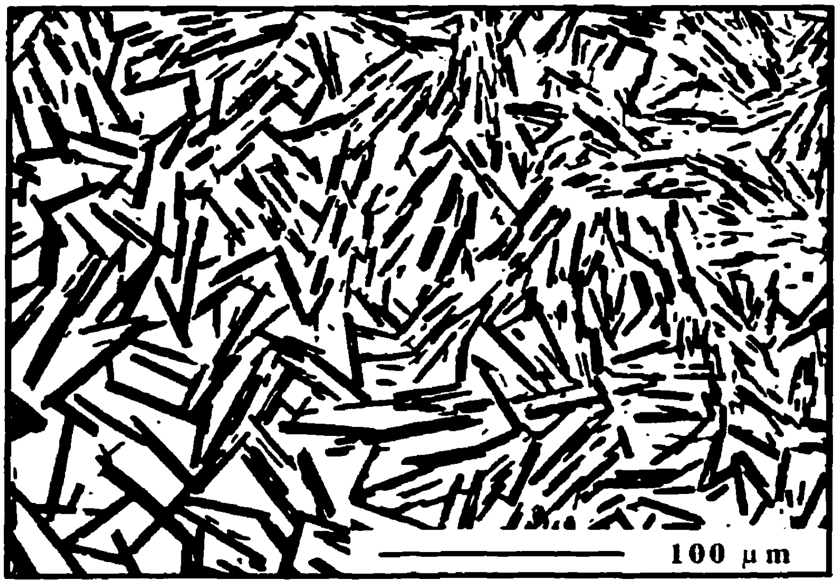

Figure 5.25. Scanning electron micrograph of the surface of the bulk fly ash glass heat treated to 1200° C

The internal crystallization of fly ash glass powder when heat-treated to 1200° C is shown in figure 5.26. The crystal size is smaller and the crystals are uniformly distributed throughout the matrix, indicating a higher rate of internal crystallization. Moreover, from the EPMA analysis it is identified there are two types of crystals anorthite and calcian albite both combined with TiO_2 form a titanium rich aluminosilicate and glass co-exist. All of the features are due the particle size of glass particles, as glass powder was chosen for the heat treatment procedure.

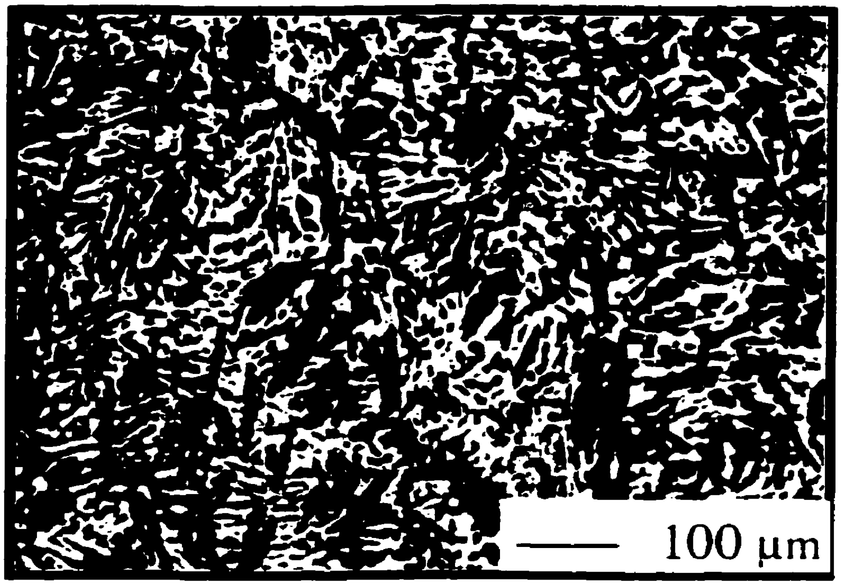

Figure 5.26. Scanning electron micrograph of powdered fly ash glass heat-treated to 1200° C

Because particle size has an effect on the final composition of each phase, it will also have an effect on the rate of nucleation of different crystal phases. It can be seen from table 5.9, that the chemical compositions correspond with anorthite crystalline phases. As the micrograph shows, there are two types of crystals, anorthite and a titanium rich complex aluminosilicate which are closely interconnecting and forming a network in glass matrix..

Table 5.9. EPMA X-ray analysis of devitrified fly ash glass powder at 1100 ° C.

Oxides										
Na_2O	MgO	CaO	SiO_2	FeO	Al_2O_3	P_2O_5	TiO_2	K_2O	MnO	Total
1.39	2.32	24.72	40.21	2.11	20.40	1.91	3.06	3.21	0.24	99.56
1.39	2.37	24.66	39.88	2.33	19.91	2.04	3.37	3.10	0.41	99.46
1.41	2.43	24.50	39.93	2.30	19.62	2.04	3.40	3.42	0.34	99.38
1.32	2.60	25.91	39.26	2.44	18.80	2.11	3.68	2.94	0.35	99.43

5.5. Mechanical Properties

5.5.1. Microhardness of Glass and Glass Ceramics

The general trend in microhardness found is that as a sample becomes more crystalline, the average microhardness increases. Table 5.8 gives values for the microhardness of glass and glass ceramics found for present work.

Table 5.10 Microhardness of glass, and glass ceramics

Sample	Hardness (H_v)
Glass	570
Glass Ceramics from Bulk Glass	652
Glass Ceramics from Sintered Glass Powder	774

The hardness values found for the devitrified glass ceramics are greater than for glass or bulk crystallized glass. Moreover the hardness value of glass ceramics obtained from sintered glass powder shows higher hardness than glass ceramics obtained from bulk glass. The microhardness trend is consistent with what can be expected based on crystallization. The glass ceramic material obtained from glass powder has two crystalline phases namely anorthite and calcian albite $(Na,Ca)Al(Si,Al)_3O_8$, combined with titanium oxide, whereas glass ceramics obtained from bulk glass has only one crystalline phase, anorthite. Figures 5.27,-5.29 show micrographs of Vickers indentation in glass, glass ceramic obtained from bulk glass and glass ceramic obtained from sintered glass powder respectively. In can be seen that the size of the indentation decreases with the amount of crystallinity, indicating an increase in hardness.

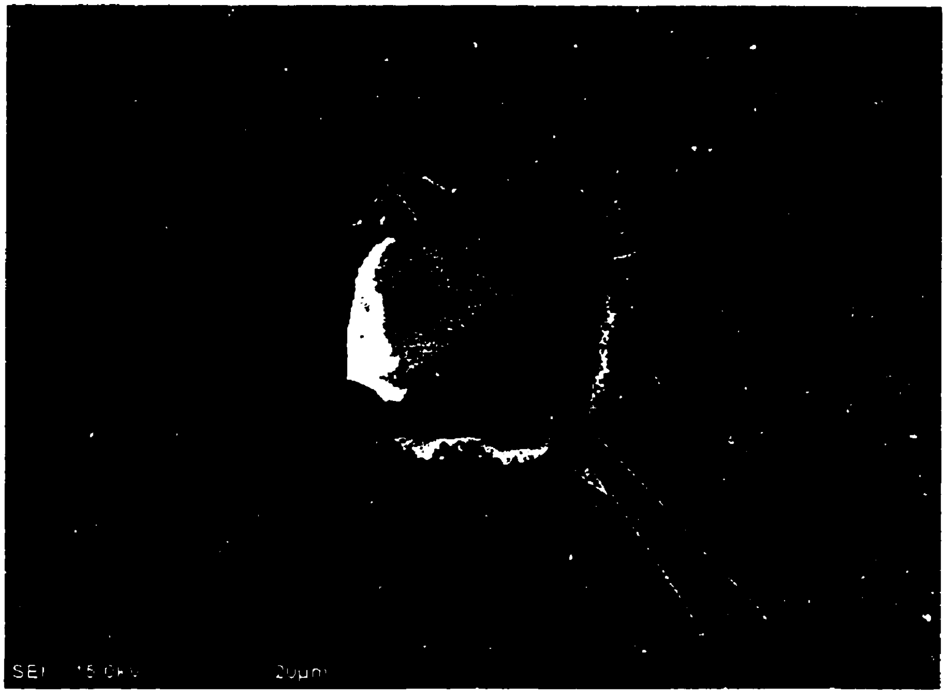

Figure 5.27. Vickers indentation in fly ash glass (load 500 g)

Figure 5.28. Vickers indentation in fly ash glass ceramic obtained from bulk glass at 1200° C (load 500 g)

Figure 5.29. Vickers indentation in fly ash glass ceramic obtained from glass powder at 1200° C (load 500 g)

5.5.2. Fracture Toughness

Fracture toughness determination using Vickers indentation could not be performed in either the glass or glass ceramics. In the glass, instead of a single crack at the indentation corners, multiple cracks occur as can be seen in figure 5.27. In glass ceramics, instead of developing half-penny like cracks, the cracks in the glass ceramics tended to propagate throw the crystal boundries as can be seen in figures 5.28 and 5.29. However, the toughness of glass and glass ceramics can be compared by the length of cracks.

It is clear from the micrographs that the length of the crack in glass is more than 100 μm compared to glass ceramics, which is around 50μm and is more tortuous in the latter case. This indicates that glass ceramics have a higher fracture toughness than a glass of the same composition.

CHAPTER VI

CONCLUSIONS

The present study was conducted to develop glass ceramic materials from pulp and paper waste incinerator ashes and from the results the following conclusions can be drawn:

- Fly ash and bottom ash are waste materials generated from the incineration of pulp and paper waste.
- These ashes represent a potential major environmental liability due to the presence of organic pollutants and the amount (volume) of waste.
- The bulk mineralogy and chemistry indicate that these ashes can be used to produced glass and glass ceramic materials.
- The chemical composition of ash is typical of a common ternary system (CAS) with significant amounts of metal oxides such as TiO_2, Fe_2O_3, and Cr_2O_3, which are able to act as nucleating agents for crystallization.
- Glass can be obtained by melting these ashes at 1500° C and quenching into water.
- Glass ceramics can be produced by controlled heat treatment process from fly ash glasses.

- The devitrification process occurs in two steps: at 1100° C nucleation takes place and crystallization occurs at 1200° C.
- The crystallization of a CAS glass system is very complex and depends on glass composition and total effective surface area of glass particles.
- Glass generally crystallizes either by surface crystallization or volume crystallization. When the ratio of the volume to the total effective surface area of all glass particles is high (decreasing particle size, bulk glass) surface nucleation occurs and the volume crystallization occurs when the effect is reverse (in glass powders).
- The devitrification of bulk glass exhibit surface crystallization whereas powdered glass exhibits volume crystallization at 1200° C
- Optimum devitrification temperature for fly ash glass was 1200° C and the final product is anorthite in surface crystallization whereas in volume crystallization the crystals were found to be anorthite and albite,
- Hardness values of glass ceramics were exceeded and the toughness of these glass ceramics were higher when compared to that of the parent glass thus the material should be useful in glass ceramic applications.

REFERENCES

1. Nemerow, N. L., Industrial Solid Wastes, Ballinger Publishing Company, (1983).
2. Pavoni, J. L., Hand Book of Solid Waste Disposal, Van Nostrand Reinhold Company (1975)
3. Gong, Y., and Kirk. D. W., "Behavior of Municipal Solid Waste Incinerator Fly Ash," Journal of Hazardous Materials, 36, (1994) 249-264
4. "Vitrification of Fly Ash," Technical Documentation, Europlasma, France (1997) 1-26
5. Barbieri, L., Lancellotti, I., 'Design, Obtainment and Properties of Glasses and Glass-Ceramics from Coal Fly Ash" Fuel 78 (1999) 271-276
6. Boccaccini, A. R., Kopf, M., Stumpfe, W., "Glass-Ceramics From Filter Dusts From Waste Incinertor," Ceramic International, 21 (1995) 231-235
7. Suzuki, S., Tanaka, M., and Kaneko, T., "Glass Ceramic From Sewage Sludge Ash," Journal of Materials Science, 32, (1997) 1775-1779
8. Boccaccini, A. R., Pititmermet, M., Wintermantel, E., "Glass-Ceramics From Municipal Incinerator Fly Ash," The American Ceramic Society Bulletin, (November 1997) 75- 78
9. Barbieri, L., Manfredini, T., "Vitrification of Fly Ash From Thermal Power Station," Glass Technology Vol. 38, (5), (1997) 165-170
10. James.P.F., "Glass Ceramics: new composition and uses, Journal of non crystalline solids 181 (1995) 1-15
11. Partridge,G., "An overview of glass ceramics. Part.I: Development and principal bulk applications" Glass Technology Vol. 35, (3), (1994) 116-127
12. Romero, M., Rawlings, R. D., and Rincon, J., Ma., " Development of a New Glass-Ceramic by Means of Controlled Vitrification and Crystallization of Inorganic Wastes from Urban Incineration" Journal of the European Ceramic Society 19 (1999) 2049-2058
13. Glenn, J., "Paper Mill Sludge: Feedstock For tomorrow" Progress in Paper Recycling (May 1998) 54-59

14. Rudiger Dorre Dipl.,"Waste incineration in the pulp and paper industry",Paper Technology (May 1995) 26-30.

15. Chin-Tson Liaw, Hui-Lan Chang et al, " A Novel method to resuse paper sludge and co-generation ashes from paper mill", Journal of Hazardous Materials, 58, (1998) 93-102.

16. Aitken,M.M., Evans, B., Lewis, J.G., "Effect of Applying paper mill sludge to arable land on soil fertility and crop yields", Soil Use and Management 14, (1998) 215-222.

17. Trepaniier,L., Gallichand,J., et.al." Environmental Impact of On-farm Stroage of Deinking Paper Mill Sludge" American Society of Agricultural Engineers Vol. 39 (5), (1996) 1853-1859.

18. Gray, M.S., Said Abubakr, Amy Smith, "Characterization of Pulp Mill Sludge", Disposal and Utilization alternatives for the Pulp and Paper industry: A Review, (November 1997) 34-36.

19. Graydon, A.R.H., Charles A.E., "Composting of Pulp and Paper Mill Fly Ash with Wastewater Treatment Sludge," Bio-resource Technology, 70 (1999) 217-224.

20. Mark Taylor, "Unique Landfill Options Spurred By Employing Mill Solid Wastes", Pulp & Paper (May 1996) 63-77.

21. Charles Holbert, JoAnn, S.L., "Trace metals behavior during the thermal treatment of paper-mill sludge" Waste management 18 (1998) 423-431.

22. By Staff writer' Change in waste incineration" Techno Japan Vol. 30, No. 3. (March 1997) 10- 12

23. Mangialardi, T., Piga, L., "Characteristics of MSW Incinerator Ash for Use in Concrete" Environmental Engineering Science, Vol. 15, No 4 (1998) 291-297

24. Wang, D., Sweigard, R. J., Characterization of Fly Ash and Bottom Ash from a Coal-fired Power Plant" (1996) 181-186

25. Wei, M.C., Wey, M.Y., "Stability of Heavy Metals in Bottom Ash and Fly Ash Under Various Incinerating Conditions" Journal of Hazardous Materials, 57 (1998) 145-154

26. Kipka, A., Luckscheiter, B. and Lutze, W., "Melting of Fly Ashes and Product Properties," Glastech. Ber. 66 (9), (1993) 215-220

27. Hjelmar, O., "Disposal Strategies for Municipal Solid Waste Incineration Residues," Journal of Hazardous Materials 47, (1996) 345-368

28. Sakai, S., Sawell, S. E., et.al "World Trends in Municipal Solid Waste Management," Waste Management, Vol. 16, (5-6), (1996) 341-350.

29. Wiegand P.S., Unwin, J.P., "Alternative Management of Pulp and Paper industry Solid Wastes" Tappi Journal Vol77, No 4, (April 1994) 91-97

30. Ito, T., Vitrification of Fly Ash by Swirliing-flow Furnace" Waste Management, Vol. 16b, No 5/6 (1996) 453-460

31. By Staff writer "Incineration Ash Melting Facilities" Techno Japan Vol. 30, No3. (March 1997) 13- 21

32. Bickford, D. F., and Schumacher, R., "Vitrification of Hazardous and Radioactive Wastes," Ceram Eng. Sci. Proc. 16(2) (1995) 1-10

33. Boccaccini, A.R., Janczar, J., " The Multibarriers-system as a Materials Science Approach for Industrial Waste Disposal and Recycling: Application of Gradient and Multilayered Microstructures" Environmental Technology, Vol. 17, (1996) 1193-1203

34. Chiang, Y. M., Dunbar, P. B., III and Kingery, W. D., Physical Ceramics, John Wiley & Sons, Inc., (1997)

35. Hemmings, R.T., Berry, E.E., 'On the Glass in Coal Fly Ashes: Recent Advances" Materials Research Society Symposium Proceedings, Vol. 113 (1988) 3-38

36. Petitmermet, M., Eckert, E., et al, "Residues of Waste Incineration Plants as Raw Materials; Processing and Characterization," (1997) 67-72.

37. McMillan, P. W., Glass-Ceramics, 2nd Edition, Academic Press (1979)

38. Strnad, Z., Glass-Ceramic Materials, Glass Science and Technology; Vol. 8, Elsevier, (1986)

39. Topping, J. A., "The fabrication of Glass-Ceramic Materials Based on Blast Furnace Slag," Journal of the Canadian Ceramic Society, 45, (1976) 63-67

40. Rincon, J. M., Romero, M., "Glass –Ceramics as Building Materials" Materials De Construccion, Vol. 46 (September 1996) 242-243
41. De Mestral, F., "Calcium Phosphate Glasses and Glass-Ceramics for Medical Applications", M. Engineering Thesis, McGill University June 1986
42. Liard, A., Lessard, R., "Product from residue: standard setting for alkaline mill residues in Quebec" Pulp and Paper Canada 100:5,(1999) 27-29
43. Jouko Latva-Somppi, Esko I.Kauppinen, "The ash formation during co-combustion of wood and sludge in industrial fluidized bed boilers", Fuel Processing Technology 54, (1998) 79- 94.
44. Oktay Bayat, "Characterization of Turkish fly ashes" Fuel, Vol. 77, No. 9 (1998) 1059-1067.
45. Jouko Latva-Somppi, Mikko Moisio, " Ash formation during fluidized-bed Incineration of paper mill Waste Sludge", Journal of Aerosol Science, Vol.29, No 4 (1998) 461-480
46. Turkdogan, E.T., " Physicochemical Properties of Molten Slags and Glasses" The Metals Society London (1996) 17-25
47. Duan, R.G., Liang, K.M., "A study on the Crystallization of CaO-Al_2O_3-SiO_2 system glasses" Journal of Materials Processing Technology 75(1998) 235-239
48. Ray, C.S., Yang. Q., "Surface and internal Crystallization in Glasses as Determined by Differential Thermal analysis", Journal of American Ceramic Society, 79 (12) (1996) 3155-60

APPENDIX

Summary of minerals in bulk raw materials after beneficiation as function of particle size fraction

Paricle Size (μm)	**Minerals**	
	Fly Ash	**Bottom Ash**
> 850	Amorphous, Anorthite	Amorphous. Anorthite
850 - 600	Amorphous, Anorthite	Amorphous, Anorthite
600 - 425	Amorphous	Amorphous, Anorthite
425 - 300	Amorphous,	Complex aluminosilicate
300 - 212	Complex aluminosilicate	Complex aluminosilicate
212 - 150	Amorphous	Anorthite
150 - 75	Quartz, Complex aluminosilicate	Quatz, Anorthite
75 - 53	Quartz	Anorthite
53 - 38	Quartz	Anorthite
< 38	Amorphous	Anorthite

Particle Size Fraction: > 850 µm

Fly Ash

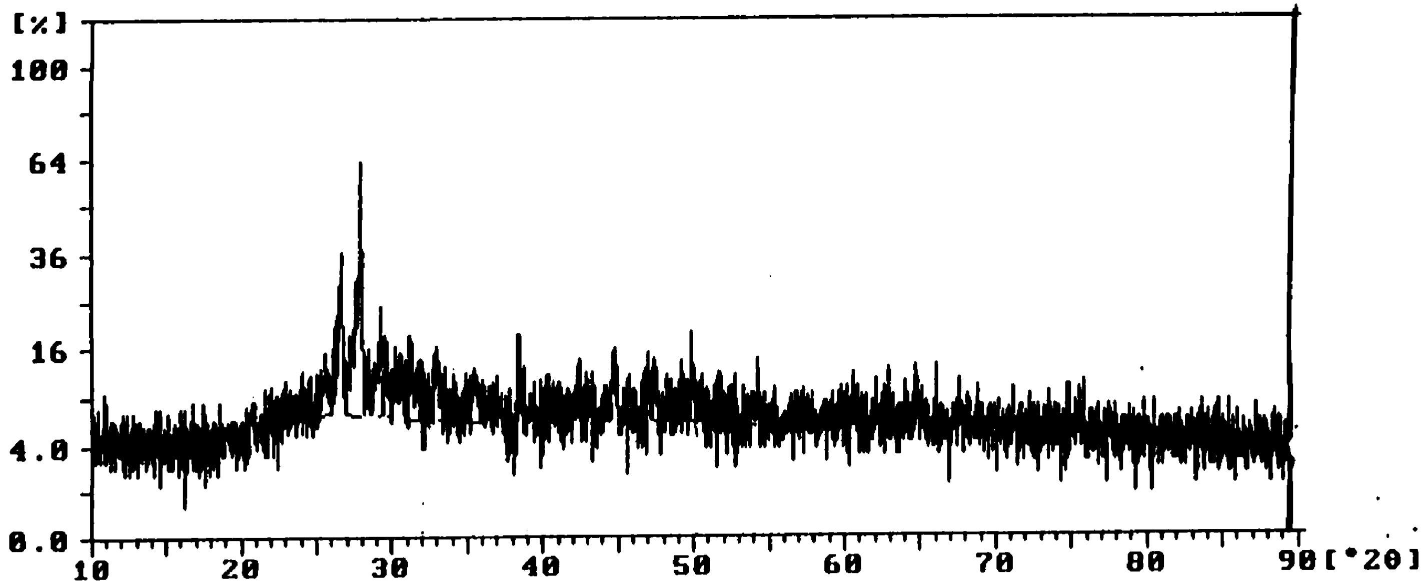

Bottom Ash

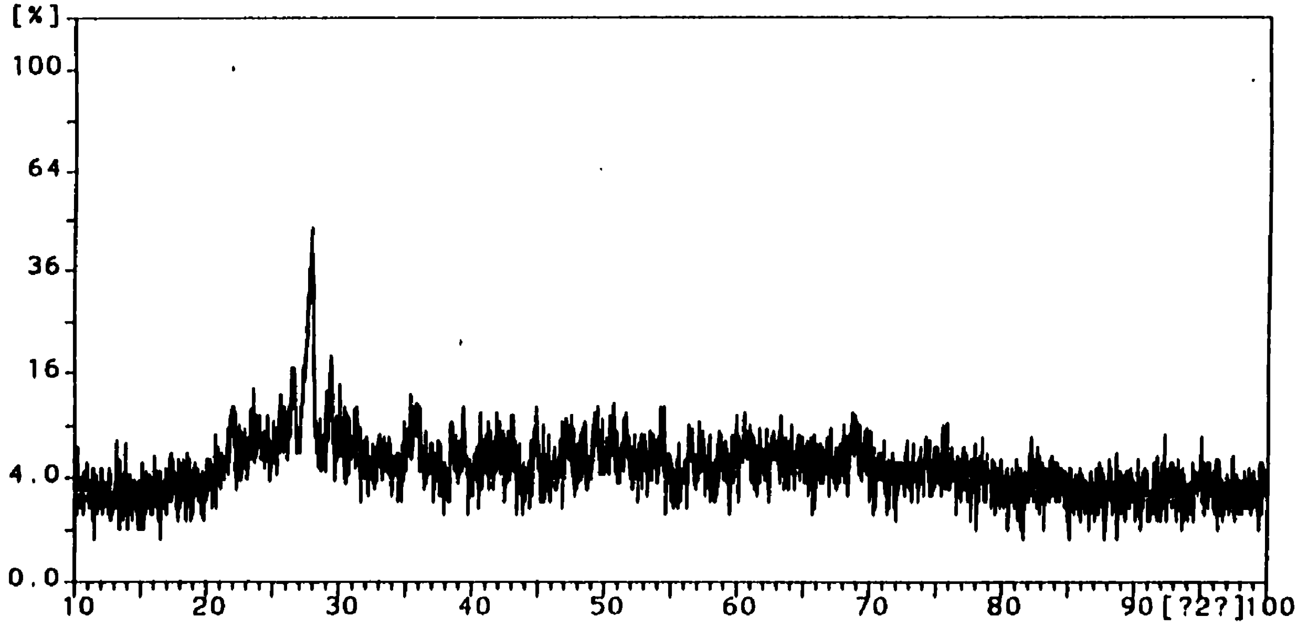

Particle Size Fraction: 850 - 600 µm

Fly Ash

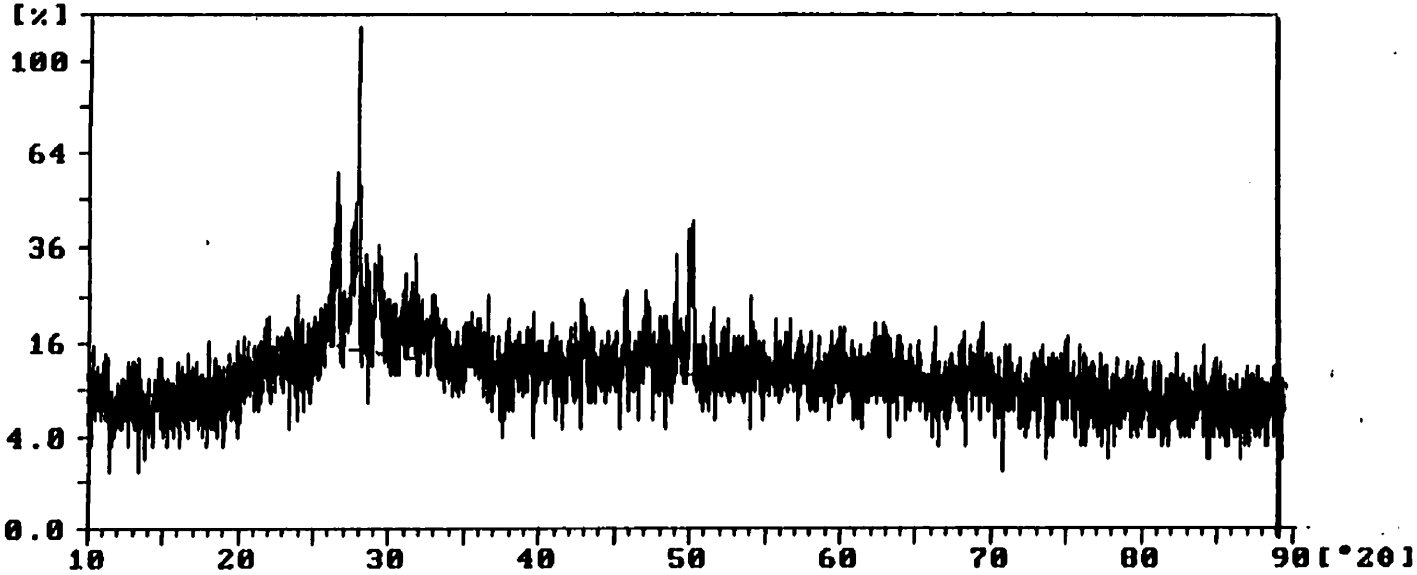

Bottom Ash

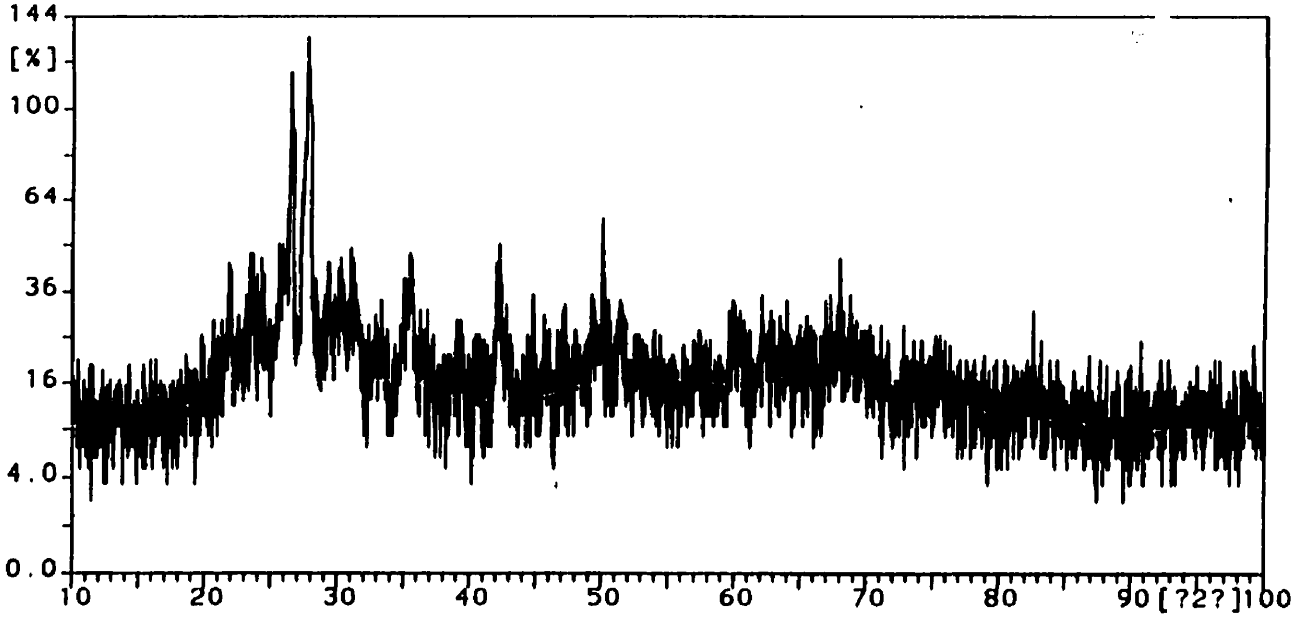

Particle Size Fraction: 600 - 425 µm

Fly Ash

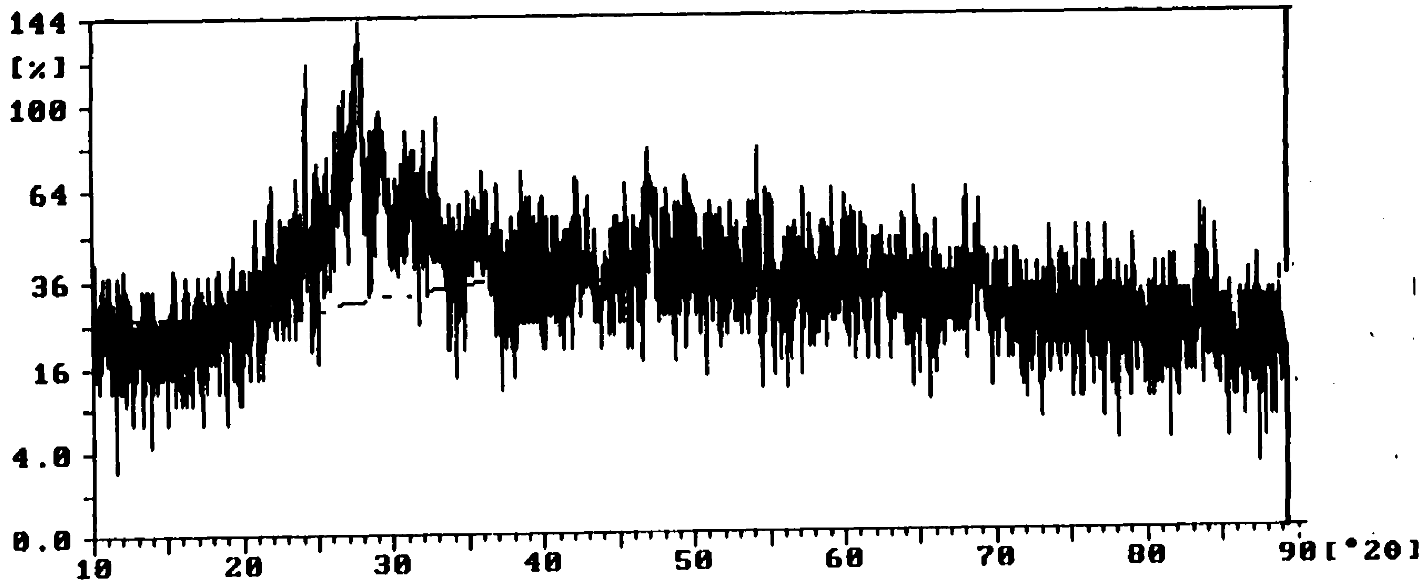

Bottom Ash

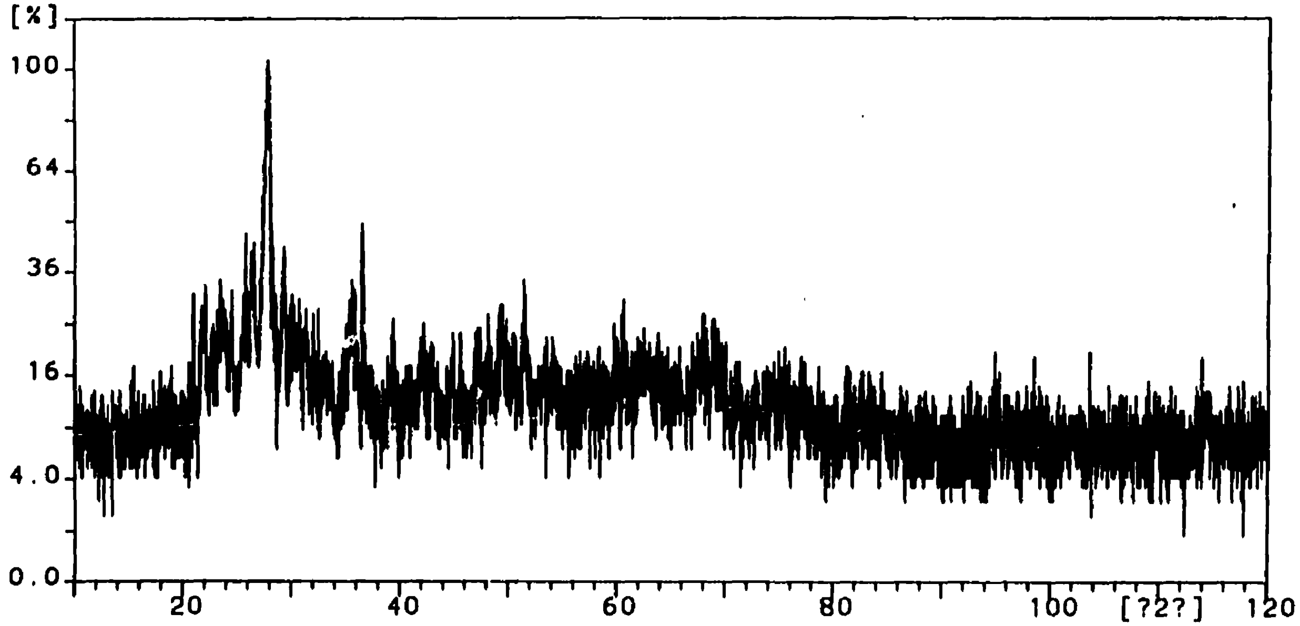

Particle Size Fraction: 425 - 300 μm

Fly Ash

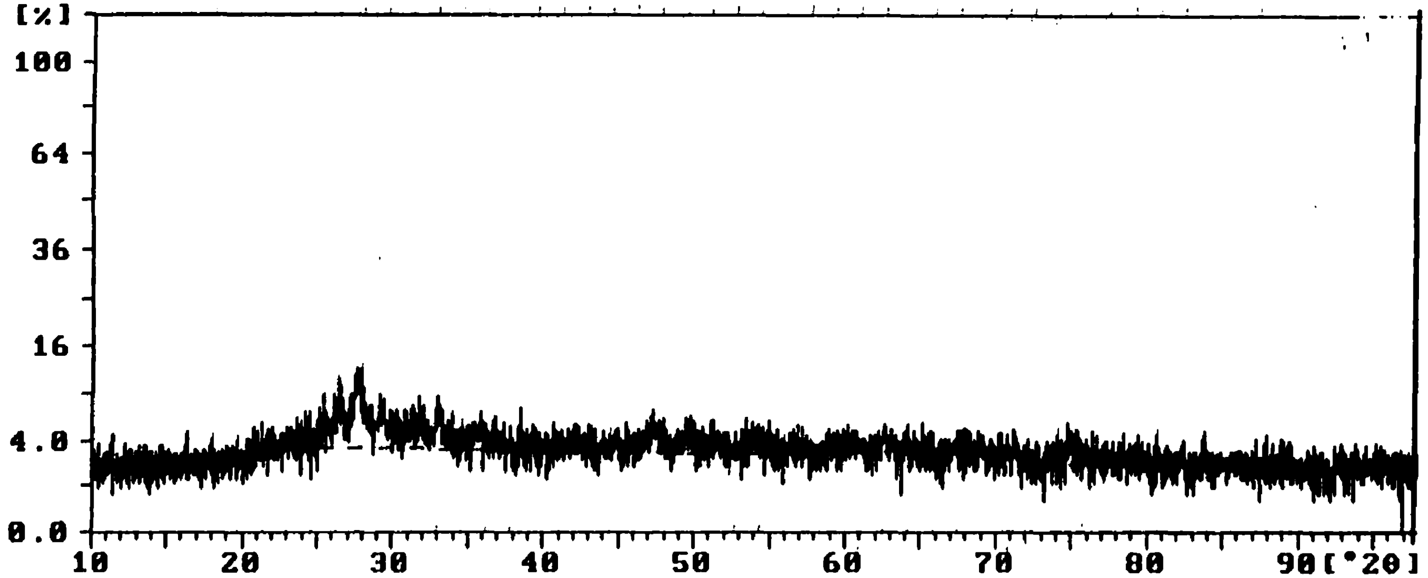

Bottom Ash

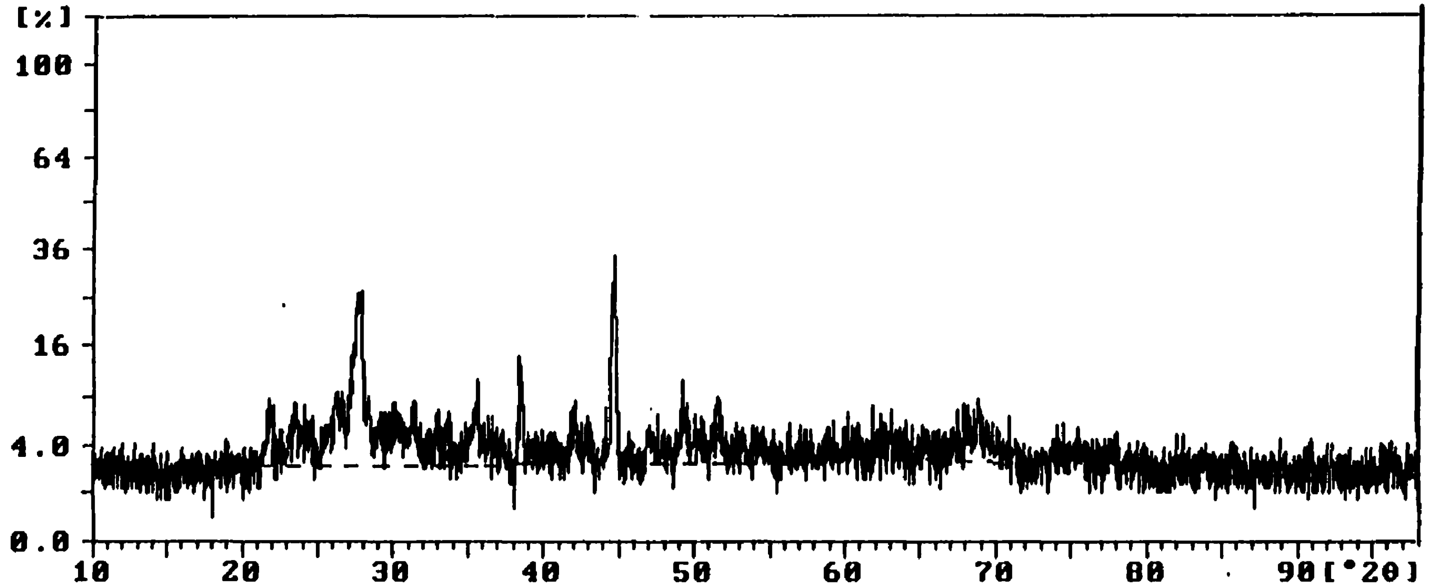

Particle Size Fraction: 300 - 212 µm

Fly Ash

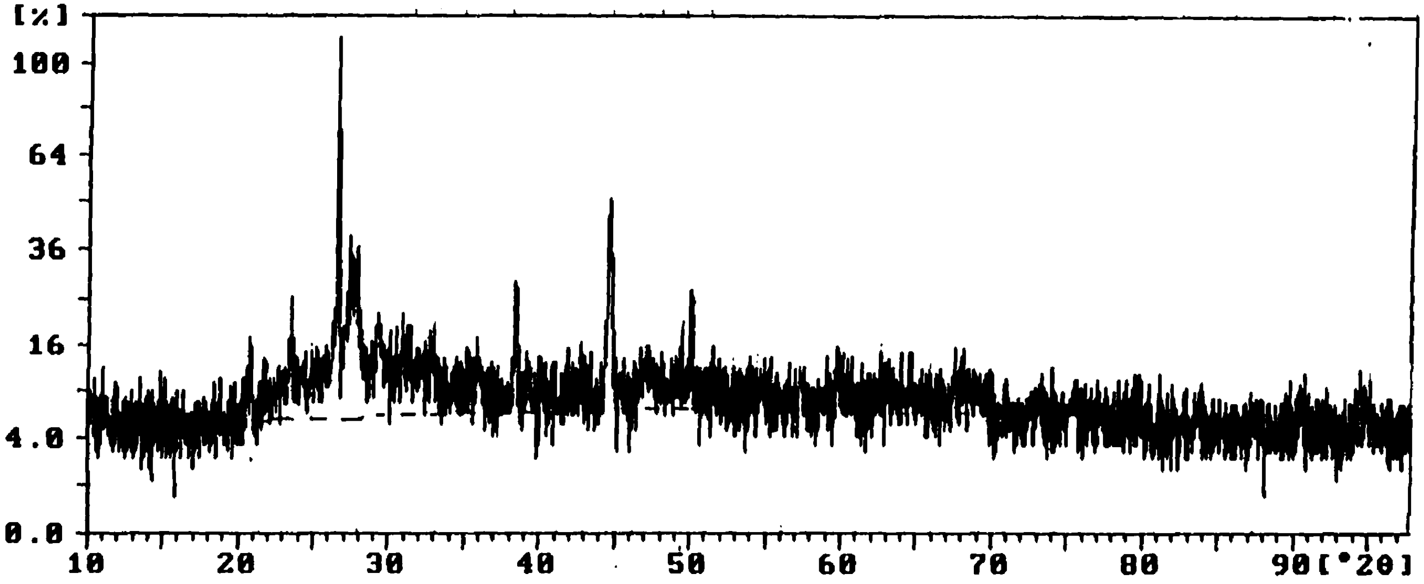

Bottom Ash

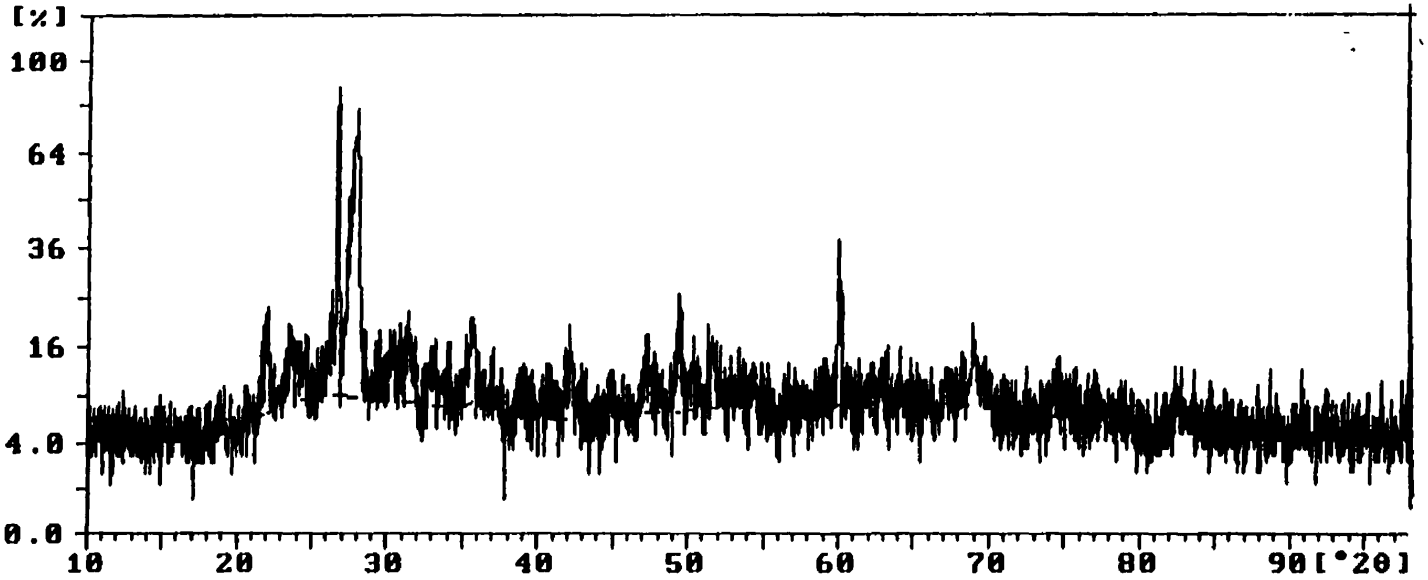

Particle Size Fraction: 212 - 150 µm

Fly Ash

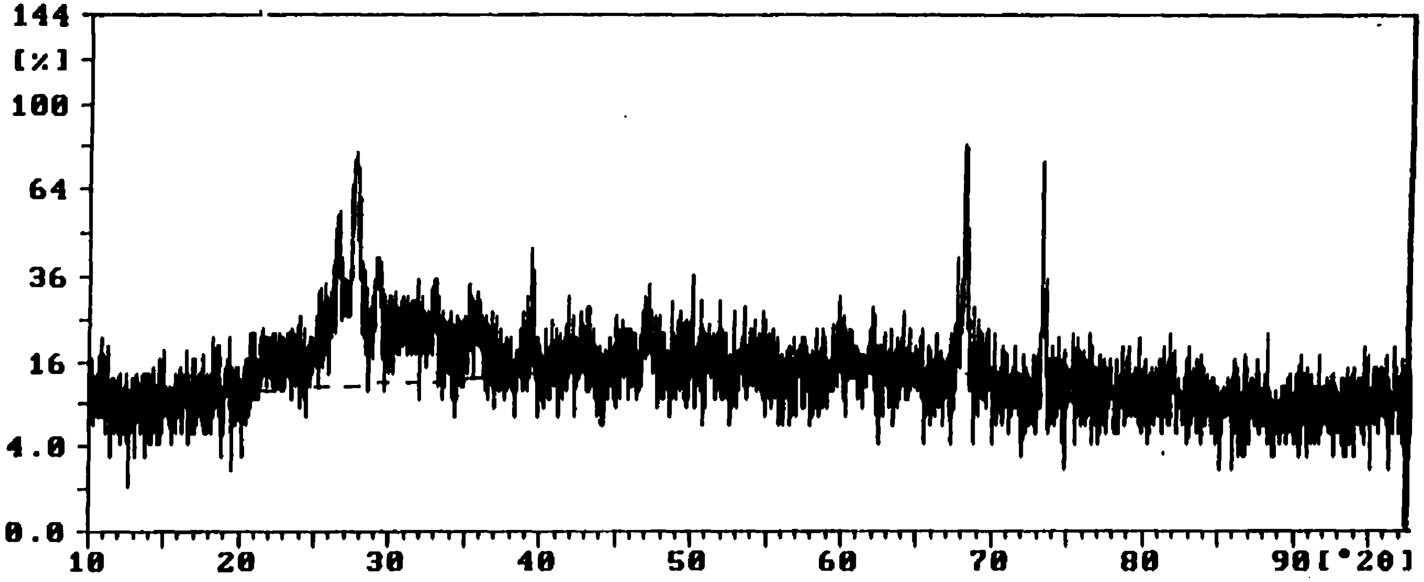

Bottom Ash

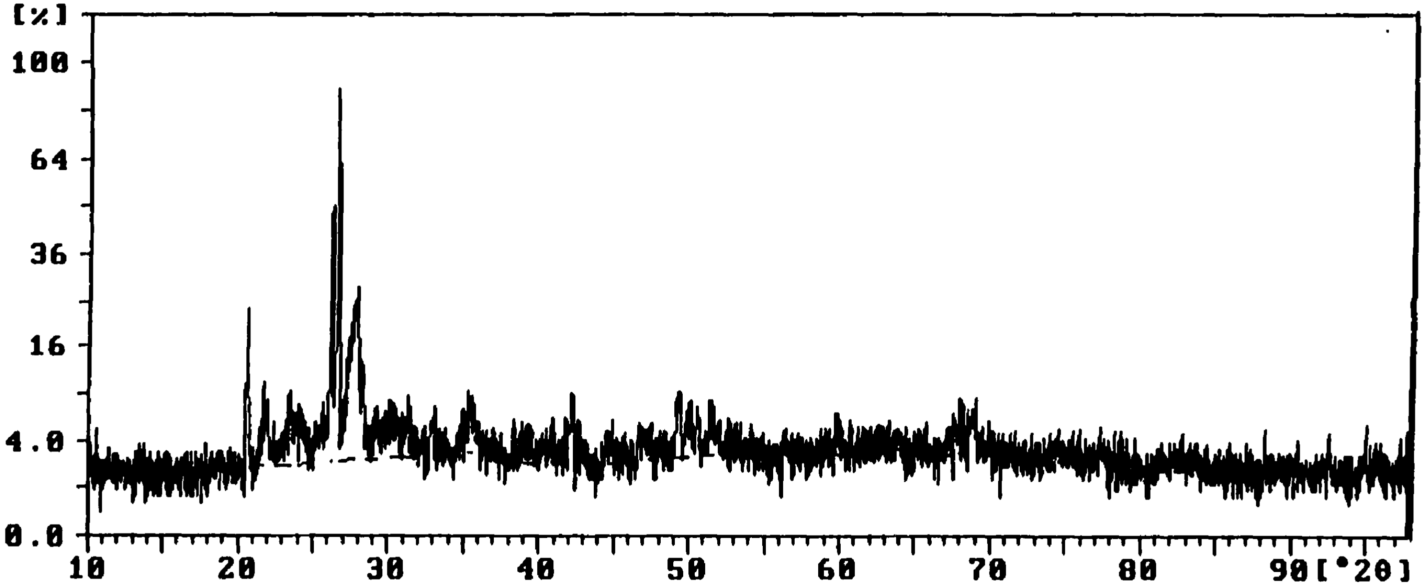

Particle Size Fraction: 150 - 75 μm

Fly Ash

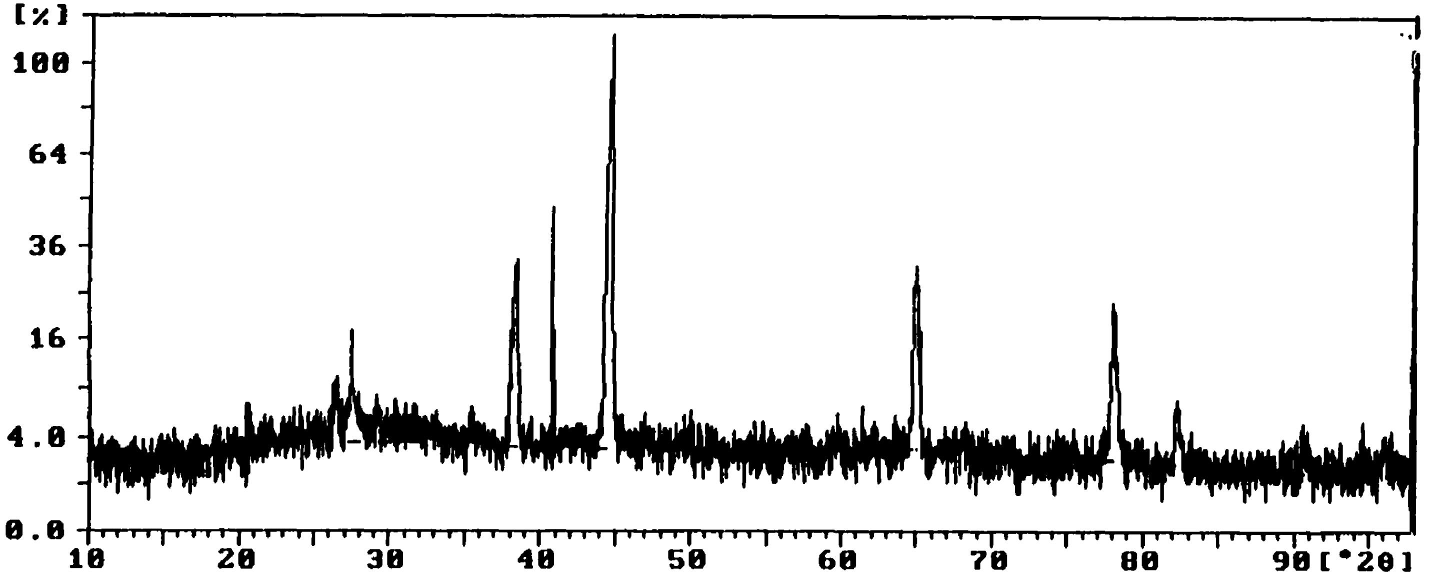

Bottom Ash

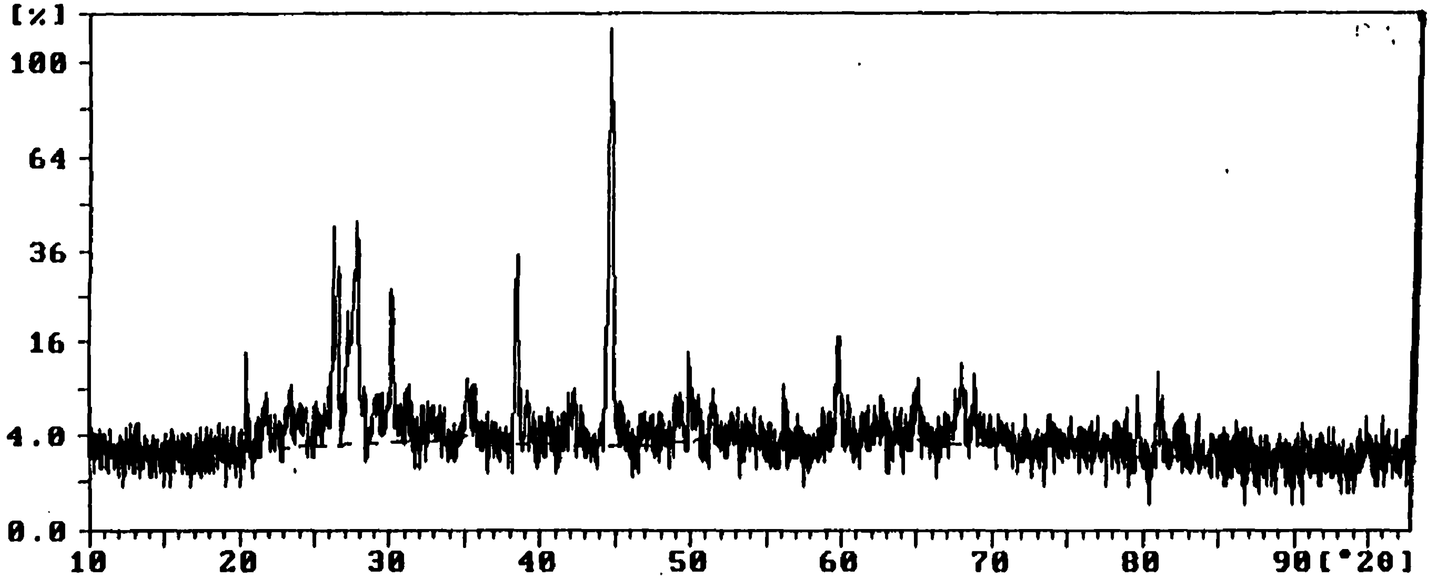

Particle Size Fraction: 75 -53 μm

Fly Ash

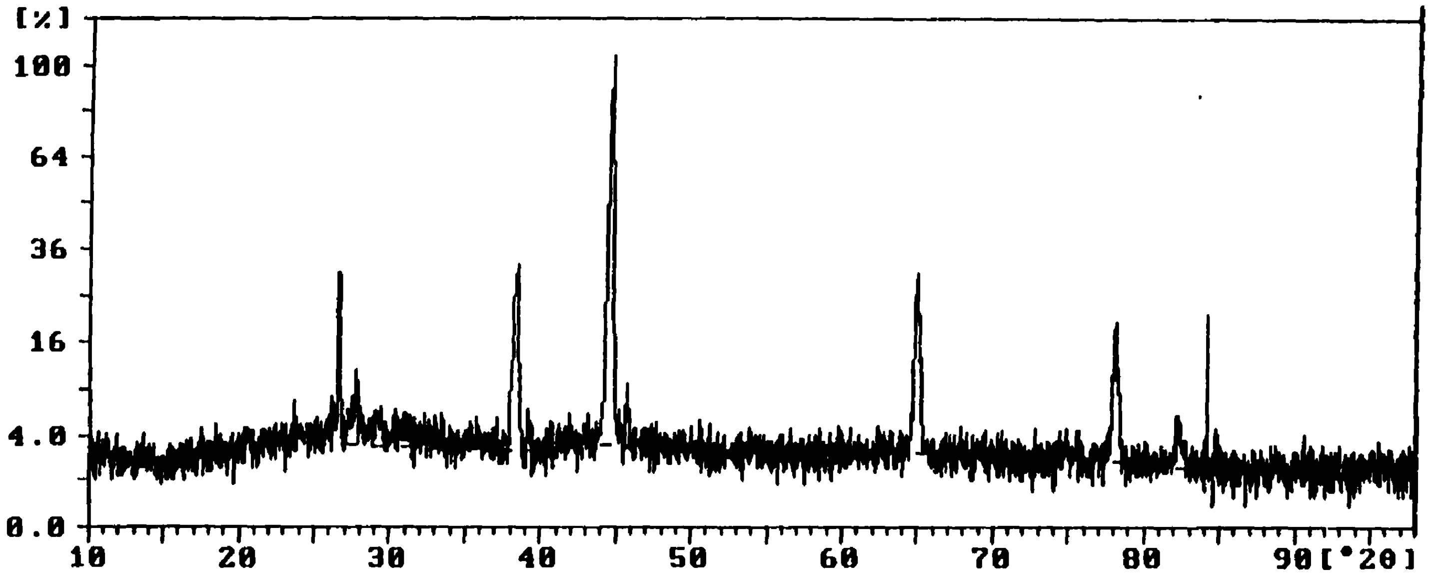

Bottom Ash

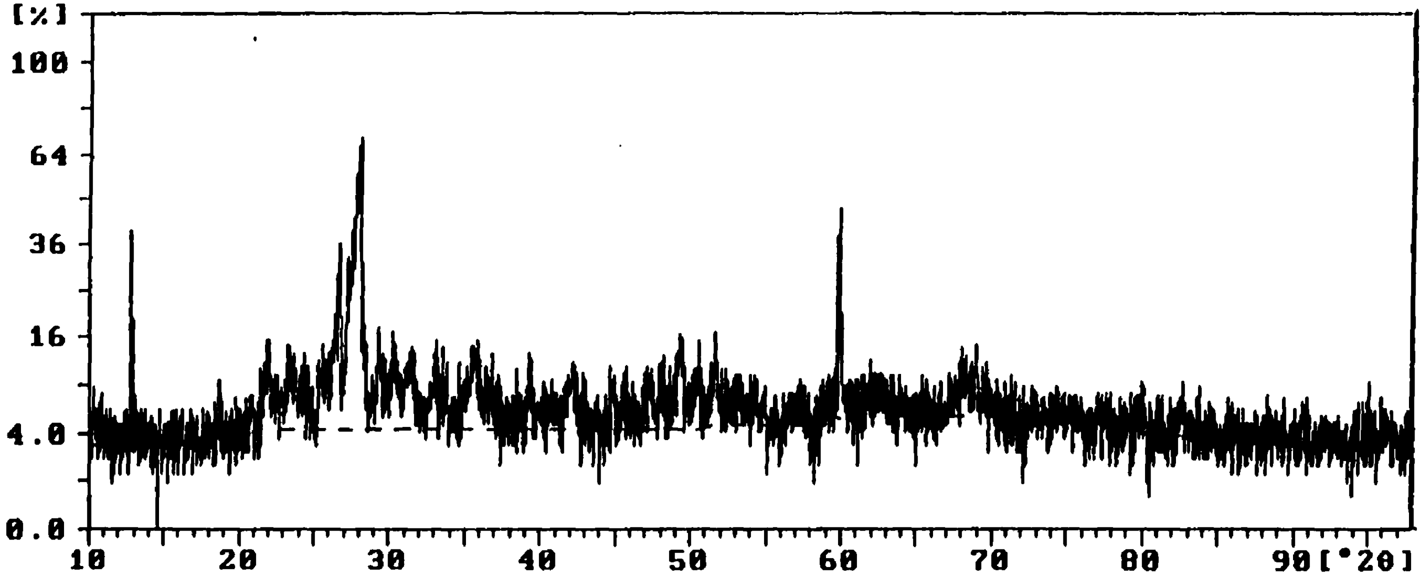

Particle Size Fraction: 53-38 μm

Fly Ash

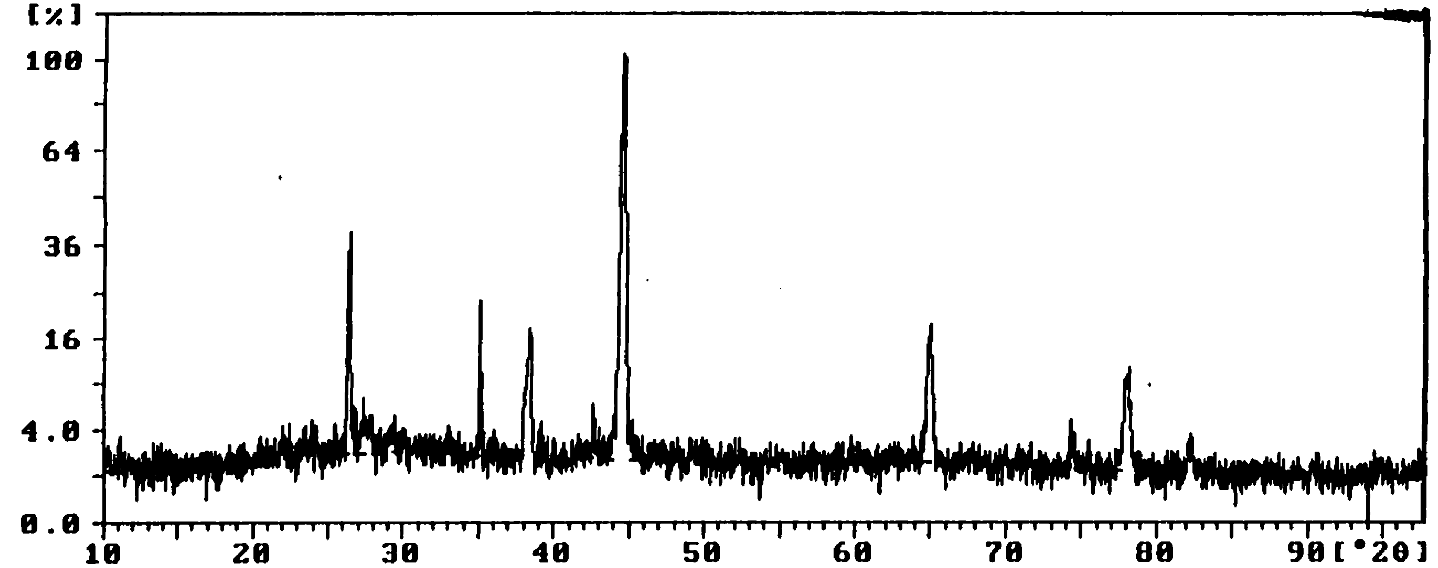

Bottom Ash

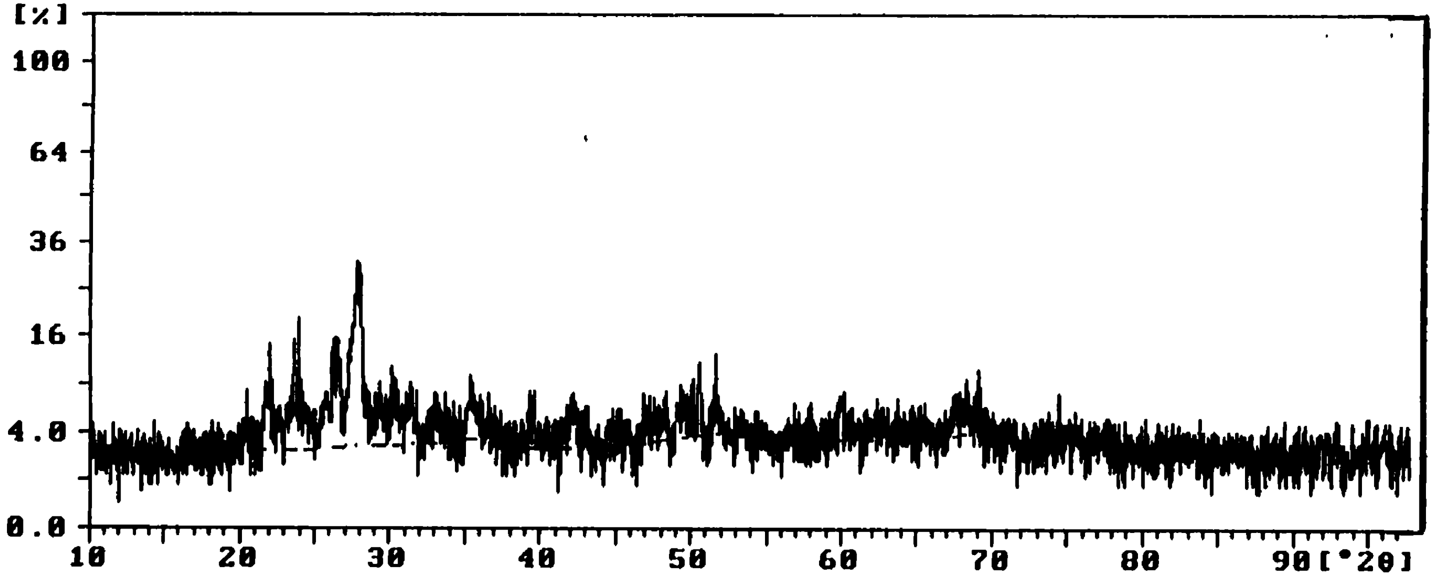

Particle Size Fraction: <38 µm

Fly Ash

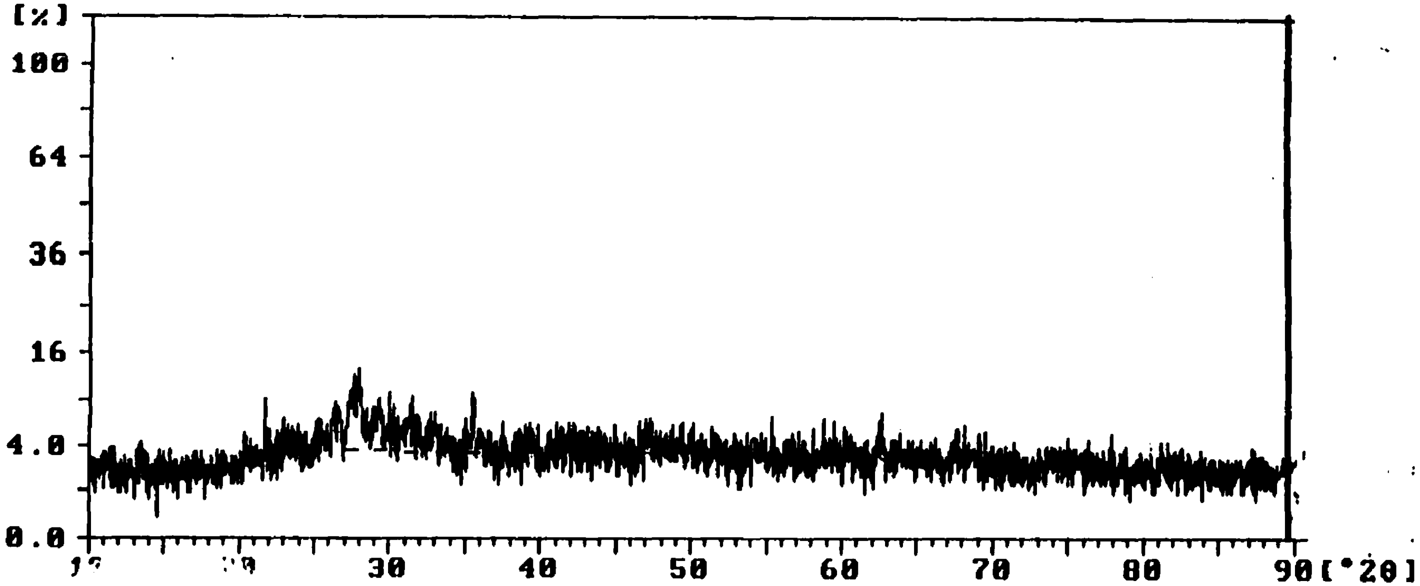

Bottom Ash